An analysis of N-Src splice variants in Xenopus development

Isobel Bradley

MSc by Research

University of York

Biology

January 2016

Abstract

The ubiquitously expressed cellular-Src (C-Src) protein kinase has a number of neural isoforms known as neural-Src (N-Src) kinases. One such isoform, N1-Src has an insert of five or six amino acids in its SH3 domain, changing target protein specificity. Previous data have shown that N1-Src expression levels correlate positively with good prognosis childhood neuroblastoma cancer; which develop from neural crest-derived tissues. In this project it was shown using RT-PCR that peaks in *N1-Src* expression correspond to stages of primary and secondary neurogenesis in the *Xenopus tropicalis* and zebrafish model organisms. An additional *Xenopus*-specific isoform, termed N3-Src, which previously had no ascribed function, possesses 22 additional amino acids in its SH3 domain. Here it was shown that *N3-Src* expression levels also peak during primary and secondary neurogenesis and that both isoforms are somewhat upregulated in *noggin* mRNA-injected animal cap explants. *In situ* hybridisation using locked nucleic acid (LNA) probes showed that the expression of these isoforms is restricted to neural and neural crest structures during early *Xenopus tropicalis* development. Antisense morpholino oligo-mediated knockdown of *Xenopus tropicalis N1-Src* and *N3-Src* resulted in locomotive defects, the expansion of the proliferative neural plate marker *sox3* and the reduction of the neural differentiation marker *n. tubulin* in neurula stage *Xenopus tropicalis* embryos and a subtle reduction in *phox2a* expression at tailbud stages; a marker of noradrenergic cells from which neuroblastoma cancers derive. Whilst *N1-Src* overexpression had no detectable effect on *Xenopus tropicalis* embryo phenotype or the expression of the neural markers analysed, *N3-Src* overexpression caused a reduction in both eye pigmentation and the expression of *phox2a*. These data support functions of neural Src isoforms in the regulation of vertebrate neural development.

Table of contents

List of figures

Chapter one: Introduction

Chapter three: Results

List of tables

Chapter two: Methods

Chapter three: Results

Acknowledgements

I would like to thank my supervisor Dr Harv Isaacs for providing me with support, confidence and an abundance of patience throughout this project – especially on Monday mornings after poor performances by Liverpool and Manchester United and when faced with broken taps! I would like to thank Dr Betsy Pownall and all other members of the Isaacs and Pownall labs for their help, encouragement and for making my time in the lab so much fun. Caitlin I will miss our injection sessions and Radio 2 sing-a-longs – Popmaster is not the same without you. Thank you also to members of my thesis advisory panel Dr Dawn Coverley and Dr Gareth Evans for your time, advice and reassurance.

Author's declaration

I, Isobel Bradley, declare that this thesis is a presentation of original work and I am the sole author. This work has not previously been presented for an award at this, or any other University. All sources are acknowledged as references.

Chapter one: Introduction

Protein phosphorylation

Protein phosphorylation is a mechanism by which proteins are post-translationally modified by the covalent addition of one or more gamma-phosphate groups from ATP, resulting in their activation or inactivation and allowing cells to rapidly signal both intracellularly and intercellularly without the need for protein synthesis. By adding phosphate groups to target proteins, kinase proteins facilitate the phosphorylation process, whilst phosphatase proteins reverse this by removing phosphate groups. Protein phosphorylation results in the activation of multiple cell signalling pathways, which modulate key cellular activities such as differentiation, cell cycle progression, cytoskeletal arrangement and cell motility (Johnson 2009).

Protein phosphorylation in higher eukaryotes occurs on serine, threonine and tyrosine residues, upon the recognition of the surrounding amino acids, known as the 'motif' (Amanchy et al. 2007).

Src Family Kinases

Src Family Kinases (SFKs) are a family of ten non-receptor tyrosine kinases known as Src, Lck, Hck, Fyn, Blk, Lyn, Fgr, Yes, Frk and Yrk (Smida & Smidová 1969; Amata et al. 2014). SFKs are a group of proteins with related structures, in the form of conserved protein domains, termed Src homology (SH) domains (Figure 1).

The first tyrosine kinase protein to be discovered, viral-Src (v-Src) is an essential oncogenic component of the transforming capability of the Rous Sarcoma Virus (RSV) after which Src and subsequently the protein family was named. RSV infection causes neoplastic transformation of chicken fibroblasts (Smida & Smidová 1969) whilst uninfected chicken cells also contain DNA that is partially complementary to the virus RNA (Baluda 1972), a feature that has been shown to be conserved in avian species (Stehelin et al. 1976) and in fact all Parazoa and Uemetazoa (Schartl &

Barnekow 1982). This proto-oncogene encodes the cellular product known as C-Src and is believed to be the gene from which the transforming capacity encoded by *v-Src* originally derived, upon its integration into the viral genome (Stehelin et al. 1976), owing to its functions in regulating proliferation, cell adhesion and cell migration (Baumgartner et al. 2008). C-Src overexpression and activation is associated with many human cancers, including cancers of the breast, brain, pancreas and colon (Irby & Yeatman 2000).

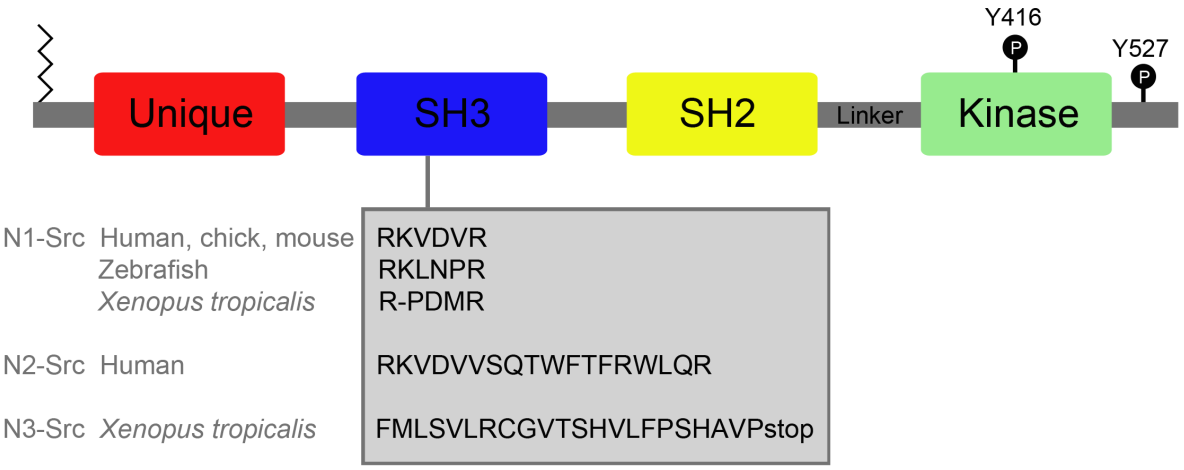

Figure 1: Src Family Kinase (SFK) domain structure: SFK proteins possess an N-terminal membrane targeting SH4 domain, a variable unique domain, a substrate-specifying SH3 domain (the site of neural microexon inclusion, the amino acid sequences of which are shown), a phosphotyrosine-binding SH2 domain and a kinase domain, which is connected to the SH2 domain via a linker. SFK proteins are subjected to regulatory phoshpohorylations; at the activating Y416 and inactivating Y527 sites. Amino acid positions refer to the chicken Src protein.

Src Family Kinase protein domains

The SH4 domain

At the amino terminus, SFK proteins are membrane targeted via the SH4 domain. This occurs via myristoylation and palmitoylation of basic arginine residues. The N terminal Met-Gly-X-X-X-Ser/Thr consensus sequence is recognised and myristoylated cotranslationally by the covalent addition of the myristate group to the glycine residue at position two by N-myristyl transferase (Resh 1993; Resh 1994). In addition to myristolylation, SFK proteins are palmitoylated at N-terminal cysteine

residues; at position three and additionally position five in the Lck protein, by palmitoyltransferase enzymes following myristoylation. Palmitoylation occurs on all members of the SFK family, with the exceptions of Src and Blk (Koegl et al. 1994). Whilst Src is not palmitoylated, its membrane association is promoted by the presence of alternate basic lysine residues at the N terminus, forming the Met-Gly-X-X-Lys-X-Lys-X motif, variants of which are shared by other SFK proteins and promote membrane association via electrostatic interactions with acidic phospholipid head groups (Silverman et al. 1993). In addition, Src contains three arginine residues at positions 14-16, which further increase this positive charge and strengthen the electrostatic interaction (Resh 1994).

Membrane targeting and anchorage of SFKs primarily targets them to the plasma membrane inner surface, which permits their function in propagating cellular signalling. Membrane localisation enables SFK proteins to interact with other membrane proteins, including transmembrane proteins (Thomas & Brugge 1997). In doing so, SFKs are able to phosphorylate proteins in association with membrane proteins, which themselves lack intrinsic kinase activity and thus enables cellular signalling (Courtneidge et al. 1993).

The unique domain

C-terminal to the membrane-targeting SH4 domain is the unique domain; an intrinsically disordered region (Maffei et al. 2015) of 50-90 amino acids in length, which is the most variable region between SFK proteins (Amata et al. 2014). Due to their intrinsically disordered nature, no single domain structure or function has be attributed to this domain, however the unique domains of specific SFK proteins are highly conserved between different species and exchanging the unique domain of Src for the unique domain of Yes switches its functions in gene expression regulation and cell morphology (Hoey et al. 2000; Summy et al. 2003), implying that this domain is important in SFK function and specificity.

The Src unique domain has been shown to interact with acidic lipids via the unique lipid-binding region (ULBR), the Src SH3 domain both intramolecularly and intermolecularly and proteins such as calcium-bound calmodulin (Pérez et al. 2013) and the adaptor protein NADH dehydrogenase subunit 2 (ND2), which bridges the binding of Src and the N-methyl-d-aspartate (NMDA) receptor (Gingrich et al. 2004).

Pérez et al. (2013) showed *in vitro* that there are multiple sites of Src unique domain phosphorylation that are able to regulate its binding. Phosphorylation of T37 or S75 of human Src (T34 and S72 of chicken Src (Amata et al. 2014)) by p25-activated Cyclin-dependent kinase 5 (Cdk5) reduces the interaction between the ULBR and acidic phospholipids. This promotes ubiquitination-mediated Src degradation, thereby regulating its levels and therefore Src activity (Pan et al. 2011). In the context of cellular function and in particular cell division, S75 phosphorylation by Cdk5 has been observed in the human Y79 retinoblastoma cell line (Kato & Maeda 1999). This is postulated to reduce lipid binding by the ULBR, changing the Src localisation to cytosolic; the location associated with cell cycle progression (David-Pfeuty 1990) and a feature of oncogenic v-Src (Willingham et al. 1979). This may encourage cancerous behaviour by changing the Src substrates to those associated with cell cycle progression, such as the Transmembrane and Associated with Src Kinases (Trask) protein, which interacts with cell adhesion and matrix proteins. These include syndecans and cadherins, whose mitotic relocalisation from the cell membrane to the cytosol is associated with the loss of adhesion observed during mitosis (Bhatt et al. 2005). In the non-cancerous state, Src S75 phosphorylation leads to the ubiquitination, limiting and therefore regulating cytosolic Src activity (Pan et al. 2011).

Pérez et al. (2013) showed that the interaction between the unique and SH3 domains is allosterically inhibited by polyproline peptide binding to the SH3 domain, whilst unique domain binding to calcium-bound Calmodulin enhances lipid binding by the ULBR. These data highlight the functional significance and regulation of this domain.

The SH3 domain

C-terminal to the unique domain is the SH3 domain. The SH3 domain functions in target protein binding (Pérez et al. 2013). The SH3 domain comprises of 55-75 amino acids, folded to form two three-stranded antiparallel beta sheets, which are packed at right angles to one another. There are three key interaction points present in the SH3 domains of SFK proteins; two recognition pockets responsible for binding proline and a specificity pocket which binds the flanking arginine or lysine residue. This forms a hydrophobic binding pocket, which binds proline rich substrate and ligand peptides; specifically the R/KxxPxxP or PxxPxR/K polyproline motifs (Yu et al. 1992; Zarrinpar et al. 2003). In addition to these interaction points, a region referred to as the specificity zone present in the SH3 domain targets the specificity of substrate binding via non-consensus sequences and is made of two loops that connect the two beta sheets. They are known as the n-Src loop and the RT loop (Saksela & Permi 2012). In addition, the Src SH3 domain is able to bind lipids and Src unique domains via the RT and n-Src loops (Pérez et al. 2013).

C-terminal to the SH3 domain are the SH2 and kinase domains, which are separated by a linker domain. The linker domain binds to the SH3 domain via its left-handed polyproline type II helix. This causes the SFK to adopt a closed and inactive conformation and is essential in regulating the SFK activity (Gonfloni et al. 1997).

The SH2 domain

The SH2 domain also participates in ligand and substrate binding, which occurs due to its affinity for phosphotyrosine (Huang et al. 2008). The SH2 domain has important functions in substrate binding and negative autoregulation of kinase activity (Filippakopoulos et al. 2009).

SFK substrate binding mediated by the SH2 domain permits the association of SFK proteins such as Src with focal adhesion kinase (FAK), via integrin-induced FAK phosphorylation at Y397 (Guan 1997;

Lindfors et al. 2012). This association allows Src to phosphorylate FAK in its kinase domain activation loop which consequentially becomes activated, forming an active FAK-Src complex (Mitra & Schlaepfer 2006). This promotes the turnover of focal adhesions, cell migration, survival and anchorage independent growth (Westhoff et al. 2004; Mitra & Schlaepfer 2006).

The negative autoregulation of SFK function imparted by the SH2 domain is facilitated by its binding to phosphorylated Y527 in Src and the corresponding phosphotyrosine residue in other SFK proteins, which is present at the carboxy terminus of SFK proteins (Filippakopoulos et al. 2009). C-Srk Kinase, the SFK regulator, performs Y527 phosphorylation. SH2 domain binding to phosphorylated Y527 causes the protein to adopt a closed and inactive conformation. The cancer-causing v-Src lacks the Y527 residue and therefore cannot be regulated in this manner, leading to unregulated Src activity, causing cancer (Okada 2012). In cancers that do not have somatic mutations in either *Src* or *Csk*, changes have been observed in the expression levels of Csk regulators such as Csk-binding protein (Cbp), which binds Csk and SFK proteins and directs membrane localisation (Kawabuchi et al. 2000; Oneyama et al. 2008).

The kinase domain

The SFK kinase domain, also known as the SH1 domain is responsible for the SFK effector kinase functions, adding phosphate groups to target proteins. Full kinase activity is attained upon phosphorylation of Y416 in the kinase domain activation loop. This is mediated by autophosphorylation and mutation of the ATP binding site (K295M) prevents Y416 phosphorylation (Irtegun et al. 2013).

Src regulation

As described, SFK proteins are subjected to regulation of their activities, thus preventing cellular transformation. It has been described that the Csk protein phosphorylates Y527, enabling its binding to the SH2

domain. This interaction is stabilised by the binding of the SH3 domain to the linker domain, which separates the SH2 and kinase domains. This closed conformation prevents the autophosphorylation of Y416 in the kinase domain activation loop, thereby rendering the SFK protein inactive. Y527 dephosphorylation is then required to reverse this process (Okada 2012).

Neural Src kinase

Brugge et al. (1985) demonstrated that the neurons of rats express 15-20 times higher Src protein levels and six times higher Src kinase activity than fibroblast cells, measured as ^{35}S-methionine levels and both ^{32}P incorporation and enolase phosphorylation respectively. Immunoprecipitated Src from neurons and fibroblasts also presented different migration properties following V8 protease digestion; a serine endoprotease, which cleaves peptide bonds C-terminal to glutamic acid residues. Two amino terminal digestion products of M_r 18,000 and 16,000 migrated more slowly in the neural immunoprecipitate. Martinez et al. (1987) showed that this corresponds to a neuron-specific six amino acid insertion into the SH3 domain, encoded by the insertion of a microexon between exons 3 and 4 and was termed Neural Src (N1-Src). The *N1-Src* splice variant has been detected in vertebrates from teleost fish to mammals (Raulf et al. 1989), where the microexon also encodes a six amino acid insert. In *Xenopus* species, the *N1-Src* microexons (of which *Xenopus tropicalis* have one and *Xenopus laevis* have two) encode inserts of five amino acid (Figure 1) (Collett & Steele 1992).

It has been observed that an additional neural Src isoform is expressed in the neurons of mammals such as humans and was termed N2-Src. This isoform has an insert of 11 additional amino acids, immediately C-terminal to the N1-Src insert, which are expressed concomitantly to produce the N2-Src protein (Figure 1) (Pyper & Bolen 1990).

The Neural-Src inserts are located in the n-Src loop in the specificity zone of the SH3 domain. The inserts change the Src target protein and substrate specificities, for example, the N1-Src insert increases the affinity of this protein for proteins such as NMDA receptors (Groveman et al. 2011), the axon guidance protein EVL (Ena/VASP-like protein) (Lambrechts et al. 2000) and the post-synaptic scaffolding protein Delphillin (Miyagi et al. 2002).

Neural Src in neuroblastoma cancer

Neuroblastoma is a cancer that develops from neural precursors known as neuroblasts. More specifically, neuroblastoma cancers develop from neuroblasts of the sympathetic branch of the autonomic nervous system, which derives from the neural crest. It is the most common cause of childhood extracranial solid tumours and arises in the adrenal glands, neck, chest abdomen and pelvis (Ciccarone et al. 1989).

Bjelfman et al. (1990) demonstrated that C-Src and N1-Src proteins are detectable in neuroblastoma cancer cell lines, whilst neuroepithelioma cell lines express only C-Src. By immunoblotting primary tumour samples of child patients, this group also showed the expression of the two Src isoforms in neuroblastoma, gangioneuroblastoma and retinoblastoma primary tumours, whilst N1-Src was undetected in ganglioneuroma, Askin tumour and an adult esthesinoneuroblastoma samples. Of the 27 neuroblastoma tumours analysed, 23 samples were positive for N1-Src expression. 12 tumours from infant patients (≤18 months old) expected to have a favourable outcome with stage 1-3 neuroblastoma cancer were analysed; nine of which expressed more N1-Src than C-Src. A tenth patient expressed equal amounts of the two isoforms and was given intensive treatment due to the high-risk nature of this cancer. In three infants with stage 4, highly malignant disease, the tumours expressed more C-Src than N1-Src, whilst in tumours of an additional three non-infant patients with stage 4 cancer, only C-Src could be detected. Five out of six of the patients with stage 4 cancers died. From this, they concluded

that age and the ratio between C-Src and N1-Src levels predicted neuroblastoma prognosis; with younger age and higher levels of N1-Src than C-Src proteins correlating with better prognosis.

Neuroblastoma cancers exhibit spontaneous regression, most often in children under 18 months of age (Brodeur & Bagatell 2014), with the neuroblast-like cancer cells differentiating to form benign tumours (Reynolds 2002).

Using developmental biology to study protein function and disease

To predict the roles of particular proteins in disease, it is necessary to understand their normal functions. To do so, the process of development can be studied. In this project, the development of the model organisms *Xenopus* and zebrafish (*Danio rerio*) were used to investigate how N1-Src functions in nervous system development. In differentiating embryonic cells, protein levels and/or activities can be modified, the consequences of which can indicate functions. It can then be inferred how proteins function aberrantly in disease. It could be argued that development is a strong model for studying childhood neuroblastoma as this is a spontaneously regressing cancer of neuroblasts, of which the prognosis worsens with age.

Neural development

Nervous system development occurs as a series of steps in which transcription factors activate and repress the expression of other transcription factors and effector proteins, ultimately patterning a fully functional nervous system that enables organisms to perceive and respond to endogenous and exogenous stimuli, in order to survive. Such processes have been revealed as highly conserved between vertebrates (Wullimann et al. 2005), supporting their use in these analyses.

Xenopus neural development

Nervous system development begins with the process of neural induction. In *Xenopus* this occurs during late blastula and gastrula stages (Kuroda et al. 2004). The early *Xenopus* blastula embryo consists of an asymmetrically pigmented hollow ball of cells with both anterioposterior and dorsoventral axes. Within the blastula stage embryo, numerous signalling pathways begin to establish the three primary germ layers; endoderm, mesoderm and ectoderm, which during gastrulation continue to be patterned and reorganise to their correct locations for function. The lighter, less pigmented and denser hemisphere is known as the vegetal pole, from which the endoderm originates and later differentiates into the gut and associated organs such as the pancreas and liver. The darker, more pigmented hemisphere is known as the animal hemisphere and comprises future ectodermal cells, which later differentiate into epithelial and nervous tissues. The intervening equatorial cells make up the future mesodermal tissues, which include blood, cartilage and bone (Yasuo & Lemaire 2001).

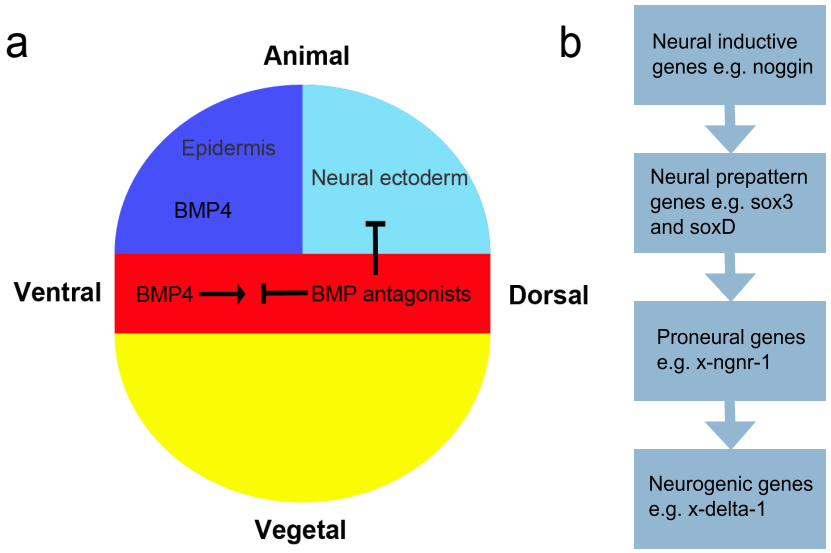

Figure 2: The cascade of transcriptional activation and repression that establishes the neurectoderm followed by differentiating neurons within this domain (a) neural induction establishes the neuroectoderm, (b) a cascade of transcriptional activation and repression establishes differentiated neurons of the nervous system.

It is the dorsal-most mesodermal cells, which have the properties of Spemann-Manngold's organiser that release the necessary signals for

neural induction. This establishes the region of the ectoderm that is competent to form the nervous system, known as the neuroectoderm (Spemann & H. Mangold 1924; Yanagi et al. 2015). Bone morphogenic proteins (BMPs) are secreted proteins expressed throughout the blastula stage embryo. Upon ligand binding, BMP cell surface receptors phosphorylate the BMP effector proteins Smad1, 5 and 8 which form complexes with the co-Smad known as Smad4 and accumulate in the nucleus where they regulate transcription. BMP signalling induces the ventral ectoderm to form epithelium whilst inhibition of BMP signalling is necessary to induce neuroectoderm. Neural inductive signals originating from Spemann-Mangold's organiser include inhibitors of BMP signalling, such as Chordin and Noggin, which are expressed due to elevated levels of β-catenin. They are secreted into the animal hemisphere where they extracellularly bind BMP dimers and prevent them from inducing epidermal fate in the dorsal ectoderm (Figure 2a) (Shi & Massagué 2003). In addition, FGF molecules in this region bind to their dimeric tyrosine kinase receptors, activating the MAP Kinase pathway. This leads to the phosphorylation of the Smad1 linker region, which inhibits its translocation to the nucleus (Pera et al. 2003), and therefore further inhibits BMP signalling and thus promotes neural fate in the dorsal ectoderm.

Following neural induction, neurogenesis ensues from gastrulation onwards in which neurons are specified in the neuroectoderm. In non-amniotic vertebrates such as *Xenopus* and zebrafish, neurogenesis occurs in two waves, known as primary and secondary neurogenesis, in which primary and secondary neurons develop respectively. Primary neurons established during primary neurogenesis enable the tail flick response of tailbud embryos and facilitate early motility in the aqueous environment. *Xenopus* primary neurons begin to differentiate and become established during gastrula stages until *Xenopus* stage 36/37 (Schlosser et al. 2002), via the cascade of transcriptional activation and repression shown in Figure 2b that ensures the neural plate is of an adequate size for the entire nervous system to develop, but that only a subset of cells in

the neural plate develop into specific neural subpopulations. The majority of primary neurons are later replaced during secondary neurogenesis that occurs within the neural tube (Schlosser et al. 2002).

At the beginning of primary neurogenesis the neural prepattern genes *sox2* and *sox3*; members of the SRY-box containing genes B1 (*SoxB1*) family are expressed in the neuroectoderm in response to neural induction. They encode transcription factors that promote cell division in the mitotically active neural plate to ensure it reaches a sufficient size for the nervous system to develop. To do this, Sox2 and Sox3 act to downregulate the expression of neurogenic genes which otherwise promote neuroblast differentiation into neurons, such as *X-ngnr* (Rogers et al. 2009). In addition, they maintain the capacity of the neuroectoderm to respond to neural inductive signals via its ability to respond to FGF signalling and promoting the repression of BMP signalling, for example by inhibiting the expression of *bmp4*; a BMP ligand (Mizuseki, Kishi, Matsui, et al. 1998; Rogers et al. 2009).

The neural prepattern gene *soxD,* which is expressed in response to BMP antagonism and *sox3* expression (Rogers et al. 2009), then sets the open neural plate down the path of neural determination by activating the expression of a neural determination factor - the early proneural gene *neurogenin* (*X-ngnr*) (Mizuseki, Kishi, Shiota, et al. 1998), which in turn activates the expression of the late proneural genes, such as the basic helix loop helix transcription factor *neuroD*; a neural differentiation factor (Cao et al. 2002; Lee et al. 1995). This pathway establishes neural differentiation, which can be visualised as populations of *n. tubulin* expression (a marker of differentiated neurons) (Kuroda et al. 2004).

During neurogenesis, three distinct neural subpopulations form on either side of the dorsal midline that can be visualised as expression domains of *neuroD* and *n. tubulin*. These subpopulations of cells differentiate in longitudinal domains positioned medially, intermediately and laterally with respect to the midline on both sides of the neural plate (Figure 3). As the

neural plate rolls and fuses to form the neural tube, the medially and laterally positioned subpopulations become positioned ventrally and dorsally respectively, with the intermediately positioned population located between (Brewster et al. 1998). These ventrally, dorsally and intermediately-positioned subpopulations go on to differentiate into motor, sensory and interneurons respectively and their positions within the neural tube enable the formation of properly formed neural circuits. The three longitudinal domains are established by Notch and Delta-mediated lateral inhibition. In this highly conserved pathway, cells in the neural plate that express the highest levels of X-ngnr activate the expression of *delta*, which encodes a transmembrane ligand. The Delta receptor, known as Notch is expressed throughout the neural plate (Yan et al. 2009). Upon Delta ligand binding, Notch receptors on the surfaces of cells located between the columns of highest *X-ngnr* expression undergo proteolysis, releasing the Notch intracellular domain. The Notch intracellular domain then enters the nucleus, where it associates with the vertebrate homologue of the *Drosophila melanogaster* DNA binding protein Suppressor of Hairless (Su(H)) . This converts it to a transcriptional activator, which activates the expression of the Enhancer of Split (Espl) complex and Hairy; inhibitors of neurogenesis. These proteins act, for example by inhibiting the expression of *X-ngnr* (Ma et al.

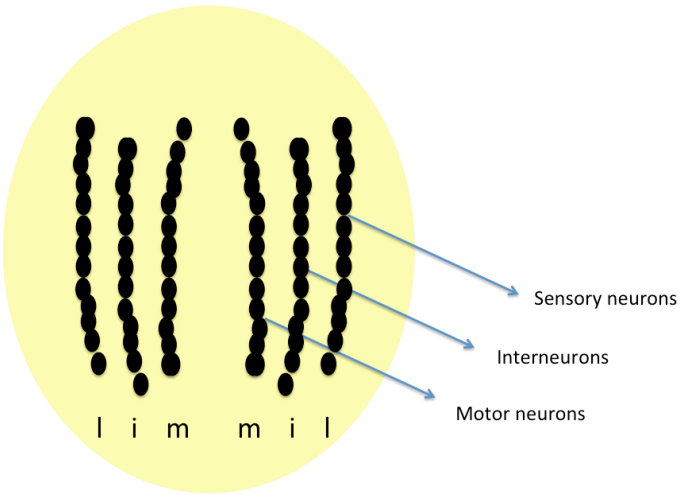

Figure 3: The longitudinal columns of *N. tubulin* expression across the mediolateral axis of neural stage *Xenopus* embryos. 'l', 'i' and 'm' refer to lateral, intermediate and medial positions across the mediolateral axis of the neural stage neural plate, which differentiate into sensory, inter and motor neurons respectively.

1996) and therefore neurons are not specified in the domains between the longitudinal columns of highest X-ngnr levels, thus creating the three distinct subpopulations described.

Secondary neurogenesis occurs in the neural tube of non-amniotic vertebrates such as *Xenopus* and zebrafish and occurs from *Xenopus* stage 46 onwards (Schlosser et al. 2002). Secondary neurogenesis has been more closely likened to amniotic neurogenesis, such as that of humans, occurring in the neural tube. It is believed that the pathways are conserved between primary and secondary neurogenesis (Wullimann et al. 2005).

Whilst differences exist, the pathways involved in neural development, such as FGF and BMP signalling and also Notch-Delta lateral inhibition are highly conserved between vertebrates, such as *Xenopus,* zebrafish and mammalian species and even invertebrates such as *Drosophila melanogaster* (Pownall & Isaacs 2010; Rogers et al. 2011; Sanes et al. 2011).

Neural crest development

Neuroblastoma cancer develops in tissues of the sympathetic nervous system, which differentiates from cells of the neural crest. The neural crest develops from cells located laterally on either side of the neural plate, which delaminate from the neuroectoderm-ectoderm margin as the neural tube rolls up, fuses and detaches from the surrounding ectoderm (Figure 4). The process of neural crest development is owing to an epithelial to mesenchymal transition, as the cells that delaminate then migrate to peripheral locations (Lim & Thiery 2012), where they contribute to peripheral nervous system development and also craniofacial cartilage and bone and also glia (Trainor 2005).

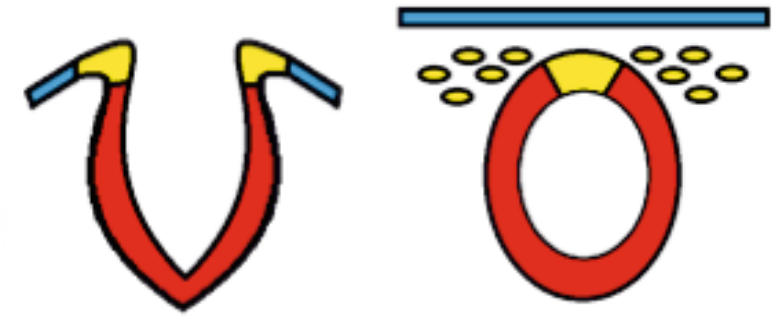

Figure 4: Neural crest cells delaminate from the neural plate-non-neural ectoderm boundary as the neural plate rolls up and fuses to form the neural tube. Non-neural ectoderm, neural crest and neural tube are represented in blue, yellow and red respectively.

The strengths of using *Xenopus* and zebrafish as model organisms to study development and disease

In this project, *Xenopus tropicalis, Xenopus laevis* and zebrafish were used to gain understanding into the function of neural Src isoforms in the context of development. These organisms provide many practical advantages due to their fully sequenced genomes and large clutch sizes. Their external development and large embryo sizes also enable the microinjection of reagents (Hirsch et al. 2002) such as antisense morpholino oligos and *in vitro* transcribed mRNA for knockdown and overexpression analyses, and additionally the microinjection of the reagents necessary to generate knockout organisms, via clustered regularly-interspaced short palindromic repeats (CRISPR)/CRISPR-associated (Cas) technology.

Previous work relevant to this project

xN1-Src expression and functional analyses

By dissecting away the neural plate from the surrounding tissue and performing RT-PCR, Collett & Steele (1992) demonstrated that the neural plate was the region of highest *Xenopus N1-Src* (*xN1-Src*) expression in neurula stage *Xenopus* embryos. In this project the spatial expression profile of the *xN1-Src* isoform during early *Xenopus tropicalis*

development was analysed using *in situ* hybridisation, which has not previously been identified.

Philip Lewis (thesis, 2014), showed using RT-PCR on early-stage *Xenopus tropicalis* embryos, that *xN1-src* transcripts are present at low levels in the maternal transcript pool, increase during primary neurogenesis and neurulation and then begin to decrease at tailbud stages, after neurulation is complete and the neural tube is closed and positioned in the dorsal side of the embryo (Schroeder 1970). In this project the temporal expression profiles of *Src* variants during *Xenopus tropicalis* neural induction and primary neurogenesis was investigated in greater detail, as well as their expression patterns at the onset of secondary neurogenesis. In addition, zebrafish primary neurogenesis and secondary neurogenesis were examined for the temporal expression patterns of *N1-Src,* as an additional model of vertebrate development.

Philip Lewis also demonstrated that COS7 fibroblast cells transfected with either mammalian or *Xenopus laevis N1-Src* constructs develop neurite-like processes. In the absence of *xN1-Src* (achieved using antisense morpholino oligos), he also showed that *Xenopus tropicalis* embryos develop a reduction and an expansion in the spatial expression patterns of *n. tubulin* and *sox3* respectively*,* along with defects in the locomotive response to touch stimuli. This project sought to investigate these effects in more detail whilst also investigating the effects on the development of the neural crest; from which neuroblastoma cancers develop.

xN3-Src

RT-PCR performed by Philip Lewis (thesis, 2014) to analyse the embryonic temporal expression pattern of *xN1-Src* revealed the expression of an additional polyadenylated *Src* splice variant with an insert between exons 3 and 4, termed *xN3-Src.* This insert includes the *xN1-Src* microexon and an additional 70 nucleotides located 5’ to the *xN1-Src* insert. The predicted protein sequence of this transcript encodes

the SH4 and unique domains and the SH3 domain amino-terminal to the xN1-Src insert followed by 22 additional amino acids, before a stop codon in the SH3 domain (Figure 1). The RT-PCR data showed that *xN3-Src* expression also increases during primary neurogenesis as primary neurons become established, peaking at stage 17, before decreasing as the neural plate rolls up.

This project sought to explore the previously unidentified spatial expression profile of this isoform using *in situ* hybridisation, as well as looking in more detail at its temporal expression profile during primary neurogenesis as well as secondary neurogenesis. This project looked to ascribe a function for this isoform using knockdown and overexpression analyses as functional analyses of this isoform had not previously been performed.

N1-Src knockout Zebrafish line

In addition to using antisense morpholino oligo-mediated neural *Src* knockdown in *Xenopus tropicalis* embryos, knockout *N1-Src* lines may offer insight into N1-Src functions. Due to their fast generation time, zebrafish are an ideal model for achieving this. To do so, CRISPR-mediated homologous recombination is a technique by which the *N1-Src* microexon could be excised, leaving the *C-Src* transcript intact.

Aims

- Establish the temporal expression profiles of *Src* variants during primary and secondary neurogenesis in *Xenopus tropicalis* and zebrafish embryos.
- Establish the spatial expression patterns of neural *Src* variants during *Xenopus tropicalis* primary neurogenesis.
- Analyse the effects of *xN1-Src* and *xN3-Src* knockdown and overexpression on embryo morphology and the expression of neural and neural crest markers.

- Generate the necessary reagents for CRISPR-mediated homologous recombination at the zebrafish *N1-Src* microexon locus.

Chapter two: Methods

Phylogenetic analyses

The vertebrate phylogenetic tree was constructed from NCBI taxonomy browser data (NCBI n.d.; Sayers et al. 2009; Benson et al. 2009), using the phyloT phylogenetic tree generator (biobyte solutions GmbH, 2014) and displayed using iTOL (version 3.0) (iTOL n.d.; Letunic & Bork 2007; Letunic & Bork 2011).

Expression of Src isoforms throughout vertebrate evolution was analysed using nucleotide and amino acid basic local alignment sequence trace (BLAST) searches, analysing expressed sequence tags, annotated and predicted sequences. Catshark transcriptome data was also analysed (John Mulley, personal communication). The NCBI Conserved Domains search tool was used to predict the amino acids to which conserved Src domains correspond (NCBI n.d.; Marchler-Bauer et al. 2014).

Embryo collection and manipulation

Xenopus embryo collection and injection

Xenopus tropicalis and *Xenopus laevis* were primed to ovulate by the injection of Human Chorionic Gonadotropin (HCG) (Winterbottom et al. 2011) by a licensed lab member, with a low dose prime the day before embryo collection and a high dose on the morning of collection.

Xenopus tropicalis testes were harvested and incubated in L15 medium with 10% Foetal Calf Serum (FCS) at 11-13°C. Testes were homogenised in this solution prior to *in vitro* fertilisation. Fertilisations were carried out on plates coated with L15/FCS solution by the application of sperm suspension. Five minutes later, embryos were flooded with Modified Ringers Solution (MRS)/9 (11.11 mM NaCl, 0.2mM KCl, 0.22 mM $CaCl_2$, 0.11mM $MgCl_2$ and 5mM Hepes/NaOH (Tindall et al. 2007)) and left to rotate. Embryos were then de-jellied using 3% L-cysteine in MRS/9 (pH 7.8-8), rinsed and incubated in MRS/9.

Xenopus laevis testes were harvested and incubated at 4°C in molecular grade water. Testes were homogenised in this solution prior to *in vitro* fertilisation. Five minutes after the application of sperm suspension, embryos were flooded in Normal Amphibian Medium (NAM)/3 (3.7mM NaCl, 0.067mM KCl, 0.033mM $Ca(NO_3)_2$, 0.033mM $MgSO_4$, 3.3μM EDTA, 5mM HEPES, pH 7.4, with 1mM $NaHCO_3$ and 25μg/ml gentamycin (Slack & Forman 1980)) and left to rotate. Embryos were then de-jellied using 3% L-cysteine hydrochloride in NAM/3 (pH7.8-8), rinsed and incubated in NAM/3.

Xenopus tropicalis and *Xenopus laevis* microinjections were carried out in 3% ficoll in MRS/9 and 5% ficoll in NAM/3 respectively using a pneumatic microinjector. Following incubation in the ficoll solutions to allow healing, *Xenopus tropicalis* and *Xenopus laevis* embryos were transferred to MRS/20 (5mM NaCl, 0.09 mM KCl, 0.1mM $CaCl_2$, 0.05mM $MgCl_2$ 5mM Hepes, with 0.1mg/ml gentamycin (Tindall et al. 2007)) and NAM/10 (1.1mM NaCl, 0.02mM KCl, 0.01mM $Ca(NO_3)_2$, 0.01mM $MgSO_4$, 1μM EDTA, 5mM HEPES, pH 7.4, with 25μg/ml gentamycin (Slack & Forman 1980)) respectively. At the relevant stages, according to the normal table of *Xenopus laevis* development (Nieuwkoop & Faber 1994), embryos were flash frozen on dry ice for RNA extraction and reverse transcription polymerase chain reaction (RT-PCR) or fixed in MEMFA (3.7% formaldehyde solution, 10% MEM salts, MEM salts: 1M MOPS, pH 7.4, 20mM EGTA, and 10mM $MgSO_4$ (Guille 1999)) for *in situ* hybridisation, following the removal of vitelline membranes.

Xenopus embryos were injected with *in vitro* synthesised mRNA for overexpression analyses and antisense morpholino oligos (AMOs) for knockdown analyses, designed by Philip Lewis and purchased from Gene Tools (Philomath OR) (Table 1). Before injection, AMOs were heated to 65°C for 10 minutes.

Table 1: Antisense morpholino oligo sequences designed by Philip Lewis to knockdown neural *Src* isoforms

Antisense morpholino oligo	Sequence
AMO A	GTCAGGTCTCCTATGGCACAGCATG
AMO D	GCCGCCGGATGGTCACATACCTCAT

Where AMO A refers to the splice acceptor-targeting AMO and AMO D refers to the splice donor-targeting AMO.

Xenopus tropicalis animal cap explants

Xenopus tropicalis embryos were injected bilaterally in the animal hemisphere as previously described at the 2-4 cell stage with 15pg *noggin* mRNA (synthesised by Hannah Brunsdon) in a final volume of 4nl. Embryos were cultured at 27°C in 3% ficoll in MRS/9 to allow healing before being transferred to MRS/20 and cultured until late blastula stages. Animal caps were then dissected using a tungsten needle in NAM and incubated at 23°C until control embryos reached stage 16/17. At this point the animal caps were flash frozen on dry ice, in addition to control animal caps dissected from water-injected or uninjected embryos. A sample of noggin-injected embryos were allowed to develop in MRS/20 to confirm that the *noggin* mRNA had exerted the expected effects.

Harvesting of *Xenopus tropicalis* adult tissues

Following the sacrifice of *Xenopus tropicalis* adult males for the harvest of testes, samples of brain, skin, muscle, heart, lung and liver were dissected and flash frozen on dry ice.

Zebrafish embryo injection and collection

Zebrafish embryos were collected and incubated at 28°C in E3 media (5mM NaCl, 0.17mM KCl, 0.33 mM $CaCl_2$ and 0.33 mM $MgSO_4$, pH6.8-6.9 (Dou et al. 2008) with $0.15x10^{-5}$% methylene blue solution to inhibit fungal growth). Embryos were injected into the yolk cell between the one cell and eight cell stage and allowed to develop at 28°C until the relevant developmental stages had been reached (according to Kimmel et al.

(1995)) at which point they were fixed in MEMFA for imaging or flash frozen on dry ice for DNA extraction.

Molecular biology methods

Gel electrophoresis

To analyse nucleic acid levels and product sizes, gel electrophoresis was used. Samples of DNA and RNA were separated on agarose gels of the specified agarose percentage in Tris-Acetate-EDTA (TAE: 40mM Tris, pH 7.6, 20mM acetic acid, 1mM EDTA (te Poele & Joel 1999) or Tris-Borate-EDTA buffer (TBE: 89mM Tris, pH 7.6, 89mM boric acid, 2mM EDTA (Meadus 2003)) at 150-200V. Gels were stained with ethidium bromide or SYBR safe and DNA sizes were predicted by running alongside the 2-log DNA ladder or low molecular weight DNA ladder (both New England BioLabs).

Nucleic acid purification

Nucleic acids were purified using phenolchloroform/chloroform extractions in which an equal volume of phenolchloroform was added, vortexed for one minute and microcentrifuged for five minutes. The aqueous phase was removed and placed in a fresh tube. An equal volume of chloroform was then added, vortexed for one minute and microcentrifuged for five minutes. The aqueous phase was removed and placed in a fresh tube.

After phenolchloroform/chloroform extraction, the nucleic acids were precipitated using by adding an equal volume of propan-2-ol (Electran) or one-tenth of the volume of 3M sodium acetate (NaOAc) and two volumes of 100% ice-cold ethanol. The method used for each of the nucleic acid precipitations are stated. In both protocols, the solutions were vortexed for one minute and then stored at -20°C overnight. Tubes were then microcentrifuged for 15 minutes and the supernatant removed. Pellets were washed with 1ml ice-cold 70% ethanol by vortexing for one minute and microcentrifuging for five minutes. The supernatant was removed and

the pellet was dried using a desiccator before being resuspended in the volume of molecular grade water indicated.

RNA extraction for semi-quantitative PCR

To extract RNA, flash-frozen embryos were homogenised by pipetting in 1ml Tri Reagent whilst adult tissue samples were homogenised in 1ml Tri Reagent using a glass tissue homogeniser. Both were then microcentrifuged for 10 minutes. The supernatant was removed, placed in a fresh tube and allowed to stand at room temperature for five minutes. Nucleic acid extraction then proceeded as described, with the adaptations described below. 200µl chloroform was added to the homogenised sample in Tri reagent, vortexed for one minute and left to stand at room temperature for five minutes, before being microcentrifuged for 15 minutes. The aqueous phase was removed and an additional chloroform purification step was performed as described previously. The aqueous phase was transferred to a fresh tube, to which 500µl propan-2-ol (Electran) was added and was placed at -20°C for 30 minutes. Tubes were microcentrifuged for 15 minutes. The supernatant was disposed of and the pellet was washed with ice-cold 70% ethanol by vortexing for one minute and microcentrifuging for five minutes. The supernatant was removed and the pellets dried in a desiccator for 5-10 minutes. Pellets were resuspended in 50µl water and 60µl 7.5M LiCl/50mM EDTA by vortexing for one minute and heating at 80°C for one minute before being stored at -80°C for at least 48 hours. After this time, solutions were microcentrifuged for 30 minutes and the supernatants discarded. Pellets were washed twice in 1ml ice-cold 70% ethanol by vortexing for one minute and then microcentrifuging for five minutes. Pellets were dried using a desiccator for 5-10 minutes and resuspended in 30µl water by heating for one minute at 80°C before vortexing for one minute. RNA concentrations were determined by use of the nanodrop.

cDNA first strand synthesis

To synthesise complementary DNA (cDNA) 1µl primer (Oligo dT or random hexamers), RNA (3µg for *Xenopus tropicalis* embryo stage series, 1µg for adult tissue and animal cap explants and 0.63µg for

zebrafish embryos), 1µl 10mM dNTPs and water up to a total volume of 12µl were mixed by gentle pipetting in a sterile PCR tube in the specified order. Tubes were incubated at 65°C for five minutes before being chilled on ice for two minutes. Tubes were then spun briefly to collect condensation. 4µl first strand buffer, 0.1M DTT and 1.0µl water were added to each tube and incubated at 42°C for two minutes. 1µl Superscript II (200 units) was added to each tube with water controls used to demonstrate the absence of genomic DNA contamination. Tubes were then incubated for an hour at 42°C before a 15 minute incubation at 72°C to inactivate the reverse transcriptase.

Table 2: Primers used to amplify *Xenopus tropicalis* cDNA and plasmid sequencing

Primer	**Sequence (5'➔3')**	**Annealing temperature (°C)**
Pan-Src forward (Philip Lewis)	ATCTCGCACCGAGACAGACT	55.5
Pan-Src reverse (Philip Lewis)	ACTGAGTGCGAGACGTGATG	55.5
N-Src forward (Philip Lewis)	ACTGTGACCTGACGCCTTTT	55.5
N-Src reverse (Philip Lewis)	CTTCCCTCATGTCAGGTCTC	55.5
C-Src specific reverse	CAGTCGCCTTCCGTGTTATT	55.5
N1-Src specific reverse	CCTCATGTCAGGTCTCGTGTT	55.5
N3-Src specific reverse	CACAGCATGTGAGGGAAAGA	55.5
L8 forward	GGGCTGTCGACTTCGCTGAA	55.5
L8 reverse	ATACGACCACCACCAGCAAC	55.5
Full length N3-Src Forward	TCTCCCGATATCTCAGGCA	54.5
Full length N3-Src Reverse	CTATGGCACAGCATGTGAGG	54.5
N3-Src+XbaI	GAGAGATCTAGACTATGGCACAGCATGTGAGG	57.6
N3-Src+BamHI	GAGAGAGGATCCATGGGTGCCACTAAAAGCAA	57.6
xN1-Src sequencing 1	GCGTCTGCTGCTGAGCCTTG	N/A
xN1-Src sequencing 2	CCACGTAGGCCATGCCTGAA	N/A
Phox2a Forward	GAGAGCGGCCAACTCTAAGA	51.1
Phox2a Reverse	TTAGAACAAATTTGCCTTCA	51.1

Semi-quantitative RT-PCR to analyse *Src* expression levels

PCR primers shown in Tables 2 and 3 for *Xenopus* and zebrafish respectively were used to amplify cDNA from embryos, adult tissues and animal cap explants, with L8 used as a housekeeping gene for *Xenopus tropicalis* and *EF1α* for zebrafish samples (*EF1α* sequences were used according to Tang et al. (2007)). The *N-Src* primers that amplify *xN1-Src* and *xN3-Src*, Pan-*Src* primers that amplify *C-Src, xN1-Src,* and *xN3-Src* and primers amplifying the housekeeping gene L8 were designed by Philip Lewis. For the PCR reaction, 8.5µl water, 1.0µl cDNA, 1.5µl forward primer (10µM), 1.5µl reverse primer (10µM) and 12.5µl 2X Promega PCR master mix were assembled and mixed by vortexing. The PCR programme used was as follows; 3 minutes at 95°C, 30 cycles of 30 seconds at 95°C, 30 seconds at the annealing temperature (specified in Table 2 or 3) and 50 seconds at 72°C before a final extension of 15 minutes at 72°C, with the annealing temperatures optimised for maximum amplification efficiency and specificity.

Table 3: Primers used to amplify zebrafish cDNA and genomic DNA

Primer	**Sequence (5'➔3')**	**Annealing temperature (°C)**
Pan-Src Forward	GCGCGGCACACAGCCCA	55
C-Src specific reverse	CCACCAGTCACCCTCCGTGT	55
N1-Src specific reverse	CCTGGGGTTCAACTTTCTCG	55
EF1α forward	CTGGAGGCCAGCTCAAACAT	55
EF1α reverse	ATCAAGAAGAGTAGTACCGCTAGCATTAC	55
N1-Src sgRNA forward	GCAGCTAATACGACTCACTATAG**GTAGGAGAAAGTTGAACCCCGTTTTAGAGC**TAGAAATA	60
Tyrosinase sgRNA forward	GCAGCTAATACGACTCACTATA**GGAGAGACGAGCTGAAGAGCGTTTTAGAGC**TAGAAATA	Synthesised by Elliot Jokl
sgRNA reverse	AAAAGCACCGACTCGGGCCACTTTTTCAAGTTGATAACGGACTAGCCTTATTTTAACTTGCTATTTCTAGCTCTAAAAC	-
CRISPR screening primer forward	GAAGCTTCTGCTGTTTGCTC	52
CRISPR screening primer reverse	CAGGTGGACAAGCAAATGGTG	52

The RT-PCR products were separated by gel electrophoresis on a 2% agarose gel as previously described. Control samples included cDNA synthesised in the absence of reverse transcriptase to check for genomic DNA contamination and primer-only controls to check for primer contamination. Time course RT-PCRs were analysed for expression levels using ImageJ.

Plasmid amplification

To amplify plasmids, including those containing *in situ* hybridisation probes and *xN1-Src* and *xN3-Src* sequences for over-expression analyses, 40µl DH5α competent bacterial cells were thawed on ice before being added to 1µl plasmid and left on ice for 30 minutes. The cells were then heat shocked at 42°C for 90 seconds. Tubes were then transferred back to ice for 2 minutes and 1ml LB culture medium was added. Tubes were incubated in a 37°C shaking incubator for one hour. 20µl and 200µl solution was each plated onto LB/Agar plates containing 100µg/ml ampicillin, and incubated overnight at 37°C. Single colonies were selected for overnight culture and added to 3ml LB medium containing 100µg/ml ampicillin. Amplified plasmids were isolated using the QIAprep Spin Miniprep Kit (Qiagen) using a microcentrifuge according to the manufacturer's instructions.

Plasmid sequencing was performed by the Technology Facility Genomics Laboratory at the University of York.

Plasmid digestion

Plasmids were digested at 37°C using the relevant restriction enzyme (Roche) and the appropriate volume of the 10x enzyme buffer. Buffers were selected that yield the highest digestion efficiency, according to the manufacturer (Table 4). The total volume was made up using molecular grade water.

Table 4: SuRE/Cut buffers used for restriction digests

Restriction enzyme	SuRE/Cut buffer used
EcoRI	H
XbaI	A
BamHI	A
NotI	H
ApaI	A
SmaI	H
NcoI	H
ClaI	H

xN3-Src cloning

The *xN3-Src* open reading frame was amplified from random hexamer-primed stage 15 cDNA using Phusion polymerase (New England Biolabs); 31.5µl molecular grade water, 10µl 5x high fidelity buffer, 1µl dNTPs (10mM), 2.5µl forward primer (10µM), 2.5µl reverse primer (10µM), 2µl cDNA and 0.5µl Phusion polymerase were assembled and mixed and the following PCR programme was used; 30 seconds at 95°C, 35 cycles of 10 seconds at 95°C, 30 seconds at 54.5°C and 30 seconds at 72°C before a final extension at 72°C for 10 minutes. After the 72°C final extension, 1µl Taq polymerase was added and the PCR reaction was maintained at 72°C for a further 15 minutes. Successful amplification was confirmed by gel electrophoresis and the PCR product was cloned into the T-Easy plasmid; 5µl 2x T-Easy ligation buffer, 1µl T-Easy vector, 2µl PCR product, 1µl T4 DNA ligase and 1µl molecular grade water were mixed and incubated at 4°C overnight.

The ligation reaction was then transformed into DH5α cells and plated out as previously described. DH5α colonies were screened for the plasmid containing the *xN3-Src* insert using colony PCR; colonies were selected by pipetting in 2µl molecular grade water. A replica plate was created by streaking the solution over the surface, with the colony solution then added to a PCR tube with 1µl forward primer (10µM) and 1µl reverse primer (10µM), 1µl molecular grade water and 5µl 2x Promega PCR

master mix. Primers were used to amplify the region between the T7 and SP6 promoters. The following PCR programme was used; two minutes at 95°C, 25 cycles of 30 seconds at 95°C, 30 seconds at 50°C and 60 seconds at 72°C before a final extension of 15 minutes at 72°C. The presence or absence of the insert was confirmed by gel electrophoresis on a 2% agarose gel as described. Clones showing an insert of the correct size were amplified by overnight culture and purified using the QIAprep Spin Miniprep Kit as described. 3µl of each of the plasmids screened was digested using 2µl EcoRI in a total volume of 20µl to confirm the presence of the insert following amplification, as described previously. Uncut plasmid and cut plasmid were run on a 1% agarose gel to confirm that the insert of the correct size was present.

xN3-Src was amplified using Phusion polymerase from *xN3-Src*-T-Easy with primers containing XbaI and BamHI restriction sites (Table 2); 10µl 5x high fidelity buffer, 1µl dNTPs (10µM), 2.5µl N3-Src XbaI primer (10µM), 2.5µl N3-Src BamHI primer (10µM), 2µl *xN3-Src*-T-Easy (0.5ng/µl), 0.5µl Phusion polymerase and molecular grade water (up to 50µl final volume) were assembled and the following PCR programme was used; 30 seconds at 95°C, 30 cycles of 10 seconds at 95°C, 30 seconds at 57.6°C and 30 seconds at 72°C before a final extension of 10 minutes at 72°C. Successful amplification and subsequent purification using the QIAquick PCR purification kit (used according to the manufacturers instructions) were confirmed by gel electrophoresis on a 1.5% agarose gel, as previously described.

20µl PCR product was digested to completion using 2µl BamHI and XbaI in a total volume of 50µl. 4µg pCS2+ plasmid was also digested as described previously using 1.5µl XbaI and 1.5µl BamHI singularly (to confirm that both enzymes are able to digest the plasmid) and in combination in a total volume of 50µl. Both reactions were incubated for 3-4 hours.

Digestion was confirmed by gel electrophoresis; undigested pCS2+ was run alongside pCS2+ digested with XbaI and/or BamHI on a 1% agarose gel. The doubly digested products were extracted using the QIAquick gel extraction kit (Qiagen), according to the manufacturer's instructions. The digested and purified *xN3-Src* and pCS2+ products were ligated; 10µl 2x ligation buffer, 3µl pCS2+, 3µl *xN3-Src*, 2µl T4 DNA ligase and 2µl molecular grade water were assembled and incubated at 4°C overnight. The ligation products were transformed into DH5α as described previously. Colonies positive for the *xN3-Src* insert were identified using colony PCR, as previously described, using primers to amplify the region between the SP6 and T3 promoters. Colonies positive for the insert were amplified using overnight culture and purified using the QIAprep Spin Miniprep Kit. To confirm that the insert was present, 2µl of each isolated clone was digested for at least two hours in a total volume of 20µl using 1µl XbaI and 1µl BamHI and run alongside undigested plasmid on a 1% agarose gel. Colonies containing the insert were then sequenced from both the T7 and SP6 promoters.

***In vitro* transcription of synthetic messenger RNA for microinjection**

xN1-Src was cloned into pCS2+ by Philip Lewis. This plasmid was sequenced from the T7 and SP6 promoters and using additional sequencing primers shown in Table 2 to confirm that the expected sequence was present. *xN1-Src*-pCS2+ and *xN3-Src*-pCS2+ plasmids were linearised by restriction digest using the Not1 restriction enzyme (Table 5); 3µg plasmid was digested for 90 minutes by 3µl Not1 in a total reaction volume of 50µl. Plasmid digestion was confirmed by gel electrophoresis on a 1% agarose gel. Once digestion to completion had been confirmed, the volume of plasmid was brought up to 200µl with water and was purified using a phenolchloroform/chloroform extraction and then sodium acetate/ethanol precipitation as described previously and resuspended in 20µl water. The presence of purified and digested plasmid was confirmed by gel electrophoresis on a 1% agarose gel.

mRNA was synthesised by *in vitro* transcription using the Megascript SP6 Transcription Kit (Ambion). At room temperature, the following components were assembled; 4.5µl RNase-free water, 2µl ATP (50mM), 2µl CTP (50mM), 2µl UTP (50mM), 2µl GTP (5mM), 2.5µl mGTP (cap, 40mM), 2µl transcription buffer, 5µl linearised plasmid and 2µl SP6 enzyme. After gentle mixing, the reaction was incubated at 37°C for four hours, after which the presence of mRNA was confirmed by gel electrophoresis on a 2% agarose gel. Once transcription had been confirmed, 1µl DNase I was added and the solution was incubated at 37°C for 15 minutes to remove the DNA template. To stop the reaction, 115µl water and 15µl ammonium acetate were added. The mRNA was extracted using a phenolchloroform/chloroform extraction and propan-2-ol precipitation as described previously and resuspended in 20µl water. mRNA concentration was measured using Nanodrop.

Generating a *phox2a* probe for *in situ* hybridisation

To synthesise an *in situ* hybridisation probe for detection of the neural crest marker phox2a, non-homeobox *phox2a* sequence was amplified by PCR and cloned. 8.5µl water, 1.0µl stage 25 cDNA, 1.5µl forward primer (10µM), 1.5µl reverse primer (10µM, primers both shown in Table 2) and 12.5µl 2x Promega PCR master mix were assembled and the following PCR programme was used; five minutes at 95°C, 35 cycles of 30 seconds at 95°C, 30 seconds at 51.1°C and 45 seconds at 72°C before a final extension of 15 minutes at 72°C. Amplification of the correct product size was confirmed by gel electrophoresis on a 1.5% agarose gel. The PCR product was purified using the QIAquick PCR purification kit (Qiagen) according to the manufacturer's instructions. The purified product was ligated to the T-Easy plasmid, transformed into DH5α cells and plated out as described previously. The colonies were screened for the *phox2a* insert using colony PCR, as described previously. Primers used to amplify this region of *phox2a* were used to screen for the insert. Clones with an insert of the expected size were sequenced to determine

the polymerase and restriction enzyme necessary to generate an antisense transcript for use in *in situ* hybridisation (Table 5).

Synthesis of probes for standard *in situ* hybridisation

To generate a template for *in situ* hybridisation probe synthesis, 2.5µg of each plasmid was linearised by digestion for 90 minutes using 3µl of the relevant restriction enzyme (Table 5**)** in a total volume of 100µl. Complete digestion was verified by gel electrophoresis - digested plasmid was run alongside undigested digested plasmid on a 0.8% agarose gel. Digested plasmid was purified by phenolchloroform/chloroform extraction and sodium acetate/ethanol precipitation as previously described. The linearised plasmid was then resuspended in 5µl water. Digested plasmid purification was confirmed by gel electrophoresis on a 0.8% agarose gel.

To synthesise the DIG-labelled RNA probes, the following components were assembled at room temperature and allowed to react for two hours at 37°C; 10µl 10x transcription buffer, 2.5µl 10x DIG NTP mix, 5µl 100mM dithiothreitol (DDT), 2µl RNasin (50 units), 2µl appropriate polymerase (150 units), 2.5µl linearised plasmid and 26µl water. After two hours, an additional 2µl polymerase (50 units) was added and incubated for a further two hours at 37°C. Transcription was confirmed by gel electrophoresis on a 2% agarose gel. Upon confirmation of transcription having taken place, 1µl RN-ase-free DNase I was added and the reaction was incubated for 20 minutes at 37°C to remove the DNA template. To confirm that the DNA template had been destroyed whilst the RNA probe had not, a sample of the probe solution was run on a 2% agarose gel. To stop the reaction and precipitate the probe, 50µl water, 25µl 10M Ammonium Acetate and 312.5µl 100% ice-cold ethanol were added and the solution was stored at -80°C for 45 minutes, before being microcentrifuged for 15 minutes. The supernatant was then removed and replaced with 100µl ice-cold 70% ethanol, which was vortexed for one minute and microcentrifuged for five minutes. The probe was then resuspended in 50µl water and stored at -80°C. For *in situ* hybridisation

reactions, the amount of probe necessary was estimated by gel electrophoresis on a 2% agarose gel, as described.

Table 5: Plasmids used to synthesise *in situ* hybridisation probes and mRNA

Insert	Vector	Restriction enzyme used	Polymerase for sense RNA	Polymerase for antisense RNA	Plasmid source
N. tubulin (beta II)	pGEM-5Zf(-)	ApaI	-	SP6+hydrolysis	Harland lab
Sox3	pBSK(+)	SmaI	-	T7	Grainger lab
Phox2a	pGEM T-Easy	NcoI	-	SP6	Own
xN1-Src	pCS2+	NotI	SP6	-	Philip Lewis
xN3-Src	pCS2+	NotI	SP6	-	Own

Due to its long length, the *n. tubulin* probe was hydrolysed to enable embryo penetration. 25µl probe was incubated at 60°C for 12.5 minutes in hydrolysis solution (80mM $NaHCO_3$ and 120mM Na_2CO_3 (Silva et al. 2006)). The incubation time was calculated according to Willars & Challiss (2004) using the equation below. Following hydrolysis, 50µl 5M ammonium acetate (NH_4OAc) and 312.5µl 100% ethanol were added to precipitate the probe and the solution was incubated overnight at -80°C. The solution was then microcentrifuged for 15 minutes. The supernatant was then removed and the pellet was washed with 70% ethanol and dried as previously described. The probe was resuspended in 25µl water and gel electrophoresis on a 2% gel was used to confirm that the probe had successfully been purified.

$$t = \frac{(\text{starting length, kb}) - (\text{desired length, kb})}{0.11(\text{starting length, kb} \times \text{desired length, kb})}$$

Where t = time, the starting length for this probe was 1.6kb and the desired length was 0.5kb

In situ hybridisation

The *in situ* hybridisation protocol was carried out as described by Harland (1991) with modifications, as described by Guiral et al. (2010) and set out

below. Embryos were prepared for *in situ* hybridisation by removal of the embryo vitteline membrane using forceps. They were then fixed by rolling for one hour in glass scintillation vials containing 10-20ml MEMFA. The MEMFA was then replaced with 100% methanol and rolled for a further five minutes to dehydrate the embryos. This was then replaced with fresh methanol, rolled for a further five minutes and stored at -20°C.

Embryos were brought to room temperature in 100% methanol and then rehydrated by washing on a roller once for 10 minutes in 75% methanol/PBSAT (PBSAT: 8mM Na2HPO4, 150mM NaCl, 2mM KH2PO4, 3mM KCl, pH7.4 and 0.1% Tween (Fehr et al. 2007)), once for 10 minutes in 50% methanol/PBSAT and a further three times for five minutes in PBSAT. Embryos were then permeabilised by treating with 10µg/ml proteinase K at room temperature with gentle stirring. Stage 14-17 embryos were treated with proteinase K for 9 minutes, stage 21 embryos for 10 minutes, stage 24-25 embryos for 11 minutes and embryos of stage 27 and above for 12 minutes. Embryos were then rinsed twice with 5ml 0.1M triethanolamine (pH 7.8) for five minutes to reduce background staining. To the second triethanolamine wash, 12.5µl acetic anhydride was added and swirled often as they mix poorly. After five minutes, a further 12.5µl acetic anhydride was added for five additional minutes. Embryos were then washed twice with PBSAT for five minutes and then refixed for 20 minutes with 10% formalin/PBSAT on the roller. They were then washed five times for five minutes with PBSAT. Embryos were transferred in 1ml PBSAT into Eppendorf tubes containing 250µl hybridisation buffer (50% formamide, 5x SSC (pH 7), 100µg/ml heparin, 1x Denhart's, 0.1% Tween, 0.1% CHAPS, 10mM EDTA), which was then replaced with 1ml fresh hybridisation buffer heated to 60°C. The hybridisation buffer was then replaced with 1ml fresh hybridisation buffer containing 1mg/ml total yeast RNA and embryos were prehybridised for two hours on a horizontal rocker at 60°C, to further reduce non-specific probe binding. DIG-labelled probes were heated to 80°C for three minutes to denature secondary structures before being added to fresh hybridisation buffer containing total yeast RNA at 60°C. 2-4µl probe was

added according to the gel electrophoresis band intensity. Embryos were incubated in this solution at 60°C overnight in the horizontal rocker.

The following day, embryos were washed twice with 1ml hybridisation buffer for 10 minutes at 60°C on the horizontal rocker. Embryos were then subjected to a series of washes to increase binding stringency, during which solutions were preheated to 60°C and embryos were rocked at 60°C. Embryos were maintained on a hot block at 60°C whilst solutions were changed. Embryos were washed three times for 20 minutes in 2x SSC with 0.1% Tween and then three times for 30 minutes in 0.2x SSC with 0.1% Tween. They were then washed twice for 15 minutes at room temperature in Maleic acid buffer (MAB; 100mM maleic acid, 150mM NaCl, pH 7.8 (Jevtić & Levy 2015)) with 0.1% Tween on the horizontal rocker. This was then replaced with MAB with 2% Boehringer Mannheim Blocking reagent (BMB) and rocked at room temperature for 30 minutes. Embryos were then pre-incubated for two hours at room temperature in 1.5ml MAB with 2% BMB and 20% heat treated lamb serum (lamb serum had previously been heat treated at 60°C for 30 minutes) to prevent non-specific binding of the anti-digoxygenin antibody. This solution was then replaced with fresh solution of MAB, BMB and lamb serum, containing 1/2000 dilution of affinity purified sheep anti-digoxygenin antibody coupled to alkaline phosphatase and rocked overnight at 4°C.

Following the second 2x SSC wash, embryos probed for *n. tubulin* were treated for 30 minutes at 37°C with 1ml 2x SSC supplemented with 20µg/ml RNase A to remove non-specifically bound probe and reduce background staining. Embryos were then washed with 2x SSC for 10 minutes at room temperature followed by three 30 minute washes in 0.2x SSC at 37°C. The protocol then continued as per the other probes.

The antibody was removed the following day and embryos were washed by rocking in MAB with 0.1% Tween three times for five minutes at room temperature. Embryos were then returned to large scintillation vials containing MAB with 0.1% Tween and washed by rocking at room

temperature three times for one hour. Embryos were then washed once for three minutes and then once for 10 minutes in Alkaline Phosphastase buffer (AP buffer; 100mM Trizma, 50mM $MgCl_2$, 100mM NaCl at pH 9.5). This was then replaced with 1ml BM purple precipitating solution (the alkaline phosphatase substrate) (Roche), and left undisturbed until staining had developed. Once staining had developed, embryos were washed twice in PBSAT for 15 minutes and re-fixed by rocking in 10% formalin overnight at room temperature and stored in the formalin solution.

To remove embryo pigmentation, embryos were washed in PBSAT and then bleached in 5% H2O2 in PBSAT by rolling under a lamp. Once pigmentation was no longer present, embryos were washed with PBST and re-fixed and stored in 10% formalin in PBSAT.

Locked nucleic acid probe *in situ* hybridisation protocol

To detect the *xN1-Src* and *xN3-Src* microexons, 19 nucleotide-long probes were designed, incorporating *xN1-Src* and *xN3-Src* reverse compliment sequences (Table 6). BLAST searches were used to confirm that no off-target sequence homologies of more than 14 nucleotides exist and Locked nucleic acids (LNAs) were incorporated at every third position, according to Darnell et al. (2010) and DIG-labelled at the 5' and 3' ends. LNA probes were purchased from and synthesised by Exiqon.

The LNA *in situ* hybridisation was carried out as per the traditional technique, with some alterations based on Sweetman (2011), with additional modifications detailed below. The hybridisation temperature was calculated using the Exiqon melting temperature calculator (Exiqon n.d.) minus 22°C, according to Darnell et al. (2010). This temperature was used for pre-hybridisation, hybridisation and subsequent SSC washes. The hybridisation time was extended to two overnight incubations in the presence of the same probe, which was retained and stored at -80°C for future use. Embryos were rocked in MAB, 2% BMB

and 20% heated lamb serum for three hours before incubation with the antibody and washed six times for one hour and then overnight in MAB with 0.1% Tween following antibody incubation. Initial incubation in BM purple was carried out until diffuse purple staining was present, at which point embryos were washed twice for ten minutes and then overnight in 4x MAB with 0.1% Tween. The BM purple solution was then replaced and the process repeated until specific staining developed. At this point, embryos were re-fixed in 10% Formalin/PBSAT overnight and stored in this solution. Embryos were then bleached as described previously and rolled in 100% methanol to reduce background staining, rinsed with PBST and re-fixed.

Table 6: LNA probe sequences for *in situ* hybridisation

Probe	Probe sequence (5'→3') (+ represents LNA)	Hybridisation temperature (°C)
xN1-Src	+TCC+CTC+ATG+TCA+GGT+CTC+G	57
xN3-Src	+AGA+ACG+TGA+GAG+GTC+ACA+C	49

sgRNA synthesis and microinjection into zebrafish embryos

sgRNA DNA templates were synthesised by PCR using partially overlapping primers and Phusion polymerase. Primers were designed according to Nakayama et al. (2014) to target the zebrafish *N1-Src* microexon and the zebrafish *tyrisonase* gene (the latter was designed by Elliot Jokl). These primers are shown in Table 3 and the gene-targeting sequences present on the forward primer are highlighted in bold. A common reverse primer was used for the syntheses of both templates. 10µl 10X high fidelity buffer, 1µl dNTPs (10mM), 5µl forward primer and 6.5µl reverse primer (both at 0.2mg/ml), 27µl molecular grade water and 0.5µl Phusion polymerase were mixed and PCR was carried out using the following programme; 98°C for 10 seconds, 35 cycles of 98°C for 10 seconds, 60°C for 30 seconds and 72°C for 15 seconds and then 72°C 10 minutes, followed by a 4°C hold. Template synthesis was confirmed by gel electrophoresis on a 2% agarose gel. *In vitro* transcription was performed using the MEGAshortscript kit (Ambion) according to the

manufacturer's instructions with non-purified 4µl DNA template. The reaction was incubated at 37°C for four hours. Once transcription was confirmed as successful by gel electrophoresis on a 2% agarose gel, 1µl DNase was added to remove the DNA template and the reaction was incubated at 37°C for 15 minutes. 15µl ammonium acetate and 115µl water were then added and the sgRNA was purified using phenolchloroform/chloroform extraction and propan-2-ol precipitation as described previously. The pellet was washed with 120µl ice-cold 70% ethanol by vortexing for one minute and microcentrifuging for five minutes. The supernatant was removed and the pellet was dried using a desiccator. The sgRNA was resuspended in 20µl molecular grade water by vortexing for one minute, heating to 80°C for one minute and then vortexing for a further minute. sgRNA purification was confirmed by gel electrophoresis on a 2% agarose gel and the concentration was measured using Nanodrop.

600pg tyrosinase sgRNA was injected into wild type zebrafish embryos alongside 1ng recombinant Cas9 protein (made by Olga Moroz, York Structural Biology Laboratory, using the plasmid and methods described in Gagon *et al.* (2014)). 600pg N1-Src sgRNA was injected alongside 1ng Cas9 protein and 100pg ssDNA oligo to guide homologous recombination (5'TCACGTCTCCTCTGTGTTTTTCCTCTACACGCTCTCGCTCGTTTAT GTAGGTTGGTAAAGTTGCTCTTGCTTTCAGCTTCTGATGAGTGTTTAT GTATGT3'), in a final volume of 3nl per embryo.

Zebrafish genomic DNA extraction and PCR genetic screen of CRISPR-targeted embryos

Zebrafish genomic DNA was extracted from targeted embryos (injected with ssDNA, sgRNA and Cas9 protein) and untargeted embryos (injected with Cas9 protein only). Single embryos were flash frozen in PCR tubes on dry ice five days post fertilisation (dpf). Prior to DNA extraction, embryos were thawed on ice. To each embryo, 200µl Tad lysis buffer was added (50mM Tris pH7, 50mM NaCl, 5mM EDTA, 0.5% SDS, 10%

Chelex and 250µg/ml Poteinase K) and incubated at 55°C for 60 minutes, 95°C for 15 minutes followed by a 4°C hold, using a PCR machine. Embryos were then vortexed and microcentrifuged for 10 minutes and the supernatant containing the genomic DNA was removed and placed in a fresh tube.

The targeted locus was amplified using PCR primers designed to amplify the region surrounding the *N1-Src* microexon (Table 3) and the following PCR programme; 95°C for 2 minutes, 30 cycles of 95°C for 30 seconds, 50°C for 30 seconds and 72°C for 30 seconds, followed by 72°C for 10 minutes and a 4°C hold. 10µl PCR product was run with 1µl 6x loading buffer on a 5% acrylamide gel (3.3ml 30% polyacrylamide, 2ml 10X TBE, 100µl APS, 30µl TEMED, 14.5ml water), alongside 5µl low molecular weight ladder. The gel was stained for 20 minutes in ethidium bromide.

Embryo imaging and ImageJ analyses

Images of embryo phenotypes and *in situ* hybridisations were taken using a LeicaMZ FLIII microscope and processed using SPOT Advanced Software and Photoshop (Adobe). Expression domains identified using *in situ* hybridisation were measured using ImageJ. Videos of locomotive phenotypes in response to touch stimuli were taken using a JVC TK-C1381 camera and processed with ArcSoft ShowBiz software. Videos of embryos responding to a touch stimulus were analysed for their behaviour and cropped to the point of contact and 0.15 seconds later. Stills from these two time points were overlaid and analysed for the distance between the centre of the right eye at these two time points using ImageJ. ImageJ was also used to semi-quantitatively analyse temporal expression profiles by densitometry. For each time point, the densitometry value was normalised to the value of the loading control; either *L8 or EF1α.*

Chapter 3: Results

3.1 Phylogenetic analysis of neural *Src* splice variants

3.1.1 Introduction

In order to understand the function of neural *Src* isoforms, it is essential to consider their evolutionary origins, as the context of their emergence may offer insight into their functions. To do so, the expression of neural-*Src* isoforms in vertebrate evolution was examined by performing basic local alignment sequence trace (BLAST) searches of available expressed sequence tags, annotated and predicted sequences on NCBI and of tissue-specific RNA-Sequencing (RNA-Seq) transcriptome Catshark data (John Mulley, personal communication).

3.1.2 Results

Figure 5 shows the expression of *N1-Src, N2-Src* and *N3-Src* across vertebrate evolution mapped onto the phylogenetic tree constructed from NCBI taxonomy browser data. The expression of *N1-Src* was detected in the *Vertebrata* subphylum of the *Chordata* phylum in species from the primitive cartilaginous fish, the Catshark, *Scyliorhinidae* to higher vertebrates including humans and *Xenopus* species. The expression of the *N1-Src* isoform was also detected in the ray-finned fish; in the subclass of *Actinopterygii* known as the *Neopterygians*, in both the *Holostei* infraclass (in in the spotted gar (*Lepisosteus oculatus*)) and the *Teleostei* infraclass (in the Tonguefish (*Cynoglossus* semilaevis) and the zebrafish (*Danio rerio*)). Whilst the expression of *N1-Src* was not detected in the *Coelacanthidae* (Coelacanths), *Dipnoi* (Lungfish), *Polypteriformes* (Bichirs and Reedfish), *Acipenseriformes* (Paddlefish and Sturgeons) or the *Amiidae* (Bowfins), this may reflect the insufficient sensitivity of the transcriptome data, rather than the absence of *N1-Src* expression across these phylogenies. This may also explain why we are unable to identify *N1-Src* in the more primitive vertebrates; the jawless fish (Lampreys and Hagfish). Conversely, it may be that the evolutionary emergence of this

isoform coincided which the evolution of the jaw, which gave rise to the *Chondrichthyes* - the sharks and rays.

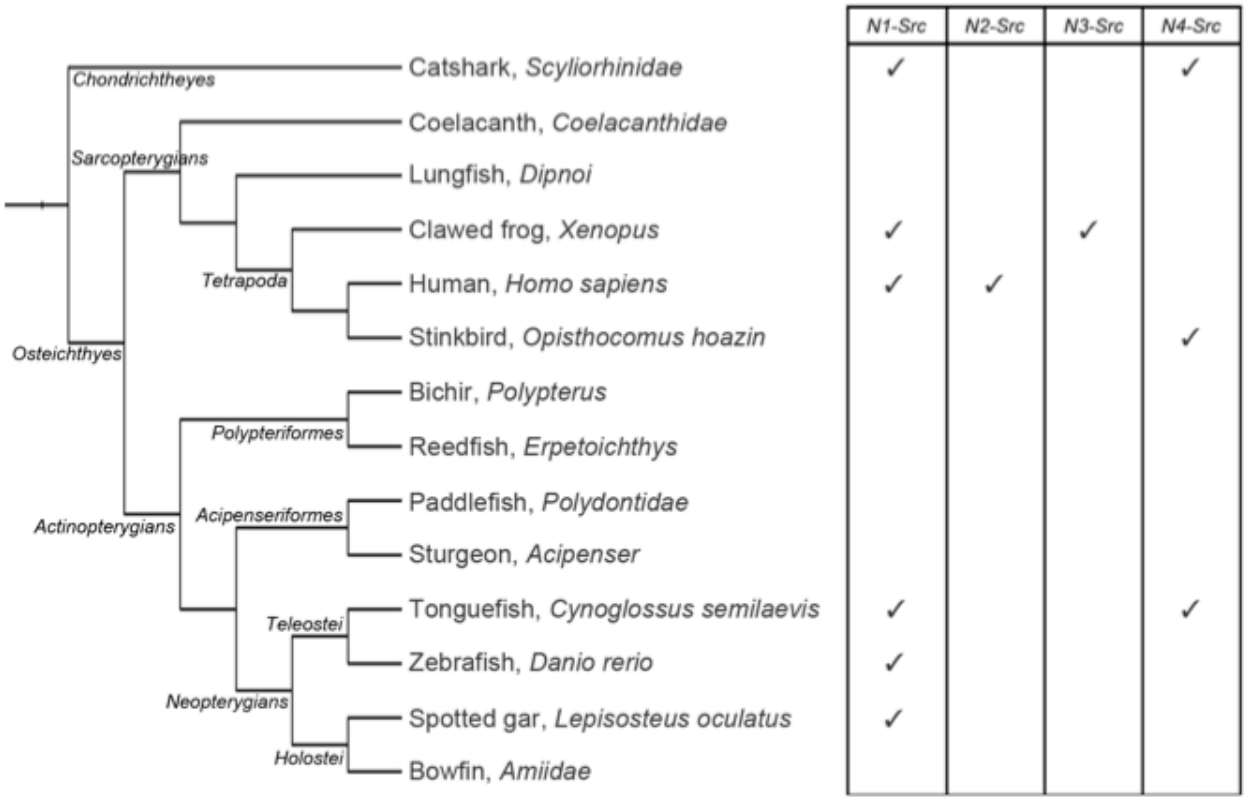

Figure 5: The expression of neural *Src* isoforms in the *Vertebrata* subphylum of *Chordata.* Ticks indicate detected expression of the relevant isoform.

Figure 6 shows the amino acids encoded by the *N1-Src* microexons detected in the species shown in Figure 5**.** At both the N and C termini of the insert in all species analysed there are conserved positively charged arginine residues. Additionally, at the second position (in organisms with a five amino acid long insert) or the third position (in organisms with a six amino acid long insert) there is a non-polar hydrophobic residue. In the

Catshark, *Scyliorhinidae*	VNNT R - L DGR EGDW
Xenopus tropicalis	VNNT R - PDMR EGDW
Xenopus laevis	VNNT R - PD I R EGDW
	VNNT R - PDMR EGDW
Human, *Homo sapiens*	VNNT RKVDVR EGDW
Tonguefish, *Cynoglossus semilaevis*	VNNT RKVNCR EGDW
Zebrafish, *Danio rerio*	VNNT RKLNPR EGDW
Spotted gar, *Lepisosteus oculatus*	VNNT RKLNCR EGDW

Figure 6: The N1-Src insert sequences detected in the species shown in Figure 5. Highlighted in grey are the amino acids present in the N1-Src protein that are flanked by amino acids found also in the C-Src protein.

most ancient vertebrate in which the insert was detected, the Catshark, the insert is five amino acids long, whereas the insert is six amino acids long in species of the *Neopterygian* subclass and the evolutionarily modern *Tetrapoda* species, the *Homo sapiens*. Surprisingly, in *Xenopus laevis* and *Xenopus tropicalis, a* more evolutionary ancient species of the *Tetrapoda* superclass, the microexon encodes only five amino acids. This amino acid discrepancy is likely to be the second position lysine, as the characteristics of the surrounding amino acids are more highly conserved.

Whilst the expression of *N1-Src* appears to be widespread across the *Vertebrata* subphylum, detection of the *N2-Src* isoform is restricted to mammals. Equally, the *xN3-Src* variant has only been detected in *Xenopus tropicalis.*

Figure 7: The predicted protein sequence of the Catshark N4-Src variant with the conserved protein domains predicted using NCBI Conserved Domain Search. The SH3 (amino acids 91-123), SH2 (amino acids 122-218) and kinase domains (245-391) are shown in yellow, red and blue respectively. The asterisk indicates the site at which the region of the C-Src SH3 domain is missing.

A BLAST search of Catshark tissue-specific RNA-Seq data revealed the expression of *N1-Src* in this ancient vertebrate and surprisingly the expression of an additional *Src* variant, which was termed '*N4-Src'*. The predicted protein sequence of this isoform, shown in Figure 7 encodes

the unique, SH2 and kinase domains of the *C-Src* and *N-Src* variants (predicted using an NCBI conserved domain search) but an incomplete SH3 domain, owing to 55 highly conserved amino acids at positions E123-E155 being absent. These amino acids correspond to the region carboxy terminal to the site of the neural Src insertions. The SH3 domain is necessary for substrate binding and autoinhibiton of kinase activity, via its association with the SH2-kinase linker domain (Ulmer et al. 2002), therefore if it is translated, this protein would have higher kinase activity and would have to rely on other domains for substrate binding, such as the unique and SH2 domains.

Figure 8 shows the tissue specific expression patterns of the *Src* variants detected in the Catshark RNA-Seq data. *C-Src* expression was detected in the pancreas but also at higher levels in the brain and liver, whilst the expression of the *N1-Src* and *N4-Src* variants was only detected in the brain. It is likely that high sequence homology explains the identical expression levels detected for the *N1-Src* and *N4-Src* variants. The expression of the *N4-Src* variant can also be detected in the *Teleost* species, the Tonguefish, in which *N1-Src* expression was also detected, as described previously. In addition, the expression of *N4-Src* was also

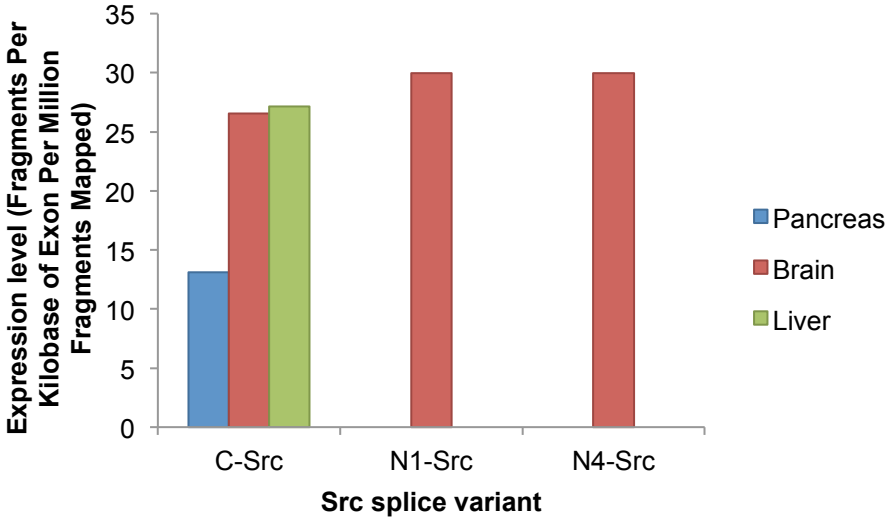

Figure 8: Tissue-specific expression of the *N4-Src* isoform in the Catshark, *Scyliorhinidae*. Expression levels measured in Fragments Per Kilobase of exon per million fragments Mapped (FPKM).

detected in the Stinkbird (*Opisthocomus hoazin*) – a member of the *Tetrapoda* superclass, of which humans are also members.

3.1.3 Discussion

N1-Src is a conserved neural *Src* variant that is expressed in vertebrates from the shark to humans, whilst the expression of other neural *Src* variants; *N2-Src* and *N3-Src* show more restricted expression during vertebrate evolution, having been detected in only mammals and *Xenopus tropicalis* respectively. *N4-Src* represents a newly identified brain-specific variant whose expression has been detected in the Catshark, *Schliorhinidae,* the Teleost fish known as the Tonguefish (*Cynoglossus* semilaevis) the tetrapod species; the Stinkbird, *Opisthocomus hoazin.* As the *N4-Src* variant lacks sequence present in *C-Src* and *N1-Src*, it may represent incomplete sequencing of these variants. However, we would expect that some RNA-seq reads will bridge the 3' and 5' ends surrounding the sequence is missing, allowing us to identify this variant in a manner analogous to identifying *C-Src* as a different variant to *N1-Src*. To confirm that this is a real variant, it must be cloned and sequenced.

More detailed analyses of RNA-seq data in addition to Pan-Src PCR priming may reveal additional isoforms to be studied using functional analyses, as was the case for *xN3-Src*, whose expression cannot be detected using BLAST searches as is not annotated or identifiable in *Xenopus* expressed sequence tags (ESTs).

3.2 Temporal and spatial expression analyses of neural *Src* splice variants

3.2.1 Introduction

To understand the function of neural Src isoforms during neurogenesis, it is important to identify their expression levels throughout the relevant developmental stages, which can be performed using reverse

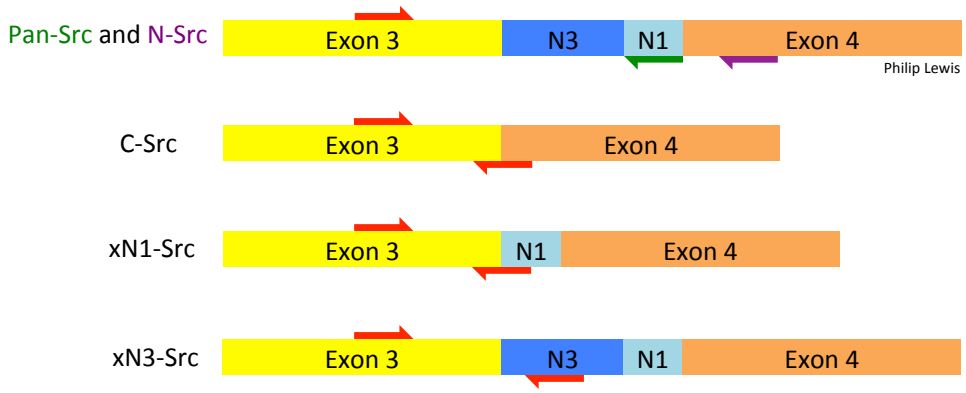

Figure 9: Priming strategy used to analyse the expression of the *Src* splice variants. The expression of the *Src* splice variants were analysed individually using Pan-*Src* primers designed by Philip Lewis that amplify cDNA of all three variants simultaneously (the red and purple primers) or the neural-*Src* isoforms together (the red and green primers).The lower primer pairs were also used to analyse the expression of each *Src* splice variant individually.

transcription PCR (RT-PCR). Understanding their expression levels during processes such as neural induction and neurogenesis may indicate specific roles of neural Src isoforms. For instance, the expression of neural *Src* variants during neural induction would imply a function earlier in nervous system development than the products of genes expressed during neurogenesis and neurulation. This allows us to put into context the effects observed when neural *Src* expression levels are perturbed. To analyse the expression levels of the *Src* splice variants in isolation from one another, variant-specific primers were designed that overlap the relevant exon boundaries to exclude amplification of the other variants (Figure 9). These primers were used in conjunction with the primers used by Philip Lewis (thesis, 2014) that amplify *C-Src, xN1-Src* and *xN3-Src* (Pan-*Src* primers) or *xN1-Src* and *xN3-Src* (*N-Src* primers).

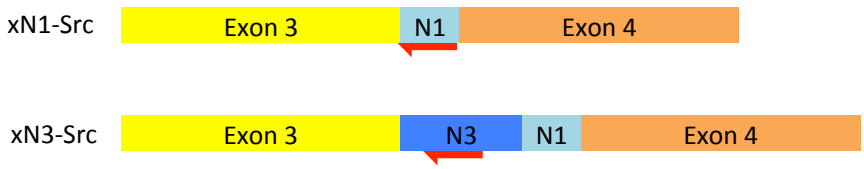

Figure 10: LNA probe transcript targeting to analyse the neural *Src* isoform spatial expression patterns

Equally, analysing the spatial expression patterns of these variants throughout early development will enable the identification of the tissues

in which these variants are expressed and from this, inferences can be made regarding their functions within the embryo at the particular stage of development. As the sequences of *C-Src, xN1-Src* and *xN3-Src* isoforms vary by the presence or absence of microexons, it was not possible to use traditional *in situ* hybridisation probes of approximately 400 nucleotides in length. Instead the probes that were used contain modified RNA nucleotides known as locked nucleic acids (LNAs) at every third nucleotide position (according to Válóczi et al. (2004); Darnell et al. (2010)), which increases the melting temperature of the probe:mRNA interaction (Braasch & Corey 2001). This allows reactions using short probes to retain specificity by permitting the hybridisation to be carried out at high temperatures. LNA probes were designed to analyse the spatial expression patterns of the *xN1-Src* microexon and the *xN3-Src* microexon (Figure 10). *Xenopus tropicalis* embryos were used in these analyses as they have only one *Src* gene, whereas *Xenopus laevis* have two.

Results

3.2.2 *Src* expression analysis during early *Xenopus tropicalis* development: Temporal expression analyses

Figure 11 shows that at stage 4, *C-Src* mRNA is present in the maternal mRNA pool, before the mid-blastula transition (pre-MBT) and the onset of zygotic transcription (Newport & Kirschner 1982). The *C-Src* expression level peaks at gastrula stage 12 before returning to the level observed at cleavage and blastula stages. From here onwards, the expression level remains relatively constant in the stages analysed.

xN1-Src mRNA and *xN3-Src* mRNA are also detectable pre-MBT at stage 4 and then increase in their expression levels during neural induction at blastula stage 8 to gastrula stages 10-12 (Kuroda et al. 2004) and increase further during primary neurogenesis from gastrula to neurula stages (which begins at stage 13 (Shuldiner et al. 1991)) to early tailbud stage 25 (Lamborghini 1980). *xN1-Src* and *xN3-Src* expression levels then decrease at stage 25 after neurulation; after the neural plate has

rolled up and closed to form a tube at stage 20 (Schroeder 1970). Their expression levels then decrease further towards the end of primary neurogenesis at late tailbud stage 35; after primary neurons have been established (Thuret et al. 2015) and the embryo is able to swim freely. Both *xN1-Src* and *xN3-Src* peak in their expression levels at neurula stage 18, whilst *xN3-Src* displays an additional but lower expression peak at blastula stage 8.

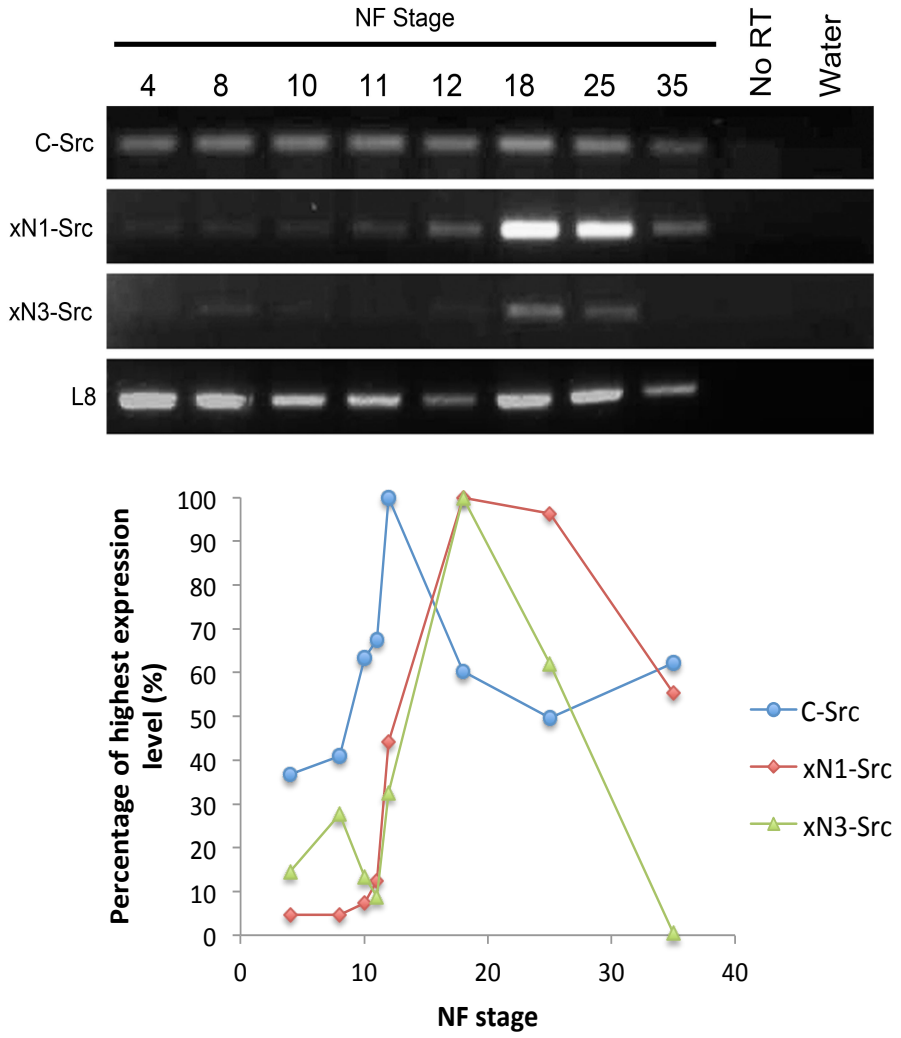

Figure 11: The temporal expression profiles of *Src* splice variants during early *Xenopus tropicalis* development analysed using RT-PCR. Densitometry measured using ImageJ and normalised to L8. NF stage = Nieuwkoop and Faber (1994) stages of *Xenopus* development. RNA extracted from stage 18 embryos was used for the no RT and water controls. This figure represents data from one experiment, n=1.

In a more detailed analysis of gastrula and neurula stage embryos (Figure 12), it was observed that from gastrula stage 10.5, *xN1-Src* and

xN3-Src expression levels increase as neural induction ensues and as gastrulation and primary neurogenesis begin, whilst *C-Src* levels remain more constant. Once the neuroectoderm has become established and as primary neurogenesis continues during neurula stages, these levels continue to increase up to stage 17, before plateauing towards the end of neurulation at stage 19. Each of these time course experiments was performed once.

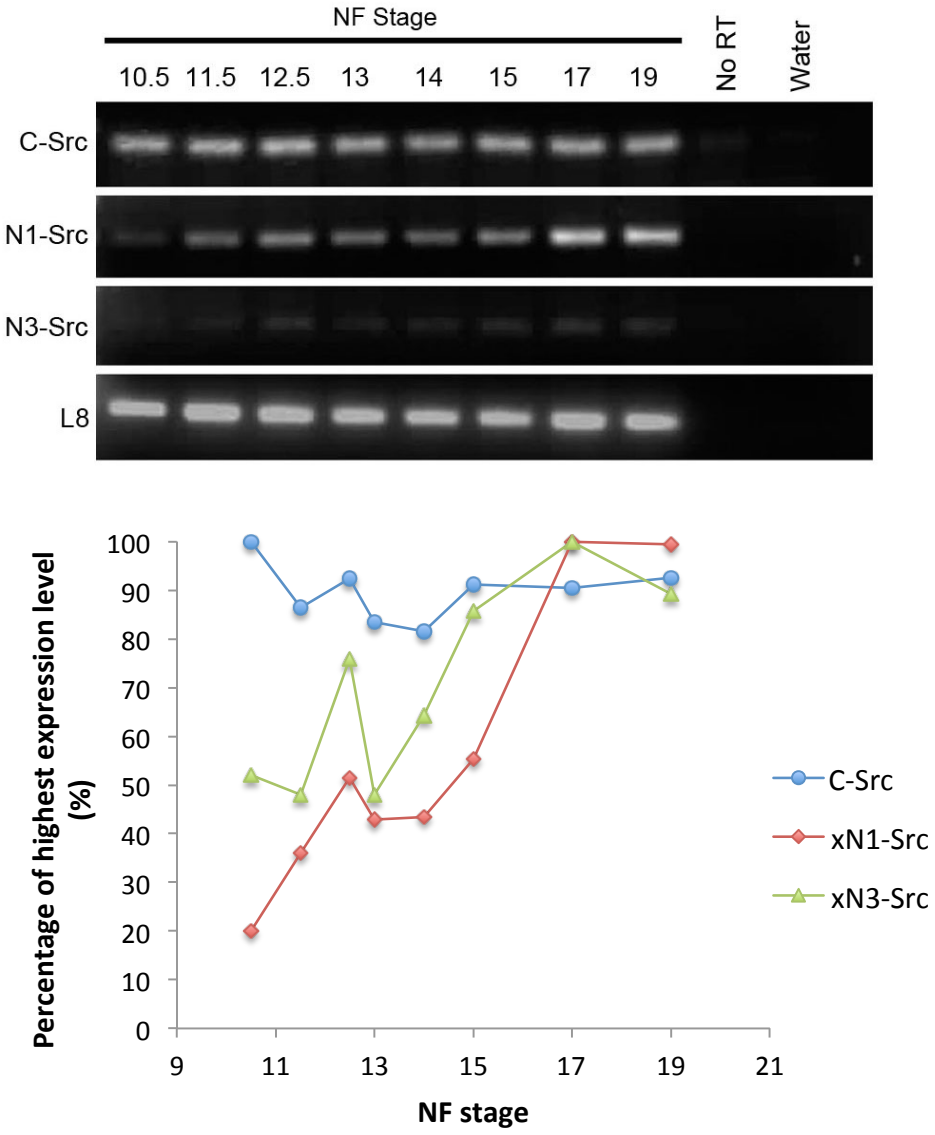

Figure 12: The temporal expression profiles of *Src* splice variants during *Xenopus tropicalis* primary neurogenesis analysed using RT-PCR. Densitometry measured using ImageJ and normalised to L8. NF stage = Nieuwkoop and Faber (1994) stages of *Xenopus* development. RNA extracted from stage 19 embryos was used for the no RT and water controls. This figure represents data from one experiment, n=1.

3.2.3 *Src* expression analysis during secondary neurogenesis: Temporal expression analysis

Figure 13 shows that following the decrease in expression levels at stages 25 and 35, both *xN1-Src* and *xN3-Src* levels subsequently increase at the beginning of secondary neurogenesis at stage 46. During secondary neurogenesis the majority of primary neurons that enable embryonic swimming reflexes are replaced by secondary neurons, which develop during a phase of neurogenesis that proceeds in the neural tube, which has been more closely likened to the neurogenesis of amniotes, such as humans (Wullimann et al. 2005). It is during secondary neurogenesis that neurons termed 'secondary neurons' differentiate, that are functional into adulthood (Forehand & Farel 1982).

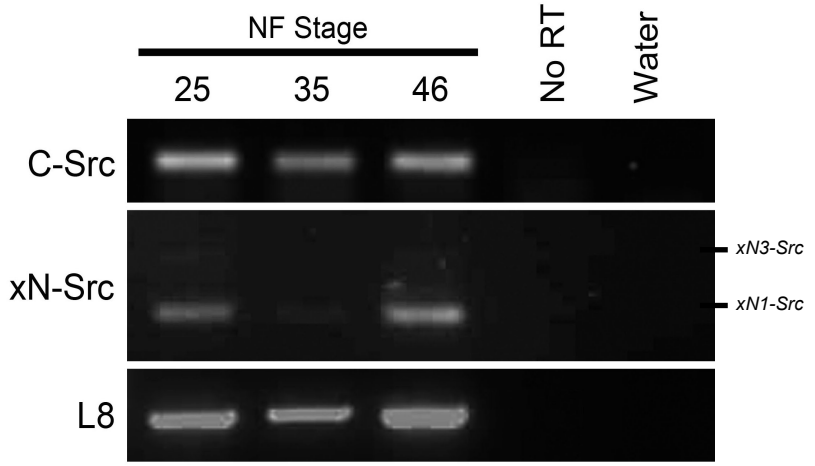

Figure 13: The temporal expression profiles of *Src* splice variants at the end of primary neurogenesis and the beginning of secondary neurogenesis analysed using RT-PCR. NF stage = Nieuwkoop and Faber (1994) stages of *Xenopus* development. RNA extracted from stage 25 embryos was used for the no RT and water controls. Neural *Src* expression was analysed using neural *Src* primers designed by Philip Lewis. This figure represents data from one experiment, n=1.

3.2.4 *Src* temporal expression analysis during zebrafish primary and secondary neurogenesis

It is important to investigate the temporal expression patterns of *Src* isoforms in multiple examples of vertebrate development as conserved patterns of gene expression enable stronger predictions to be made regarding their expression in other vertebrate species, such as humans.

Zebrafish neurogenesis was studied for the expression levels of the *Src* splice variants as an additional example of vertebrate development.

Figure 14 shows that in the 4-cell stage zebrafish embryo, before the onset of zygotic transcription (pre-MBT) (Kane & Kimmel 1993), both *C-Src* and *N1-Src* are expressed in the maternal mRNA pool at relatively high levels. At the blastula stage, when neural induction begins (Schmidt et al. 2013) known as the high stage, *C-Src* and *N1-Src* expression can also be detected. Both *C-Src* and *N1-Src* expression levels then decrease but remain detectable during gastrulation at stages 75% epiboly

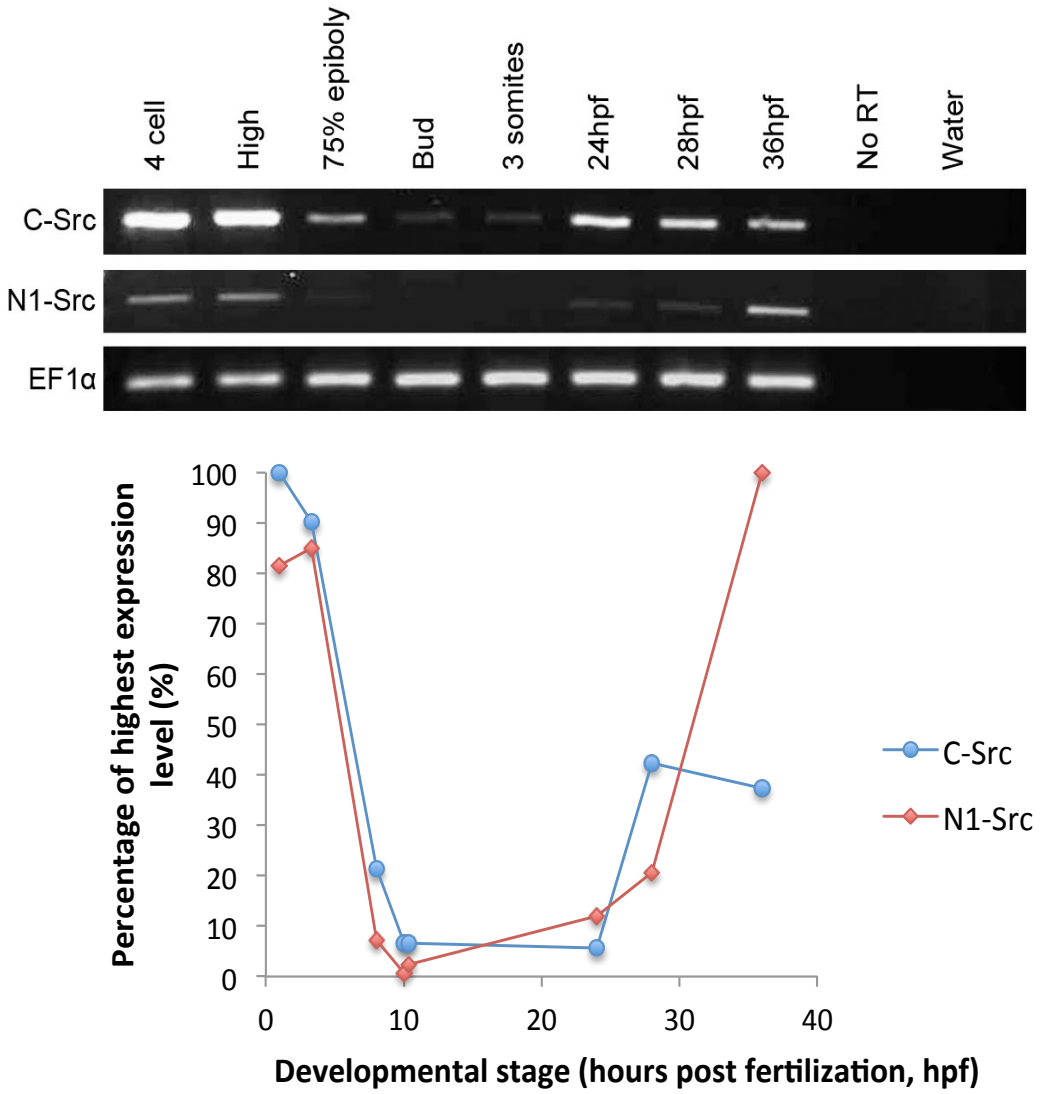

Figure 14: The temporal expression profiles of *Src* splice variants during early zebrafish development analysed using RT-PCR. Densitometry measured using ImageJ and normalised to EF1α. Zebrafish embryos were staged according to Kimmel *et al.* (1995). RNA extracted from embryos at 24hpf was used for no RT and water controls. This figure represents data from one experiment, n=1.

to bud stage, as neural induction continues and neurogenesis begins (Schmidt et al. 2013) and then increase as primary neurogenesis continues at the three-somite stage. It is during somitogenesis that a process equivalent to *Xenopus* neurulation occurs as the neural keel forms from the neural plate and hollows out to form the neural tube (Fahrbach 2013). Whilst *C-Src* expression then plateaus at 24 hours post fertilisation (hpf), *N-Src* expression continues to increase as primary neurogenesis continues at 24hpf. *N1-Src* expression then increases further as primary neurogenesis ends and secondary neurogenesis begins at 28hpf (Zhao et al. 2011). Pan-Src priming, which amplifies *C-Src* and insertions at the *N1-Src* microexon locus, detected no additional *Src* splice products (data not shown).

3.2.5 *Src* expression analysis during early *Xenopus* development: Spatial expression analysis of the *xN1-Src* microexon

Figure 15a and 15b show that the LNA probe designed to analyse the spatial expression pattern of the *xN1-Src* microexon (present in both *xN1-Src* and *xN3-Src* transcripts), detected higher expression in the animal hemisphere than the ventral hemisphere at the blastula stage 9. As neural induction and neurogenesis proceed, expression of the *xN1-Src* microexon can be seen throughout the neural plate, akin to *sox3* expression (Rogers et al. 2009) (indicated by the black arrows in Figures 15c and 15d). In stage 20-21 embryos *xN1-Src* microexon expression remains restricted to this region after the neural plate has rolled up to form the neural tube during neurulation (Figures 15e and 15f). At tailbud stage 26, the expression of the *xN1-Src* microexon is detectable in the neural tube and also in the anterior head region. Expression is also detectable in the branchial arches; a structure populated by neural crest cells (indicated by the red arrow) (Koestner et al. 2008). When the embryo was dissected laterally at stage 26, higher expression was detected in the neural tube of the anterior section, corresponding to the head region (Figure 15g) than the posterior tail section (Figure 15h).

Whilst existing protocol recommends preabsorption of LNA probes six times to increase probe specificity (as described by Warrander et al. 2015), there was no noticeable difference in the amount of background staining when preabsorbed or fresh probe was used (data not shown).

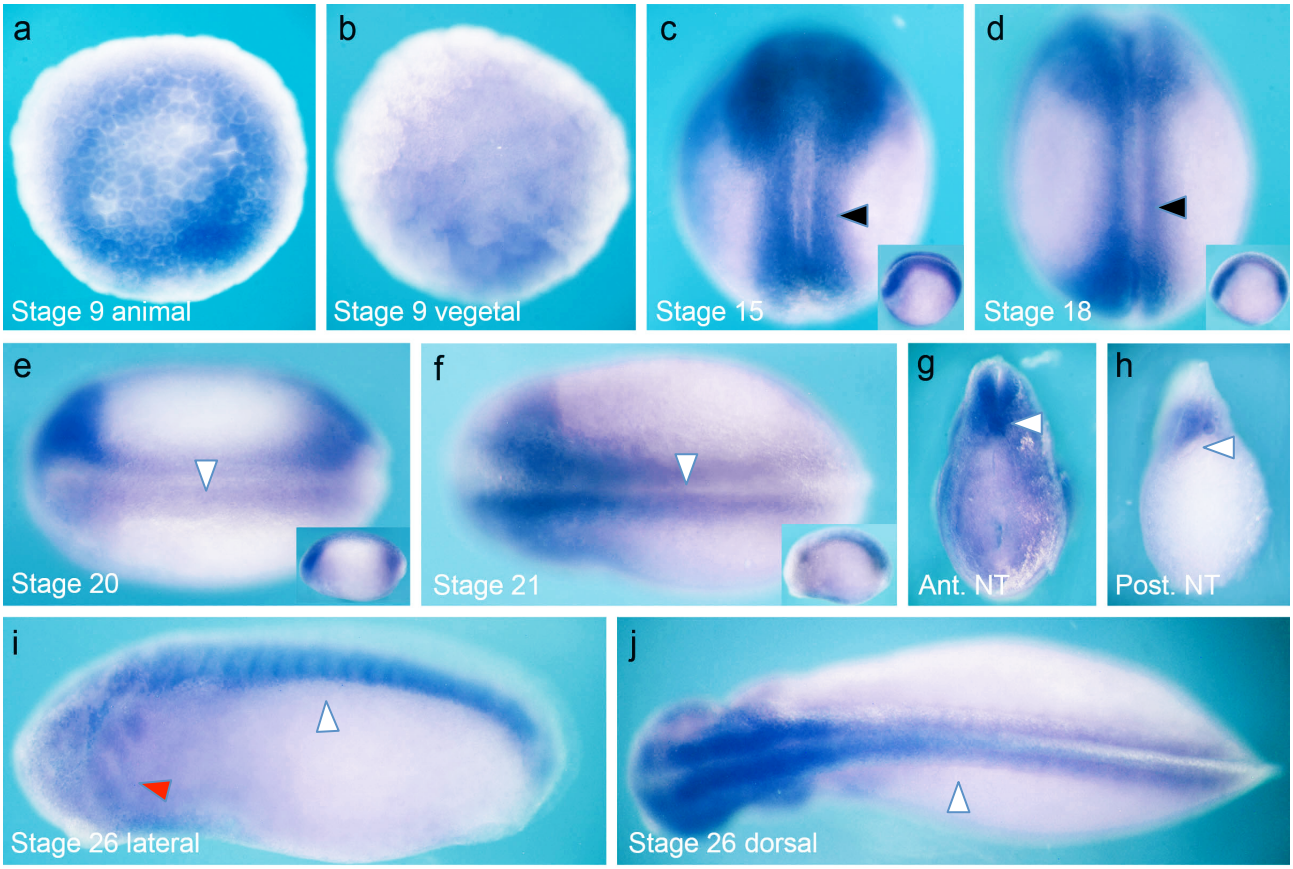

Figure 15: The spatial expression pattern of the *xN1-Src* microexon during early *Xenopus tropicalis* development analysed using *in situ* hybridisation with an LNA probe. (a) stage 9 animal view, (b) stage 9 vegetal view, (c+d) stage 15 and stage 18 dorsal views, anterior to the top, (e+f) stage 20 and 21 dorsal views, anterior to the left, (g+h) anterior and posterior lateral sections of stage 26 embryo, dorsal to the top, (i) stage 26 lateral view, anterior to the left, dorsal to the top, (j) stage 26 dorsal view, anterior to the left. Inset (stages 15-21) are lateral views anterior to the left, dorsal to the top. Black arrows indicate the neural plate, white arrows indicate the closed neural tube, red arrows indicate the brachial arches. Embryos were staged according to Nieuwkoop and Faber (1994) stages of *Xenopus* development. Ant. NT = anterior neural tube, Post. NT = posterior neural tube.

3.2.6 *Src* expression analysis during early *Xenopus* development: Spatial expression analysis of *xN3-Src*

Figure 16c shows that at stage 5, there is an animal to ventral gradient of *xN3-Src* expression with *xN3-Src* transcripts localised to the animal hemisphere (Figures 16a and 16b). At stages 12-20 (Figures 16d-g), as neurogenesis and neurulation proceeds, *xN3-Src* is expressed at highest

levels in the neural plate and then the neural tube. At tailbud stages 25-39 (Figures 16h, 16i and 16l), expression is detectable in the neural tube and also the eye. Expression is also localised to the branchial arches. Lateral sections of stage 34 and 39 embryos show that *xN3-Src* expression is more diffuse in the anterior head region than the posterior tail region (Figures 16j, 16k, 16m and16n).

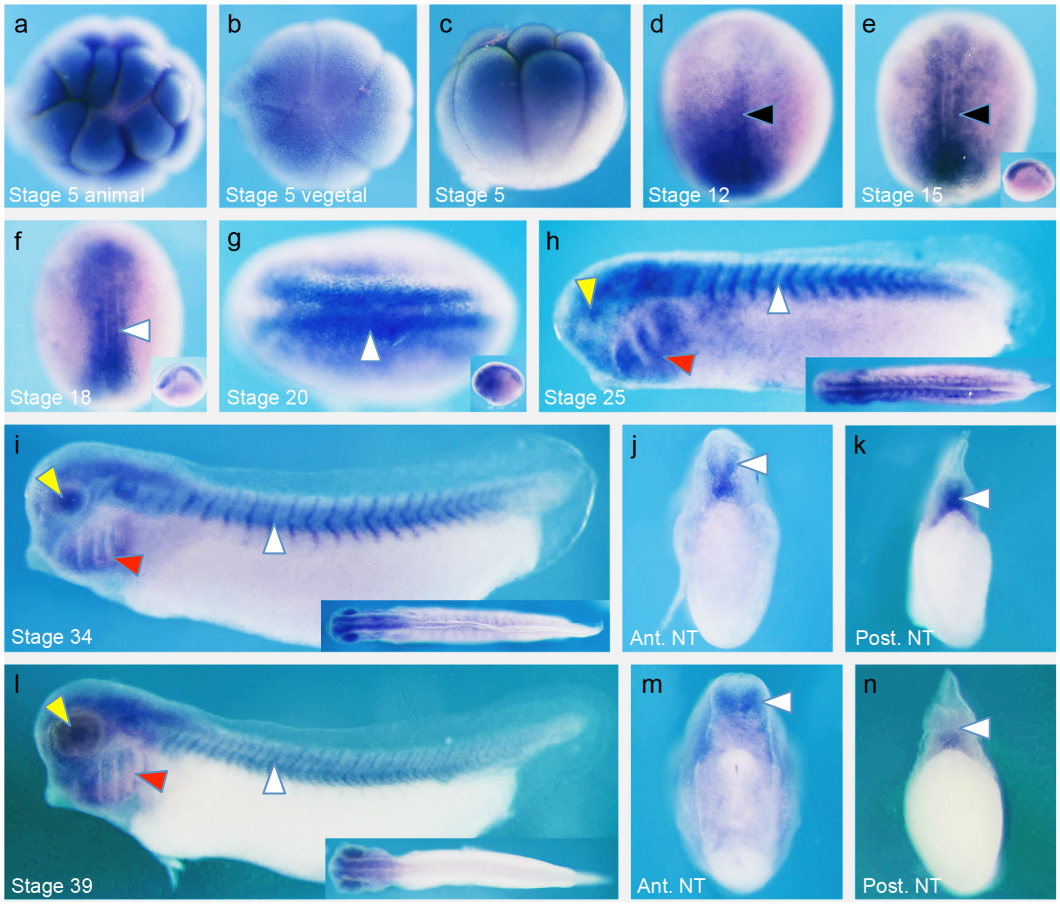

Figure 16: The spatial expression pattern of the *xN3-Src* microexon during early *Xenopus tropicalis* development analysed using *in situ* hybridisation with an LNA probe. Embryos were staged according to Nieuwkoop and Faber (1994) stages of *Xenopus* development. (a) stage 5 animal view, (b) stage 5 vegetal view, (c) stage 5 lateral view, animal pole to the top, (d-f) stage 12, 15, 18 dorsal views, anterior to the top, (g) dorsal view, anterior to the left, (h, i, l) stage 25, 34, 39 lateral views, anterior to the left, dorsal to the top, (j+K) anterior and posterior lateral sections of stage 34 embryo, dorsal to the top, (m+n) anterior and posterior lateral sections of stage 29 embryo, dorsal to the top. Inset (stages 15-20) are lateral views; anterior to the left, dorsal to the top. Inset (stages 25-39) are dorsal views; anterior to the left. Black arrows indicate the neural plate, white arrows indicate the closed neural tube, red arrows indicate the brachial arches and yellow arrows indicate the eye. Ant. NT = anterior neural tube, Post. NT = posterior neural tube.

3.2.7 Neural-inductive signals upregulate neural-*Src* splice variants

Neural induction occurs partly as a result of the BMP inhibition by molecules such as Noggin and Chordin; dorsalising factors released by

Spemann-Mangold's organizer (Spemann & Hilde Mangold 1924; Smith & Harland 1992; Sasai et al. 1994). Microinjection of *noggin* mRNA results in embryo dorsalization (Smith & Harland 1992; Holley et al. 1996), visible in the phenotype shown in figure 17b; a positive control for *noggin* translation and activity. In an experiment that was performed once, when undissected control embryos reached stage 16-17 (Figure 17a), animal cap explants dissected from sibling embryos injected with *noggin* mRNA exhibited a slight increase in expression of *xN1-Src* and *xN3-Src* relative to animal cap explants from uninjected embryos, whilst *C-Src* expression remained unchanged (Figure 17c).

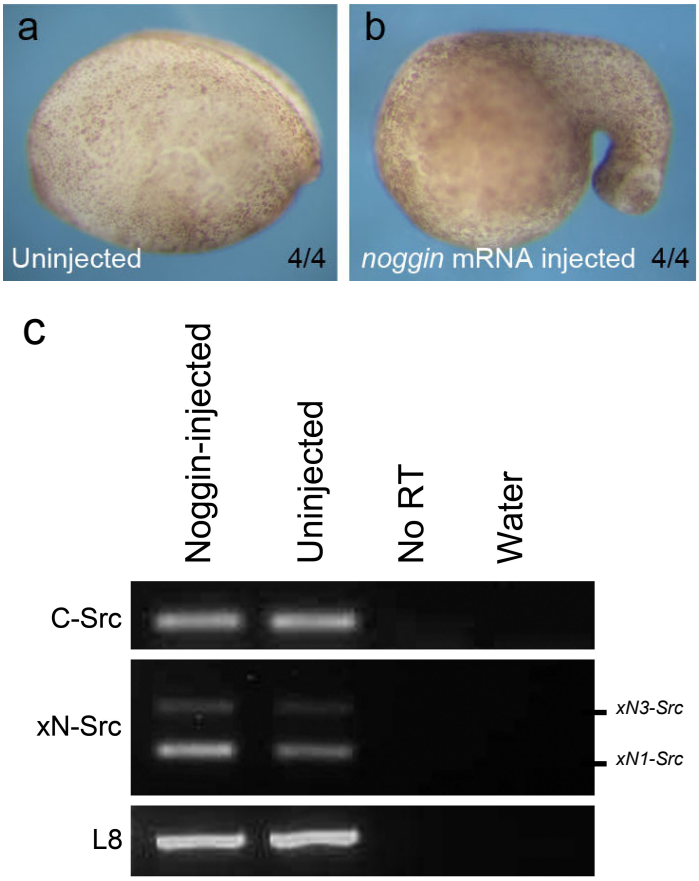

Figure 17: Noggin-induced upregulation of neural *Src* isoforms in animal cap explants analysed using RT-PCR. (a) uninjected neurula stage embryos, (b) *noggin* mRNA-injected phenotype, (c) RT-PCR of animal cap explants. RNA extracted from uninjected animal caps was used for no RT and water controls. Neural *Src* expression was analysed using neural *Src* primers designed by Philip Lewis This figure represents data from one experiment, n=1.

3.2.8 *Src* expression analysis in adult *Xenopus tropicalis* tissues

N1-Src expression has previously been detected in the human foetal brain and at lower levels in the adult brain but is absent in other adult and

foetal tissues, including the pancreas, liver and lung (Pyper & Bolen 1990). Conversely, it was unknown as to whether the expression of the novel xN3-Src isoform is restricted to embryogenesis or whether its expression was maintained into adulthood and if so, in which tissues it is expressed. In an experiment performed once, RT-PCR performed on RNA extracted from *Xenopus tropicalis* adult tissues showed as expected, that *xN1-Src* expression is detectable in the brain, and more surprisingly at lower levels in the heart (Figure 18). Additionally, *xN3-Src* expression is also detectable in these two tissues but neither isoform is detectable in the other tissues analysed. Pan-*Src* priming detected no additional *Src* splicing between exons three and four (data not shown). *C-Src* expression was detected in all adult tissues analysed.

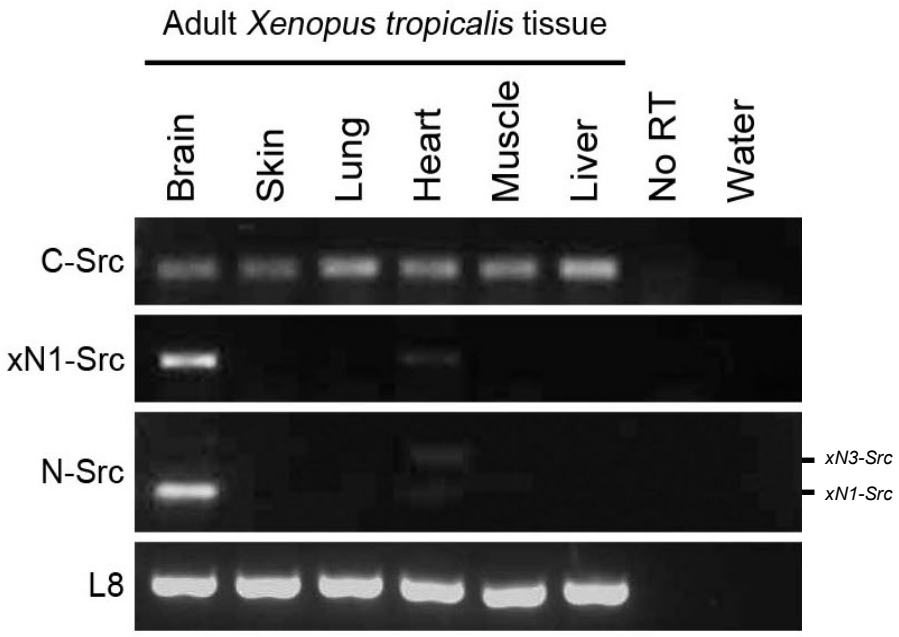

Figure 18: The expression of *Src* isoforms in adult *Xenopus tropicalis* tissues measured using RT-PCR. RNA extracted from the brain was used for no RT and water controls. *xN1-Src* expression was analysed using *xN1-Src*-specific primers. Both *xN1-Src* and *xN3-Src* expression levels were analysed using neural *Src* primers designed by Philip Lewis This figure represents data from one experiment, n=1.

3.2.9 Discussion

Temporal expression analyses

RT-PCR analyses of *Xenopus tropicalis* and zebrafish embryos showed that expression levels of neural *Src* variants correlate with primary and secondary neurogenesis and that *Xenopus tropicalis xN1-Src and xN3-*

Src expression is maintained into adulthood, where expression is restricted to the brain and the heart. This recapitulates the findings of Philip Lewis (thesis, 2014) who showed that expression of the neural *Src* variants were detectable in the maternal mRNA pool and increased in expression towards a peak during primary neurogenesis. Additionally, this project builds his work, where Pan-*Src* priming (which detected *C-Src, xN1-Src* and *xN3*-Src expression) and neural-*Src* priming (which detected *xN1-Src* and *xN3-Src* expression) were used to analyse the expression of *Src* isoforms during primary neurogenesis. In these experiments, isoform-specific primers have been used to analyse the temporal expression patterns of the specific splice variants in isolation from one another during both primary and secondary neurogenesis. In addition to the detailed temporal expression analyses of *Src* isoforms during *Xenopus tropicalis* neural development, the temporal expression patterns of *N1-Src* isoforms was also shown to peak during zebrafish primary and secondary neurogenesis and provides an additional example of vertebrate development. These RT-PCR experiments and densitometries should be repeated for statistical validation. For more quantitative analyses, quantitative PCR (qPCR) should be used. In addition, the isoform-specific primers must be validated. To do so, the primers should be shown to amplify cloned cDNA of the specific isoform they are intended, and not the other isoforms. In addition, the products should be cloned and sequenced to confirm their identities. Due to time constraints, this was not possible during this project.

During neural induction at blastula and gastrula stages*, xN1-Src* and *xN3-Src* expression levels were shown to increase from low levels of maternal mRNA that was deposited pre-MBT. Upregulation of the neural *Src* isoforms during neural induction was recapitulated in the noggin-injected animal explants, where it was observed that overexpression of the BMP inhibitor noggin caused a slight increase in the expression levels of both *xN1-Src* and *xN3-Src*, relative to the basal level expressed in the animal caps dissected from uninjected control embryos. This experiment must be repeated to confirm that the subtle changes observed are statistically

significant. In addition, qPCR should be used to measure such small changes in gene expression, however this was not possible due to time constraints.

To normalise the expression patterns of the *Src* variants using RT-PCR, expression levels of the house keeping genes *L8* and *elongation factor 1α* (*EF1α*) were used for *Xenopus tropicalis* and zebrafish respectively. The expression levels of mRNA encoding the ribosomal protein L8 has been shown to be constant in its expression levels up until stage 19 in *Xenopus laevis*, relative to the total RNA levels (Sindelka et al. 2006) and whilst *EF1α* levels were shown to be stably expressed during development, compared with other housekeeping genes studied (McCurley & Callard 2008), more accurate levels of gene expression may be calculated by comparison with total RNA levels, though this is a more difficult and time consuming approach.

Spatial expression analyses

The *in situ* hybridisation experiments using LNA probes demonstrated the neural, eye and neural crest expression pattern of the *xN1-Src* microexon during *Xenopus tropicalis* primary neurogenesis. It is important to note that the LNA probe designed to detect the *xN1-Src* microexon is likely to detect *xN3-Src* transcripts in addition to *xN1-Src* transcripts, and therefore should be referred to as the '*N-Src* LNA probe'. This is because the *xN1-Src* microexon is present in the *xN3-Src* transcript. It is unlikely that the two nucleotides at the 3' end of the probe that are homologous to the 3' end of exon 3 enable the probe to distinguish between the *xN1-src* and *xN3-Src* isoforms (You et al. 2006). To analyse the spatial expression pattern of *xN1-Src* specifically, it would be necessary to design an LNA probe that spans more of the 3' end of exon 3, therefore excluding binding of the LNA probe to the *xN3-Src* microexon, in a manner analogous to the RT-PCR primer design used in the time course experiments. To increase the specificity further, additional LNAs may be introduced (You et al. 2006).

In addition to using designing additional LNA probes to analyse the expression patterns of these microexons, work must be done to validate their specificities. The LNA probes were designed to have as little sequence homology to other transcripts as possible; using BLAST searches to predict off-target binding via sequence homology. Darnell et al. (2010) showed using chicken embryos that signal could be detected from LNA *in situ* hybridisation probes of 14 nucleotides but not probes of 12 nucleotides in length. For this reason, probes were designed that had sequence homology of less than 14 nucleotides to off-target transcripts. *xN3-Src* expression cannot be detected using BLAST searches of published *Xenopus* transcriptome data; therefore it is possible that BLAST searches are of insufficient sensitivity to predict off-target binding. These LNA *in situ* hybridisation experiments therefore require stronger negative controls, such as LNA probes with mismatches to the *xN1-Src* and *xN3-Src* microexons or random sequences that are not predicted to bind to any transcripts in the *Xenopus tropicalis* transcriptome. This is necessary to demonstrate that the staining observed is not background staining that can occur when performing *in situ* hybridisation. Conversely, an LNA probe designed against a transcript of a known but different neural expression pattern such as *n. tubulin* would act as a positive control for the use of these probes in assessing different expression patterns. Alternatively, to support the expression patterns observed using the *N3-Src* LNA probe, multiple LNA probes could be generated, targeting different regions of the 70-nucleotide insert. This is not possible for the *xN1-Src* probe due to the short microexon sequence length. Due to time limitations it was not possible to perform these controls during this project, however they are essential in supporting this data. Nevertheless, these experiments represent the first detailed analyses of the neural and neural-crest-restricted expression patterns of neural *Src* isoforms during embryogenesis.

SFK proteins are subjected to many posttranslational modifications, some of which alter protein levels. For example, the unique domain phosphorylation at Thr37 or Ser75 in human Src by p25-activated cyclin

dependent kinase 5 (cdk5) promotes ubiquitination-mediated Src degradation (Pan et al. 2011). Whilst analyses of mRNA levels show the temporal and tissue-specific splicing of the neural *Src* RNA to produce mature mRNA and may indicate protein levels, this highlights the importance of studying protein levels to understand fully the tissues in which the neural Src proteins isoforms are expressed and the developmental stages at which this occurs. To do so, anti-neural-Src antibodies are required for western blot analyses of temporal expression patterns and immunostaining analyses of spatial expression patterns.

In conclusion, in *Xenopus tropicalis, xN1-Src* and *xN3-Src* are expressed in neural tissues during primary and secondary neurogenesis, placing their expression in the correct time and place for a role in neural development.

3.3 Functional analyses of neural Src isoforms

3.3.1 Introduction

Owing to the large sizes of *Xenopus* and zebrafish embryos and their consequential ease of injection, understanding of protein function can be gained from microinjecting the reagents necessary for overexpression and knockdown/knockout technologies and observing their effects on developmental processes. To understand the function of *xN3-Src* using overexpression analyses in *Xenopus tropicalis* embryos, it was necessary to clone this isoform, from which mRNA was synthesised *in vitro* and microinjected. As *xN1-Src* has previously been cloned (by Philip Lewis), synthetic mRNA could be transcribed.

Figure 19: The splice-blocking antisense morpholino oligo (AMO) strategy used to knockdown the neural *Src* isoforms

Two antisense morpholino oligos (AMOs) were previously designed by Philip Lewis to knockdown the expression of the neural *Src* variants in *Xenopus tropicalis* by binding to and inhibiting the splice donor and

acceptor sites of x*N1-Src* via their complementary sequences (Figure 19, sequences shown in Table 1, page 31), whilst leaving the expression of *C-Src* mRNA unaffected. We may predict that injecting the splice acceptor site-inhibiting AMO (AMO A) singularly may knockdown *xN1-Src* expression alone, as an alternative splice acceptor is spliced to exon 3 to produce mature *xN3-Src* mRNA. Conversely, we may expect that microinjecting AMOs targeting the splice donor site (AMO D) would knock down both *xN1-Src* and *xN3-Src* as this site is used to produce both mature mRNAs by being spliced to exon 4. Furthermore, we may hypothesise that when used in combination, these AMOs would knock down *xN1-Src* expression by inhibiting the splice acceptor site and both *xN1-Src* and *xN3-Src* expression by inhibiting the splice donor site used for the expression of the both neural variants (as shown in Table 7). *Xenopus tropicalis* embryos were used in these analyses as they have only one *Src* gene, whereas *Xenopus laevis* have two.

Table 7: The predicted effects of Antisense Morpholino Oligo microinjection on *Src* splice variant expression

Antisense morpholino oligo	Predicted effects on *Src* splice variant expression		
	C-Src	*xN1-Src*	*xN3-Src*
Acceptor	✔	✖	✔
Donor	✔	✖	✖
Acceptor + Donor	✔	✖	✖

Where ✔ indicates the expression of the isoform and ✖ indicates the splicing of the transcript is inhibited

To understand the functions of these proteins using overexpression and knockdown analyses, embryos injected with these constructs can be observed for changes in phenotype and analysed for changes in the expression of neural and neural crest markers using *in situ* hybridisation. Unilateral injection of mRNA and AMOs allow subtle changes in gene expression to be identified using *in situ* hybridisation as the expression patterns in the two embryo hemispheres can be compared, rather than

comparing large population averages. It could also be argued that this is a more accurate method of analysing changes in gene expression. Such markers include *sox3* (a marker of the proliferating neural plate, (Rogers et al. 2009)), *n. tubulin* (a marker of differentiated neurons (Kuroda et al. 2004)) and *phox2a* (a marker of neural crest). Phox2a is a transcription factor that is responsible for regulating the expression of *tyrosine hydroxylase* and *dopamine beta-hydroxylase*; enzymes which are required for noradrenergic neuron development (Lo et al. 1999) – a subpopulation of neurons of the peripheral autonomic nervous system derived from the neural crest, from which neuroblastoma cancers develop in humans (Wylie et al. 2015).

In addition to analysing neural *Src* morphant *Xenopus tropicalis* embryos,

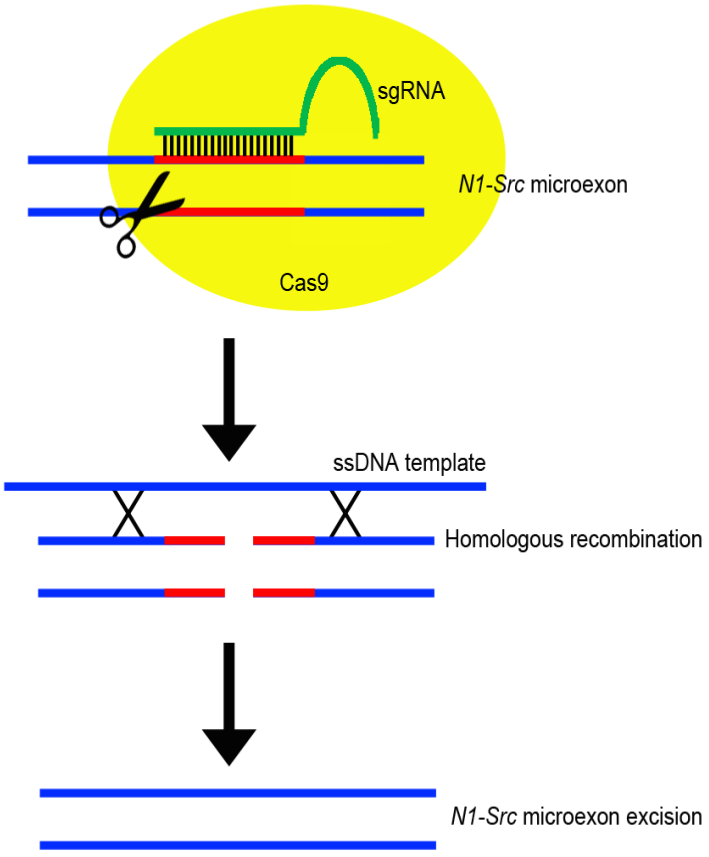

Figure 20: CRISPR-mediated homologous recombination strategy for creating an *N1-Src* knockout zebrafish line. A single guide RNA (sgRNA, green) guiding cleavage of the *N1-Src* microexon (red) by Cas9 protein (yellow) would create double strand breaks at the DNA locus. This can be repaired by homologous recombination, guided by a single stranded DNA (ssDNA) template containing the sequence surrounding but not including the *N1-Src* microexon (blue) to excise the *N1-Src* microexon from the genomic locus. Figure designed by author.

clustered regularly interspaced palindromic repeats (CRISPR)/CRISPR-associated (Cas)-mediated homologous recombination may allow the removal of the *N1-Src* microexon from the genome, whilst leaving *C-Src* splicing and transcription unaffected (Figure 20). To do so, microinjection of Cas9 protein alongside single guide RNA (sgRNA) that is complementary to the *N1-Src* microexon would in theory recruit this endonuclease to the *N1-Src* locus and guide its cleavage, creating double strand breaks. Alone, this would be repaired by non-homologous end joining (NHEJ), an error-prone DNA repair mechanism (Ran et al. 2013) which may knockout the function of *N1-Src* via the formation of indels but may also affect the closely positioned exons of other splice variants and may therefore have off-target effects. Co-injecting a single stranded DNA (ssDNA) oligo template containing 50 nucleotides of homologous sequence immediately before and after but not including the *N1-Src* microexon would provide a guide for DNA repair (Ward 2015), allowing the error free mechanism of DNA repair known as homology directed repair (HDR) or homologous recombination to take place and the excision of the *N1-Src* microexon (Maruyama et al. 2015).

As the *xN1-Src* splice acceptor site is necessary to generate both *xN1-Src* and *xN3-Src* transcripts in *Xenopus*, and zebrafish show no additional *Src* splicing between exons 3 and 4, the zebrafish model offers the opportunity to study the function of *N1-Src* in isolation using this method, as this would hypothetically affect neither *C-Src* nor additional *Src* isoforms. In addition, whilst being tetraploid, zebrafish have only one *Src* gene and therefore only one gene must be targeted to generate null organisms.

Results

3.3.2 Unilateral injection technique

To demonstrate the method of unilateral embryo injection in *Xenopus tropicalis*, *TdTomato* mRNA was injected at the two to eight-cell stage. Embryos were then observed for the unilateral expression of the

fluorescent protein. Figure 21 shows that the fluorescent protein can be detected unilaterally at tailbud stage. Due to the formation of the lighter pigmented gray crescent in the animal pole of early cleavage stage embryos following cortical rotation, it is possible to distinguish the left and right embryo hemispheres (Huxley & Beer 2015). This provides an accurate and reproducible way of targeting mRNAs and AMOs to one particular hemisphere, without the need for co-injecting tracers that mark the injected hemisphere. In subsequent experiments, embryos were injected into the left hemisphere.

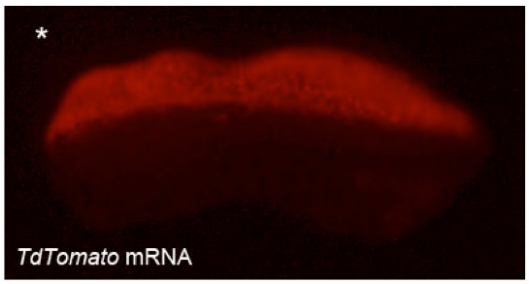

Figure 21: Unilateral microinjection technique demonstrated by the injection of *TdTomato* mRNA. Dorsal view of stage 23 embryo.

3.3.3 Antisense-morpholino oligo knockdown of neural *Src* splice variants

To test the effects of the splice-blocking antisense morpholino oligos (AMOs) on the splicing of *Src* isoforms, embryos were injected bilaterally with the AMOs singularly or in combination and RT-PCR was then performed at stage 16-17; a time point at which high *xN1-Src* and *xN3-Src* expression is ordinarily observed. Figure 22 shows that that injecting the AMOs singularly or in combination results in the knockdown of both *xN1-Src* and *xN3-Src* variants and therefore the AMOs cannot be used to specifically target *xN1-Src*, as predicted in Table 7. The death rate observed in embryos injected with AMO A and AMO D individually was 13% and 14% respectively, higher than the uninjected ficoll control embryos (3%), however no embryos injected with the AMOs in combination died, therefore it is unlikely that toxicity is associated with the injection of these AMOs.

AMO A was microinjected alone in subsequent experiments, as Figure 22 shows that it is sufficient to knockdown the expression of the neural *Src* isoforms.

The injection of AMO A was used to assess the specificity of the *xN-Src* LNA probe as a reduction in staining was expected upon the inhibition of neural *Src* splicing. Embryos injected unilaterally with AMO A showed no reduction in staining using this probe at neurula stage and embryos displayed the expression pattern shown in Figure 15c (n=8, data not shown).

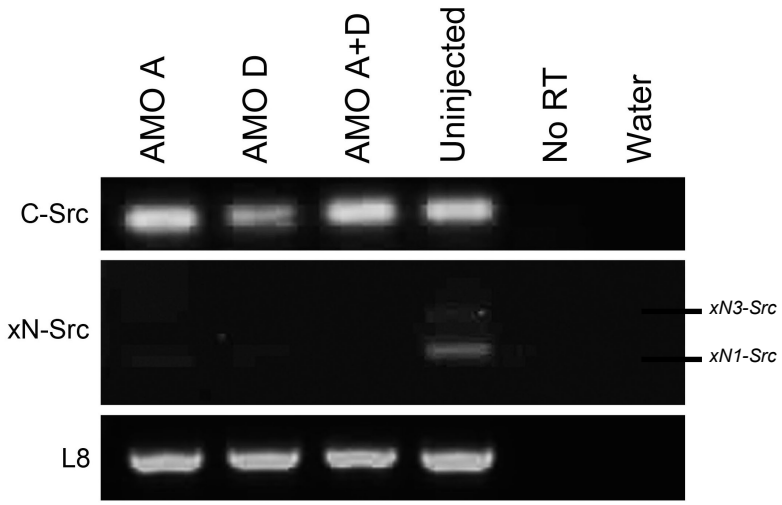

Figure 22: Antisense morpholino oligo mediated knockdown of the neural *Src* isoforms, analysed using RT-PCR. RNA extracted from uninjected embryos was used for no RT and water controls. Neural *Src* expression was analysed using neural *Src* primers designed by Philip Lewis This figure represents data from one experiment, n=1.

3.3.4 The effects of *xN1-Src* and *xN3-Src* knockdown on the locomotive responses of *Xenopus tropicalis* embryos

To analyse whether the knockdown of *xN1-Src* and *xN3-Src* has an effect on the overall development of neural circuitry, the swimming response to a light touch stimulus to the tail was analysed. The responses of free-swimming embryos to this stimulus was categorised as either 'dart' or 'twitch' responses (according to Lewis (2014)). The normal and expected response is the embryo righting itself and rapidly swimming away, which is referred to as the 'dart' response. In contrast, a 'twitch' response consists of the embryo remaining horizontal and swimming only a short

distance, owing to abnormal, convulsing-type swimming (both phenotypes are shown as an overlay of stills taken immediately after the touch stimulus and 0.15 seconds later in Figures 23a and 23b). Figure 23d shows that of embryos of one fertilisation, 94% of ficoll-cultured embryos (uninjected embryos cultured in the same medium as injected embryos) and 100% of water-injected embryos exhibited the dart response, and the remaining 6% of ficoll-cultured embryos showed the twitch response (n=18 and 5 respectively). In contrast, 71% of AMO A-injected embryos exhibited the dart response, and the remaining 29% showed the twitch response (n=21). Video figures attached are labelled with swimming phenotype categorisations (Figures 23f-h).

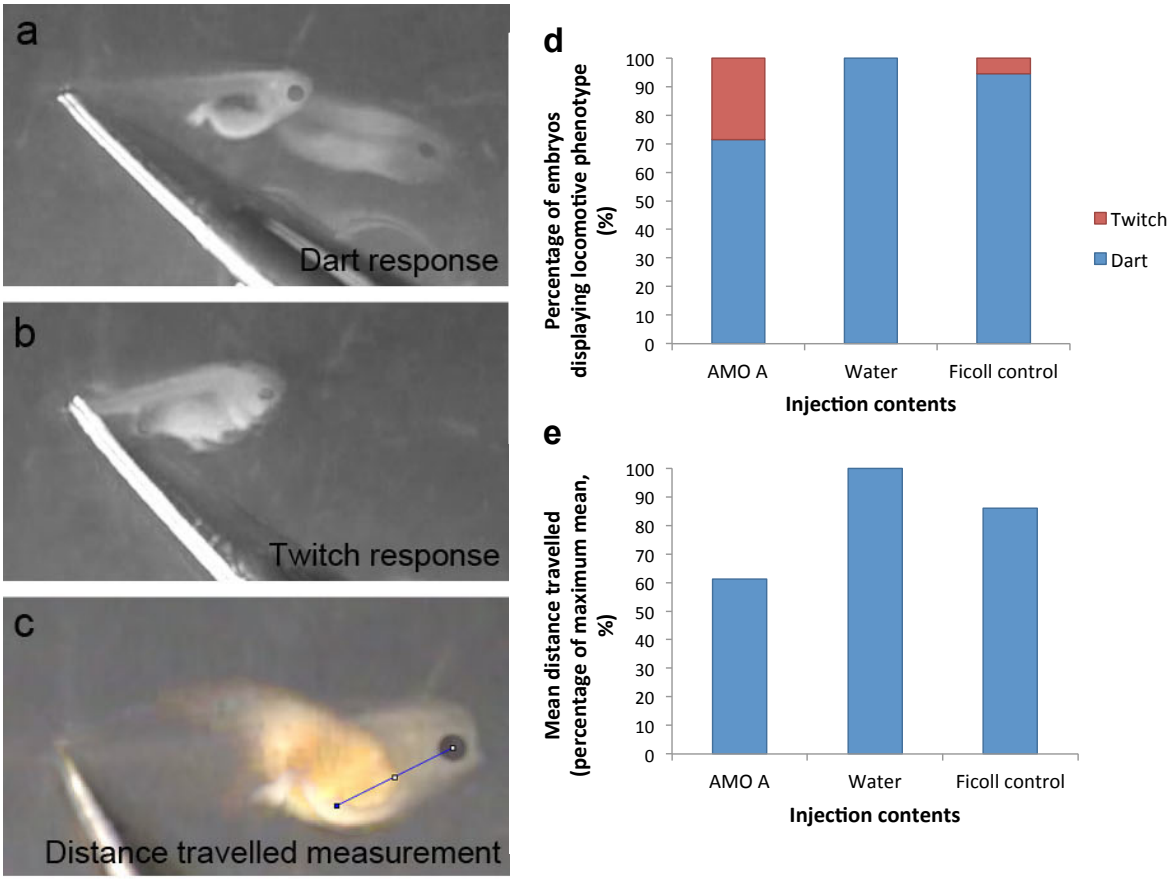

Figure 23: The effects of antisense morpholino oligo-mediated knockdown of neural *Src* isoforms on the locomotive phenotype of *Xenopus tropicalis* embryos. (a) overlay of the 'dart' phenotype, (b) overlay of the 'twitch' phenotype, (c) overlay method used to measure the distance travelled in the first 0.15 seconds after a touch stimulus to the tail, (d) quantification of the phenotypes shown in a and b, (e) quantification of the distances travelled as shown in c relative to mean of the distance travelled by water-injected embryos. Video figures 23f-h are available on the attached CD. All embryos injected and analysed were from a single set of fertilisations; therefore this data represents a single experiment, with 21 AMO-injected, 5 water-injected and 18 ficoll control embryos analysed.

In addition, the distance travelled by these embryos was quantified using ImageJ by overlaying the stills taken at the point of contact and 0.15 seconds later and measuring the distance travelled by the embryo as the distance between the centre of the eye at these two time points (as shown in Figure 23c). Figure 23e shows that water-injected and ficoll-treated embryos travelled 1.4 and 1.6 times further respectively than embryos injected with AMO A in the first 0.15 seconds after the touch stimulus. Therefore, not only is coordinated movement reduced in AMO A-injected embryos, characterised by their swimming responses, but this also impedes their escape from a touch stimulus.

3.3.5 Generating probes for *in situ* hybridisation including *phox2a* cloning

Existing *sox3* and *n. tubulin* constructs, from which antisense *in situ* hybridisation probes could be synthesised offer the ability to analyse the proliferating versus differentiating status of the neural plate, in the presence of knocked-down and overexpressed neural *Src* variants. To analyse the effects on neural crest development, *phox2a* was cloned and an antisense probe transcript was synthesised. RT-PCR was used to amplify *phox2a* from stage 25 cDNA (Figure 24a). A non-homeobox region of the *phox2a* transcript was amplified, cloned and sequenced and an antisense *in situ* hybridisation probe was synthesised. Non-homeobox sequence was chosen, aiming to reduce background staining via off-target binding to other homeobox domain-containing proteins. Figure 24b shows that that the probe synthesised from this construct enables the

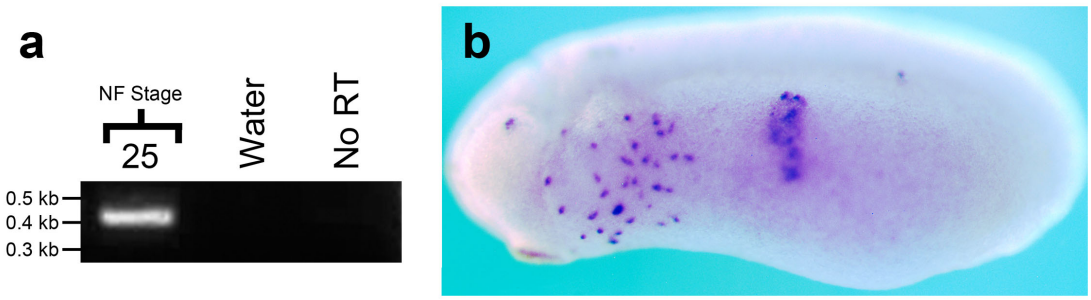

Figure 24: Generating an *in situ* hybridisation probe to analyse the spatial expression pattern of the neural crest marker *phox2a*. (a) RT-PCR of stage 25 cDNA using primers to amplify non-homeobox domain *phox2a* sequence, (b) spatial expression pattern of *phox2a* at the tailbud stage in *Xenopus tropicalis.* Lateral view of stage 23 embryo.

detection of the developing noradrenergic neurons from the neural crest in *Xenopus tropicalis.*

3.3.6 The effects of *xN1-Src* and *xN3-Src* knockdown on the expression of neural and neural crest markers

To investigate the effects of AMO A on neurogenesis that may explain the observed defects in locomotion, the expression of neurogenic markers *n. tubulin* and *sox3* were analysed in unilaterally injected embryos – comparing the injected and uninjected hemispheres.

75% of embryos showed reduced *n. tubulin* expression in the hemisphere injected with AMO A relative to the uninjected hemisphere (n=12), with the remaining 17% and 8% of embryos showing reduced *n. tubulin*

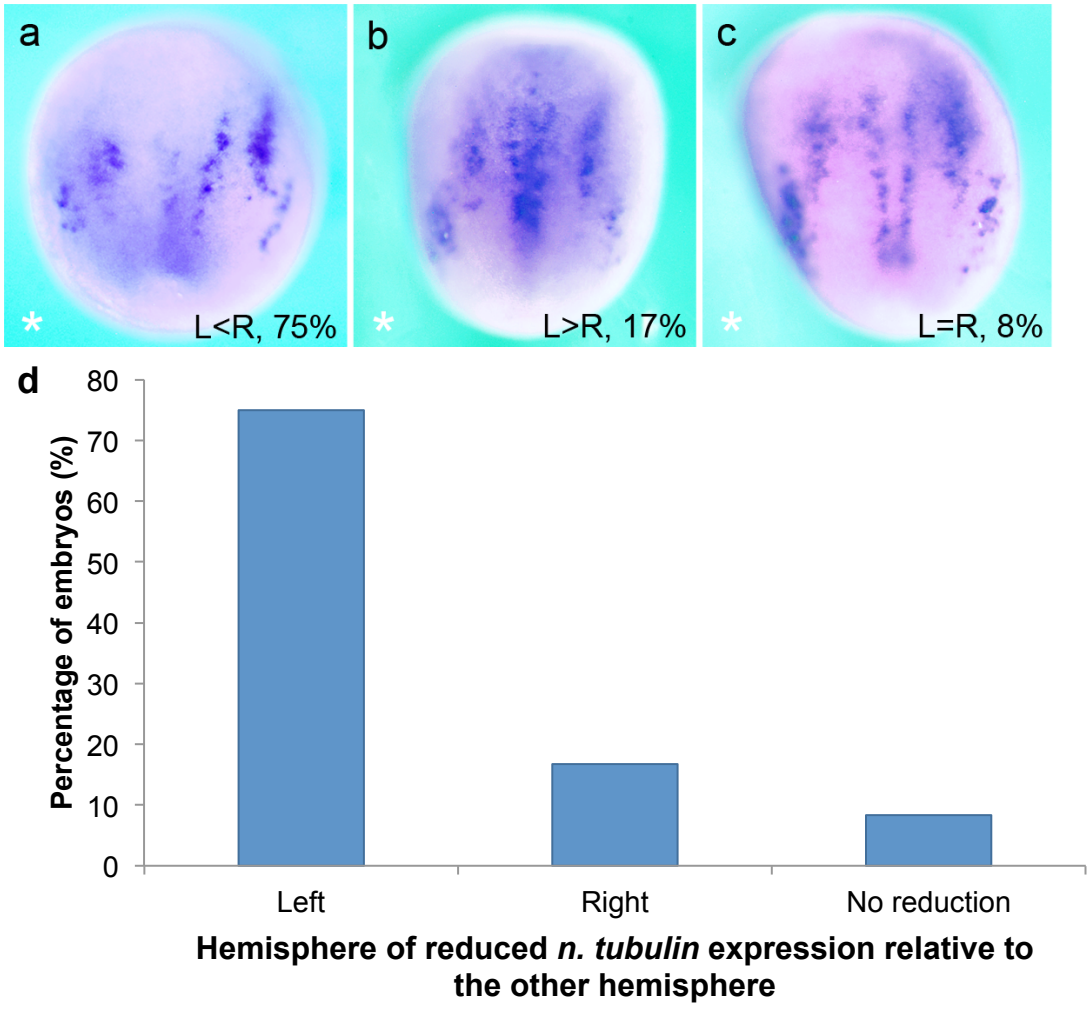

Figure 25: The effect of neural *Src* knockdown on the expression pattern of *n. tubulin* in embryos injected in the left hemisphere. (a) loss of left hemisphere staining, (b) loss of right hemisphere staining, (c) loss of staining in neither hemisphere, (d) quantification of a-c. Dorsal views of neurula stage embryos. 14 embryos were analysed from a single set of fertilisations; therefore this data represents a single experiment.

expression in the right (uninjected) hemisphere or no reduction respectively (Figure 25). Reduced *n. tubulin* staining was observed across all three longitudinal domains that mark the motor neurons, interneurons and sensory neurons (shown in Figure 3, page 22).

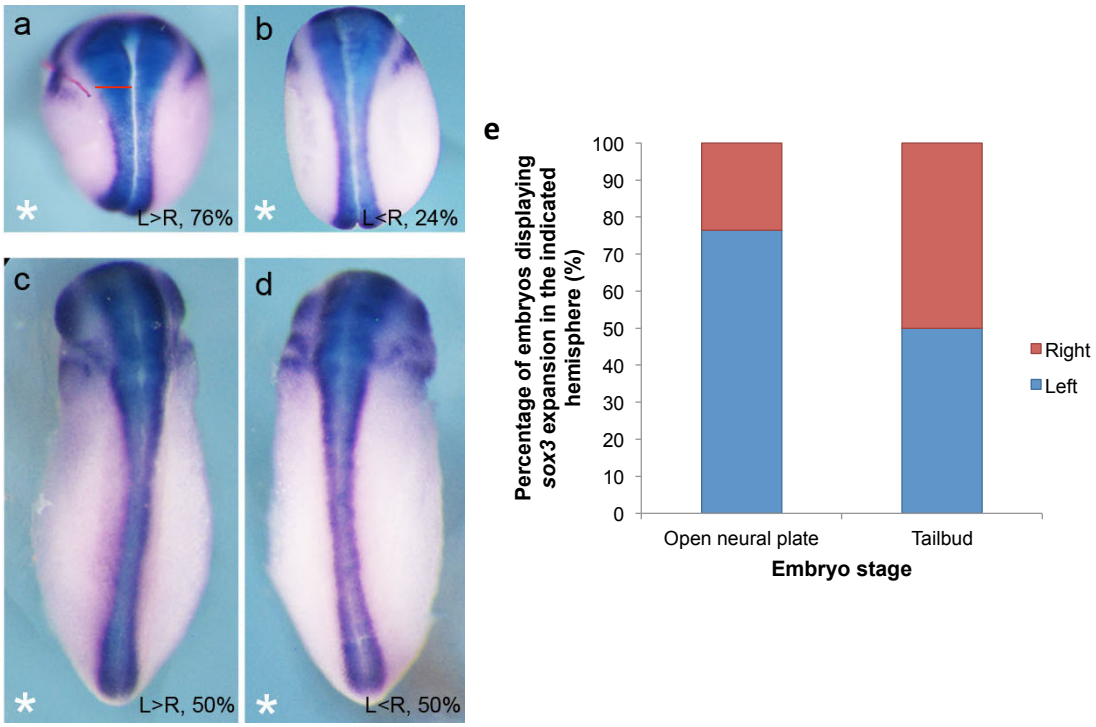

Figure 26: The effect of neural *Src* knockdown on the expression pattern of *sox3* in embryos injected in the left hemisphere, measured using ImageJ. (a) expansion of *sox3* expression in the left hemisphere at neurula stage. Indicated by the red line is an illustration of how measurements of the width of the *sox3*-positive domain were taken. Please note that this is not an actual measurement. (b) expansion of *sox3* expression in the right hemisphere at neurula stage, (c) expansion of *sox3* expression in the left hemisphere at tailbud stage, (d) expansion of *sox3* expression in the left hemisphere at tailbud stage, (e) quantification of a-d. Dorsal views of neurula and tailbud stage embryos. 17 neurula stage embryos were pooled from two sets of fertilisations and 7 tailbud stage embryos were used from one set of fertilisations, therefore these data represent single experiments.

As the expression of the neural differentiation marker *n. tubulin* was reduced upon neural *Src* knockdown, AMO A-injected embryos were analysed for a corresponding effect on the expression of *sox3* as a reduction in the number of proliferating neural precursors or an expansion of the number of proliferating neural precursors at the expense of differentiation would both explain this observation. In each hemisphere, the width of the *sox3*-positive domain was measured using ImageJ as a straight line (as indicated by the red line in Figure 26a), at a point at which there was a clear distinction between stained and unstained cells. The the ratio of the widths of these domains was then calculated for each

embryo, where a value of one represents equally sized domains and a value greater than one represents a larger *sox3* positive domain in the injected hemisphere and vice versa. When a cut off for expanded *sox3* expression was defined as a 1% difference between the widths in the two hemispheres (a ratio of the injected:uninjected widths of 1.01 or above), *sox3*-domain expansion was identified in the AMO A-injected hemisphere

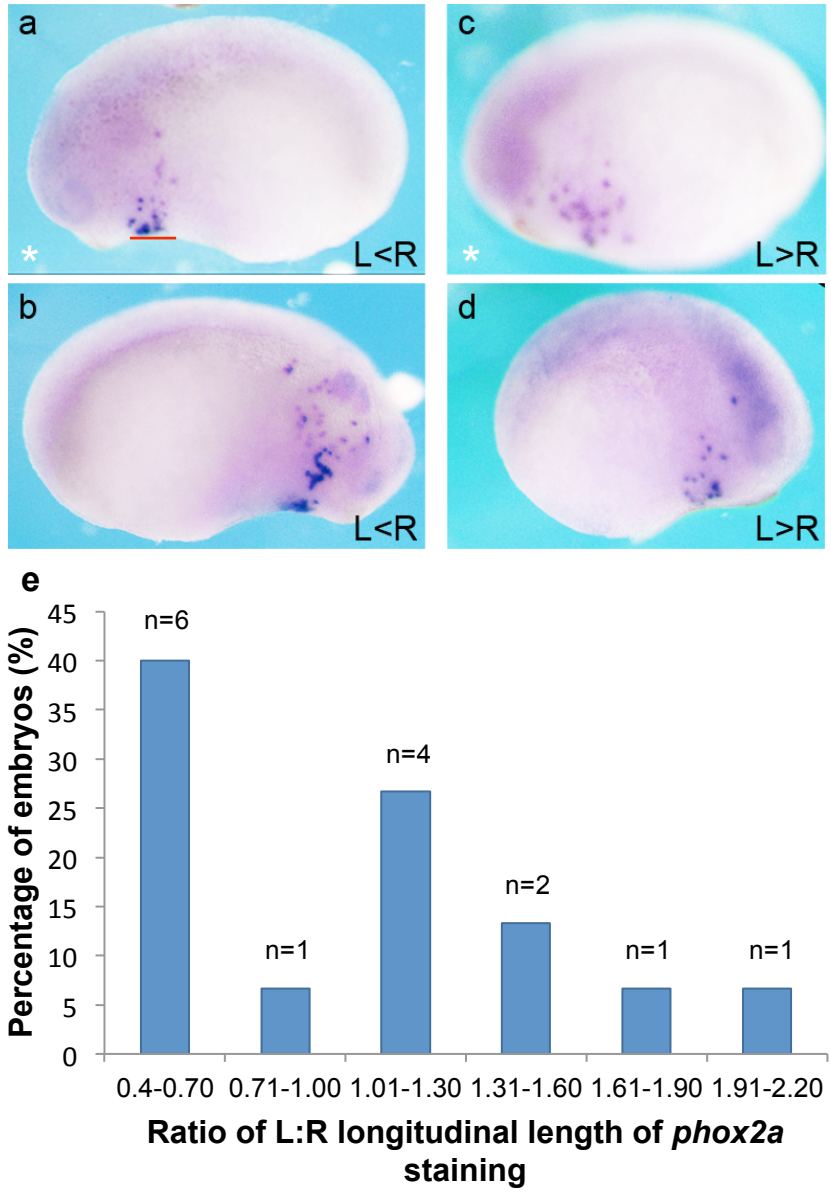

Figure 27: The effect of neural *Src* knockdown on the expression pattern of *phox2a* in embryos injected in the left hemisphere, measured using ImageJ. (a) and (b) reduced length of *phox2a* domain in the left hemisphere. Indicated by the red line in (a) is an illustration of how measurements of the *phox2a*-positive domain were taken. Please note that this is not an actual measurement. (c) and (d) reduced length of *phox2a* domain in the right hemisphere, (e) quantification of a-d phenoptypes. Lateral views of early tailbud stage embryos. 15 embryos were pooled from two sets of fertilisations; therefore these data represent a single experiment.

(left) of 76% of embryos relative to the uninjected hemisphere, compared to 24% of embryos that showed expansion in the uninjected hemisphere relative to the injected hemisphere at neurula stages (Figures 26a, 26b, 26e). When the threshold of expansion was increased to 10% (a ratio of 1.1), 71% of embryos displayed expansion in the left hemisphere and 18% and 12% of embryos showed expansion in the uninjected (right) hemisphere and neither hemisphere respectively (n=17). At early tailbud stage, when neurulation is complete, expansion of the *sox3*-positive domain was detected in both hemispheres in equal proportions (Figures 26c-e, n=8).

ImageJ was also used to measure the longitudinal length of the *phox2a* expression domain at the surface of either side of the embryo from the first to the last cell along the rostrocaudal axis at early tailbud stages (indicated by the red line, Figure 27a). The ratios of the sizes of these domains were calculated as described for the *sox3* analyses. 40% of embryos showed ratios of 0.4-0.7, a higher proportion of embryos than the 27% of embryos with ratios of 1.31-2.20 (n=15), therefore more embryos exhibited a smaller *phox2a* positive domain in the injected hemisphere when sizes of the two domains differed by more than 30%.

Embryos were injected with AMO A in eight injection sessions. Control embryos were either injected with control AMOs, water, or incubated in ficoll in seven of these sessions. Across these experiments, a death rate of 39% was observed in AMO A-injected embryos, higher than 30% of control AMO or water-injected embryos and 23% of ficoll control embryos.

3.3.7 *xN1-Src* overexpression

To analyse the function of *xN1-Src* and *xN3-Src in vivo*, mRNA was transcribed *in vitro* for overexpression analyses in *Xenopus* embryos. *Xenopus laevis xN1-Src* mRNA was transcribed from *xN1-Src*-pCS2+ (cloned by Philip Lewis (thesis, 2014)).

Unilateral and bilateral *xN1-Src* mRNA microinjection yielded no obvious phenotypic effects on *Xenopus laevis* or *Xenopus tropicalis* embryos (data not shown). Embryos microinjected unilaterally were analysed for the spatial expression patterns of the neural markers *n. tubulin* and *sox3* and the neural crest marker *phox2a* to assess for subtle changes in neurogenic gene expression between the injected and uninjected hemispheres that did not result in phenotypic defects.

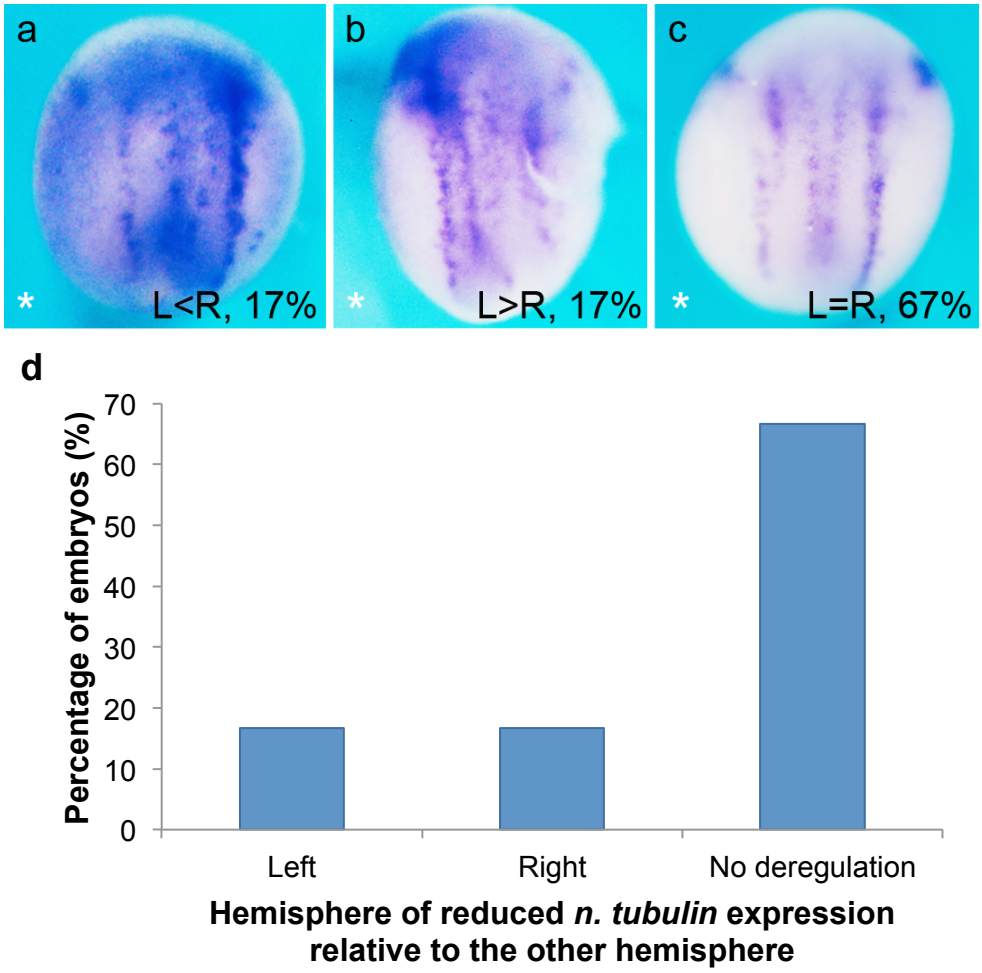

Figure 28: The effect of *xN1-Src* overexpression on the expression pattern of *n. tubulin* in embryos injected in the left hemisphere. (a) loss of left hemisphere staining, (b) loss of right hemisphere staining, (c) loss of staining in neither hemisphere, (d) quantification of a-c. Dorsal views of neurula stage embryos. 12 embryos were analysed from a single set of fertilisations; therefore these data represent a single experiment.

In the *xN1-Src* mRNA-injected hemisphere (the left hemisphere), there was no effect on the spatial expression pattern of *n. tubulin*, with an equal

proportion embryos showing reduced *n. tubulin* expression each of the two hemispheres relative to the other (17%) with the remaining 67% of embryos showing no relative reduction in either hemisphere (figure 28, n=12).

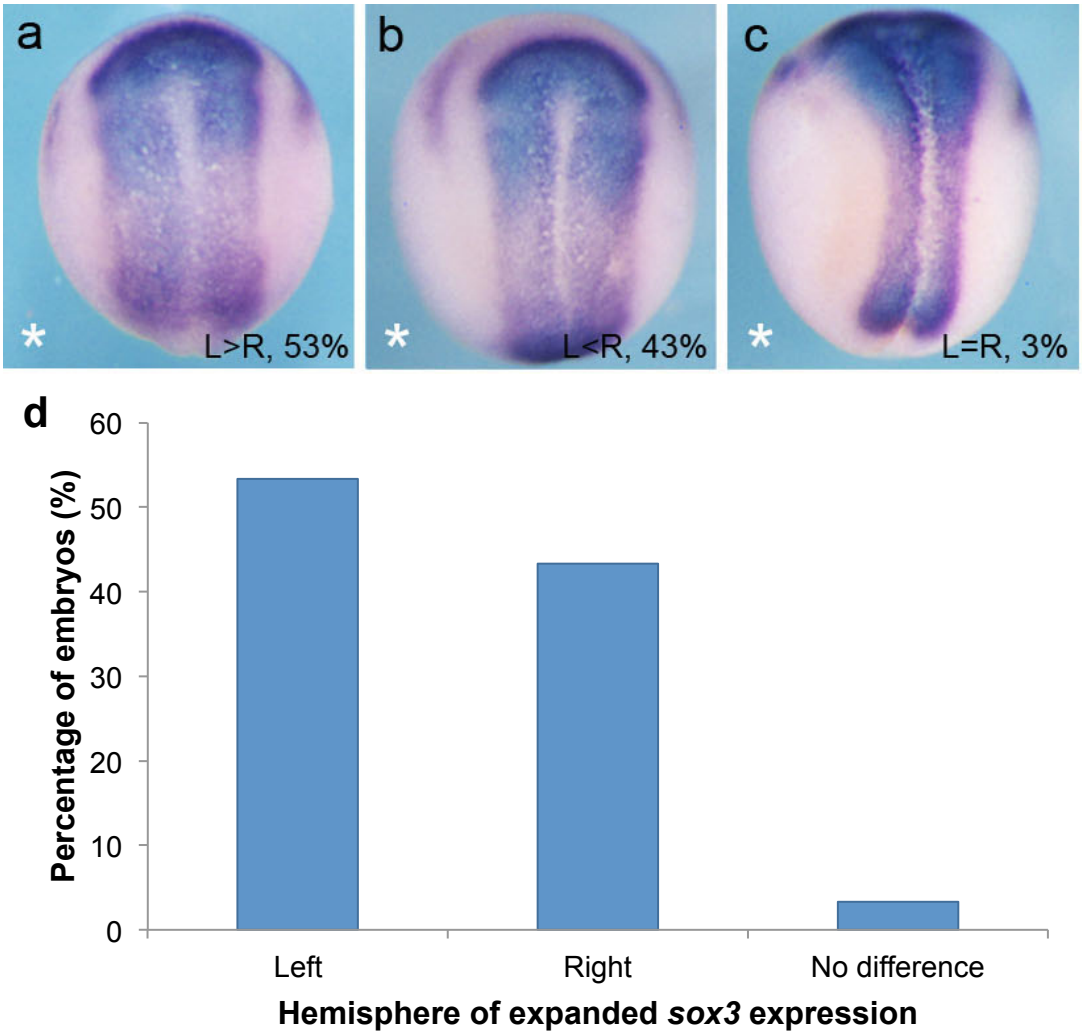

Figure 29: The effect of *xN1-Src* overexpression on the expression pattern of *sox3* in embryos injected in the left hemisphere, measured using ImageJ. (a) expansion of *sox3* expression in the left hemisphere at neurula stage, (b) expansion of *sox3* expression in the right hemisphere at neurula stage, (c) expansion of *sox3* expression in neither hemisphere at neurula stage, (d) quantification of a-c. Dorsal views of neurula stage embryos. 30 embryos were analysed from a single set of fertilisations; therefore these data represent a single experiment.

In embryos injected unilaterally with *xN1-Src* mRNA, 10% more embryos showed mediolateral expansion of the *sox3* expression domain (measured as described previously), which may represent a subtle difference in the expression pattern, with 53% and 43% of embryos

showing expansion in the left and right hemispheres respectively (Figure 29, n=30).

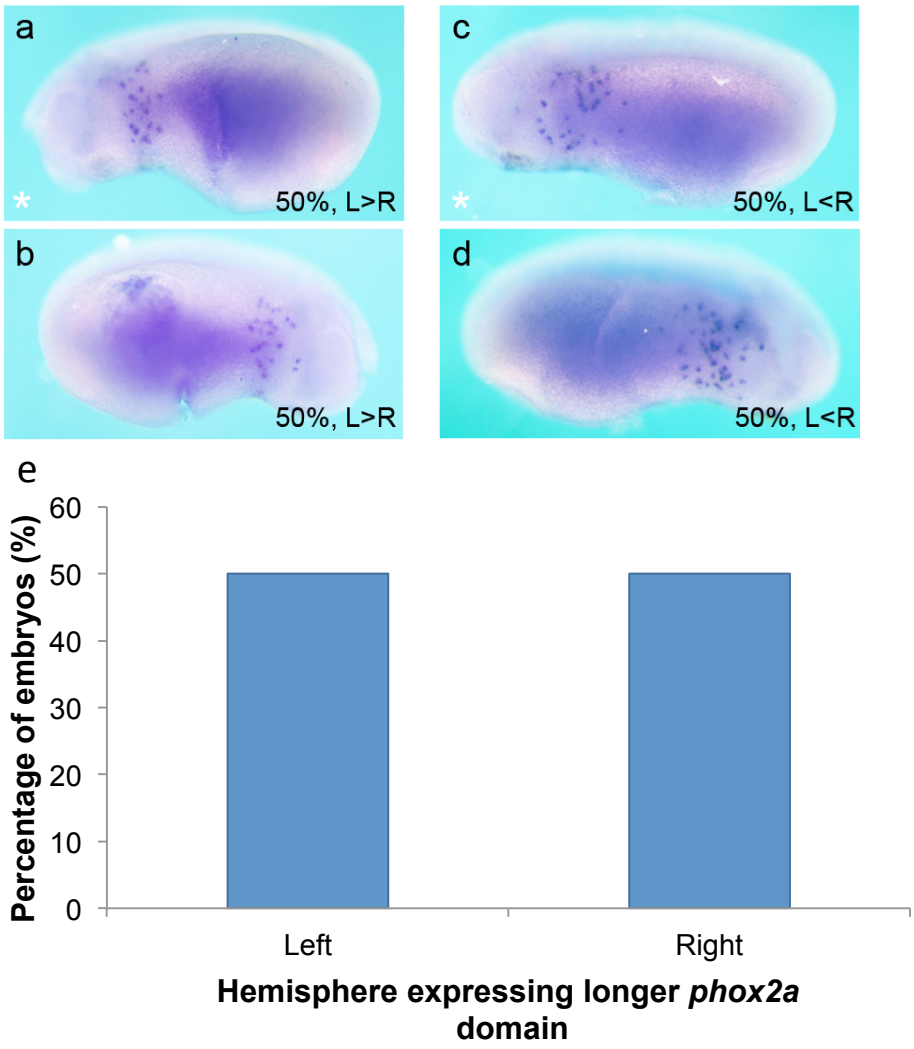

Figure 30: The effect of *xN1-Src* overexpression on the expression pattern of *phox2a* in embryos injected in the left hemisphere, measured using ImageJ. (a) and (b) increased length of *phox2a* domain in the left hemisphere, (c) and (d) increased length of *phox2a* domain in the right hemisphere, (e) quantification of a-d phenoptypes. Lateral views of early tailbud stage embryos. 8 embryos were analysed from a single set of fertilisations; therefore these data represent a single experiment.

To compare the lengths of the *phox2a* positive domains in the left and right hemispheres of *xN1-Src* mRNA-injected embryos, it was necessary to calculate the longitudinal length of the domain as a proportion of the embryo length (owing to differences in magnifications). When the ratios of these proportions were compared, it was observed that *xN1-Src* mRNA had no effect on the length of the *phox2a* positive domain, as 50% of embryos showed expansion in each of the two hemispheres (n=8).

Embryos were injected unilaterally with *xN1-Src* mRNA or incubated in ficoll across three injection sessions. A higher death rate was observed in *xN1-Src* mRNA injected embryos (24%) than the control embryos (16%), though this may be attributable to the injection process, rather than resulting from *xN1-Src* over-expression.

3.3.8 *xN3-Src* cloning

xN3-Src was cloned from stage 15 cDNA synthesised by random hexamer priming. Primers amplifying the full coding sequence were designed for Phusion polymerase-mediated PCR, to generate an error-free template. This product was then cloned into the pGEM T-Easy vector, from which directional cloning was achieved by amplifying the product using PCR primers containing restriction enzyme sites also present in the pCS2+ plasmid. Both the plasmid and PCR product were digested with these enzymes, purified and ligated together to produce cloned *xN3-Src*, from which full-length, polyadenylated transcripts were synthesised for embryo microinjection.

Sequencing of the pCS2-*xN3-Src* construct revealed an A-G point mutation present at nucleotide position 357, encoding a D111N missense mutation in the predicted amino acid sequence.

3.3.9 *xN3-Src* overexpression

Across three injection sessions, 1ng and/or 500pg *xN3-Src* mRNA was injected bilaterally, with control embryos injected with an equal volume of water and additional control embryos incubated in ficoll. Bilaterally over-expressing *xN3-Src* mRNA resulted in the loss of eye pigmentation and/or reduced eye size (Figure 31a-c). With increased *xN3-Src* dose from 500pg to 1ng, there was a dose-dependent increase in the number of embryos displaying reduced eye pigmentation and/or size. Unilateral and bilateral reduction in eye pigmentation and/or size was each observed in 7% of embryos injected with 500pg *xN3-Src* mRNA, whilst

9% and 39% of embryos injected with 1ng *xN3-Src* mRNA displayed these phenotypes respectively, compared to water-injected embryos (2% and 2% of embryos) and ficoll control embryos (2% and 4% of embryos, respectively) (Figure 31d).

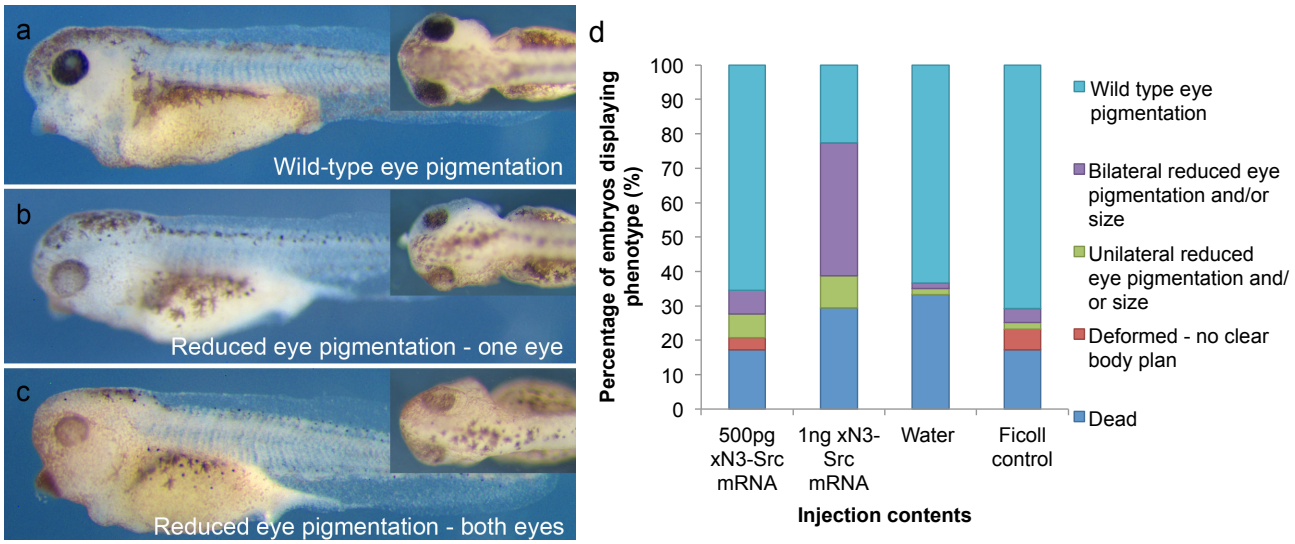

Figure 31: The effect of *xN3-Src* overexpression on *Xenopus tropicalis* eye pigmentation in bilaterally injected embryos. (a) wild type eye pigmentation, (b) unilateral reduced eye pigmentation (lateral and dorsal views of separate embryos), (c) bilateral reduced eye pigmentation, (d) quantification of phenotypes shown in a-c. Lateral and dorsal views of stage 40 embryos. Embryos were injected and analysed from three fertilisations; in two injection sessions *xN3-Src* mRNA was injected in the two quantities, alongside water and embryos were injected with ficoll. In the third injection session embryos were injected with 1ng *xN3-Src* mRNA, water or incubated in ficoll. In total, 29 embryos were injected with 500pg *xN3-Src* mRNA, 75 with 1ng *xN3-Src* mRNA, 60 with water and 99 were incubated with ficoll.

There was an increased death rate from 17% to 29% observed with increased dose of *xN3-Src* mRNA, higher than the ficoll control embryos (17%), however this was lower than the death rate of water-injected embryos (33%), therefore it is unlikely that microinjection of *xN3-Src* mRNA is detrimental to embryo survival, beyond the microinjection process itself.

Xenopus tropicalis embryos were injected unilaterally in the left hemisphere with *xN3-Src* mRNA in two injection sessions. In each set of injections embryos were either injected with an equal volume of water or incubated in ficoll. A death rate of 14% was observed in ficoll control embryos, 17% of water-injected embryos and 20% of *xN3-Src*-injected embryos.

Unilateral *xN3-Src* mRNA injection had no effect on the spatial expression pattern of *n. tubulin*, with 40% of embryos showing reduced expression in each hemisphere relative to the other and the remaining 20% of embryos showing reduction in neither hemisphere relative to the other (n=10, Figure 32).

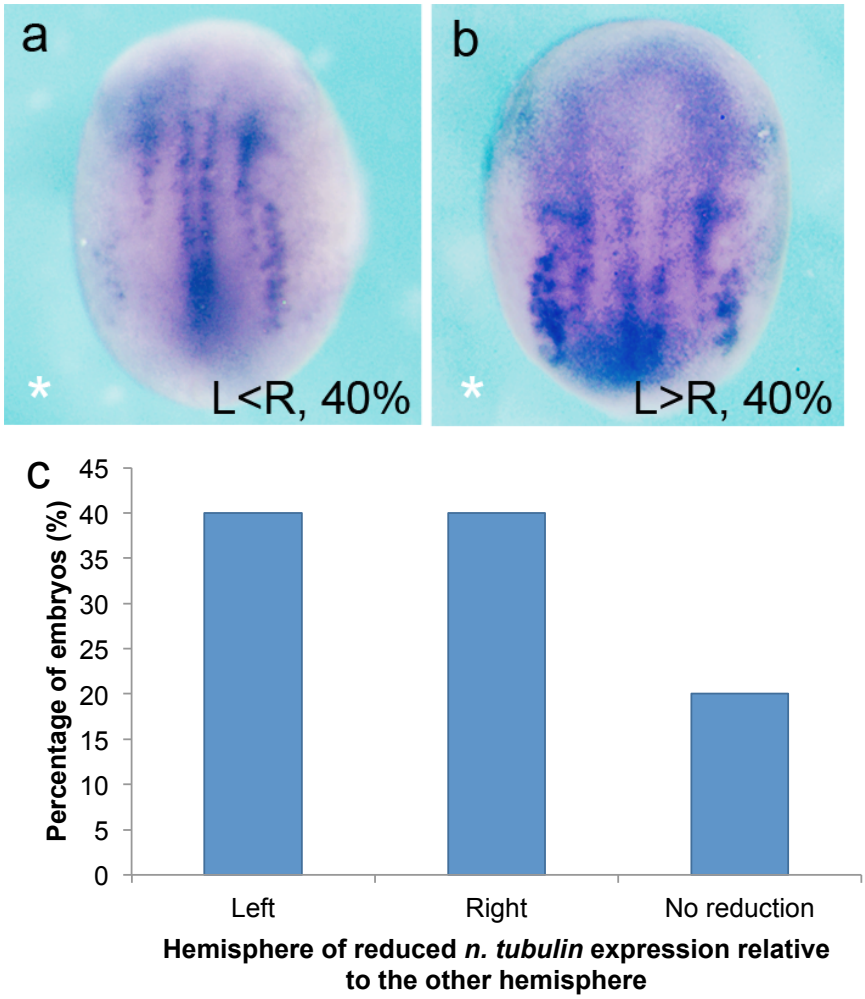

Figure 32: The effect of *xN3-Src* overexpression on the expression pattern of *n. tubulin* in embryos injected in the left hemisphere. (a) loss of left hemisphere staining, (b) loss of right hemisphere staining, (c) quantification of the dorsal views of neurula stage embryos. 10 embryos were analysed from a single set of fertilisations therefore these data represent a single experiment.

By measuring the width of the anterior neural plate *sox3* expression domains as described previously in embryos injected unilaterally with *xN3-Src* mRNA, it was observed that 44% of embryos show expanded expression in each of the right and left hemispheres, relative to the other, with the remaining 11% of embryos showing expansion of the *sox3*

expression domain in neither hemisphere (n=9, Figure 33), indicating that there was no effect of *xN3-Src* mRNA overexpression on the size of this domain.

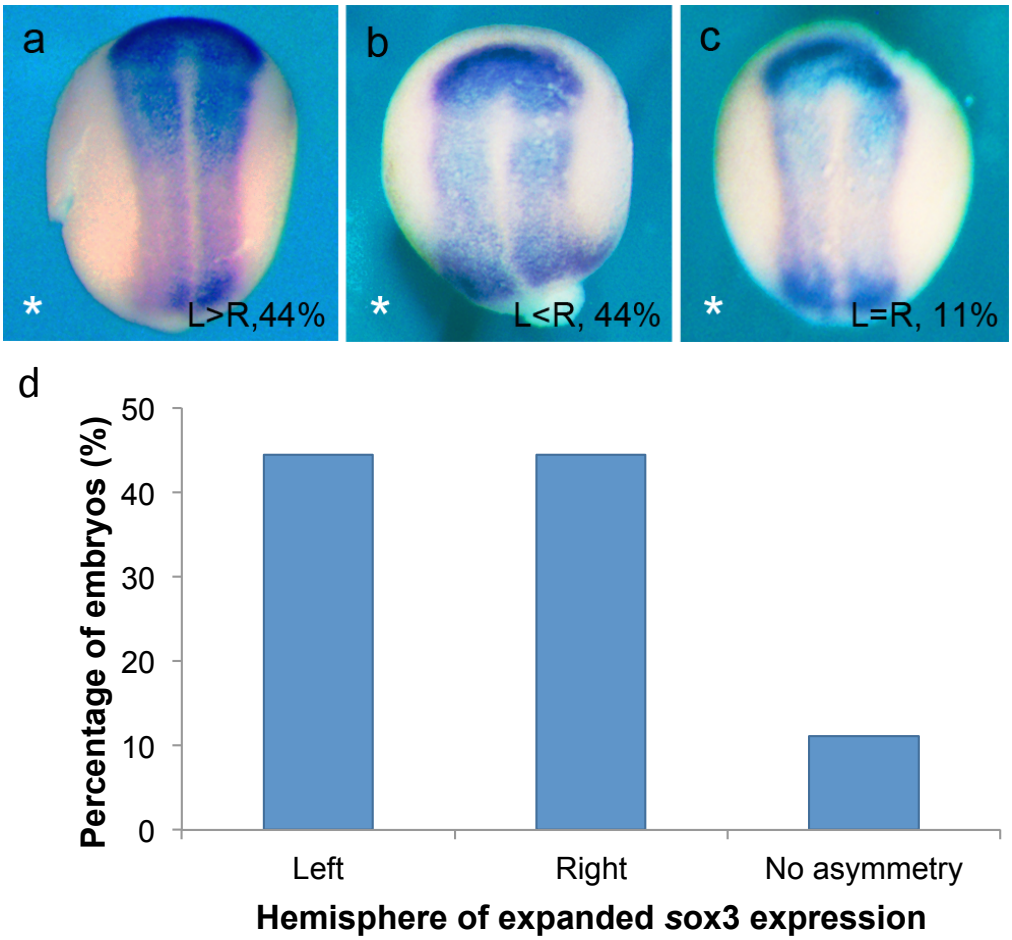

Figure 33: The effect of *xN3-Src* overexpression on the expression pattern of *sox3* in embryos injected in the left hemisphere, measured using ImageJ. (a) expansion of *sox3* expression in the left hemisphere at neurula stage, (b) expansion of *sox3* expression in the right hemisphere at neurula stage, (c) expansion of *sox3* expression in neither hemisphere at neurula stage, (d) quantification of a-c. Dorsal views of neurula stage embryos. 9 embryos were analysed from a single set of fertilisations; therefore these data represent a single experiment.

Figure 34 shows that at tailbud stage, the *phox2a* expression domain was reduced in the injected hemisphere relative to the uninjected hemisphere in 70% of embryos, compared to 30% of embryos that showed a reduction in *phox2a* staining in the uninjected hemisphere relative to the

injected hemisphere. 10% of embryos showed no change in the expression of *phox2a* (n=10).

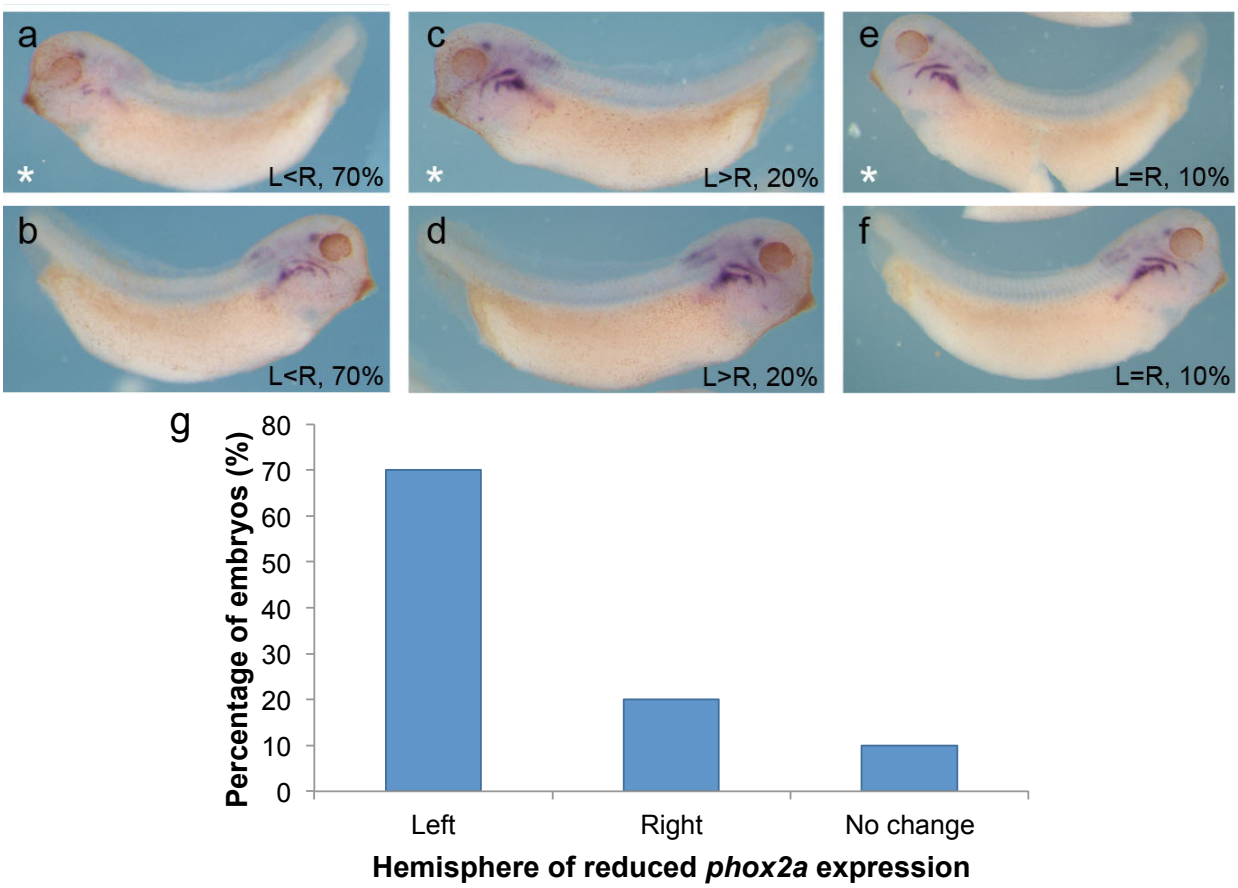

Figure 34: The effect of *xN3-Src* overexpression of the spatial expression pattern of *phox2a* in tailbud stage embryos injected into the left hemisphere. (a) and (b) loss of left hemisphere staining, (c) and (d) loss of right hemisphere staining, (e) and (f) loss of staining in neither hemisphere, (g) quantification of phenotypes shown in a-f. Lateral views of stage 24 embryos. 10 embryos were analysed from a single se of fertilisations; therefore these data represent a single experiment. *phox2a* expression domains were not measured using ImageJ for this experiment.

3.3.11 Generating the necessary reagents to perform CRISPR-mediated homologous recombination and excision of the *N1-Src* microexon in zebrafish embryos

PCR using partially overlapping primers yielded template DNA from which gene-specific sgRNA was transcribed *in vitro* (the sequence of which was used according to Nakayama et al. (2014)), for microinjection alongside Cas9 protein (synthesised by Olga Moroz, according to Gagnon et al. (2014)). To specifically target *N1-Src* whilst leaving *C-Src* unaffected, CRISPR-mediated homologous recombination was used. By designing and co-injecting a ssDNA oligo containing the DNA sequence 5' and 3' to

but not including the *N1-Src* microexon, alongside sgRNA and Cas9 protein, the aim was to induce homologous recombination at the N1-Src locus, excising the N1-Src microexon whilst leaving the surrounding sequence intact.

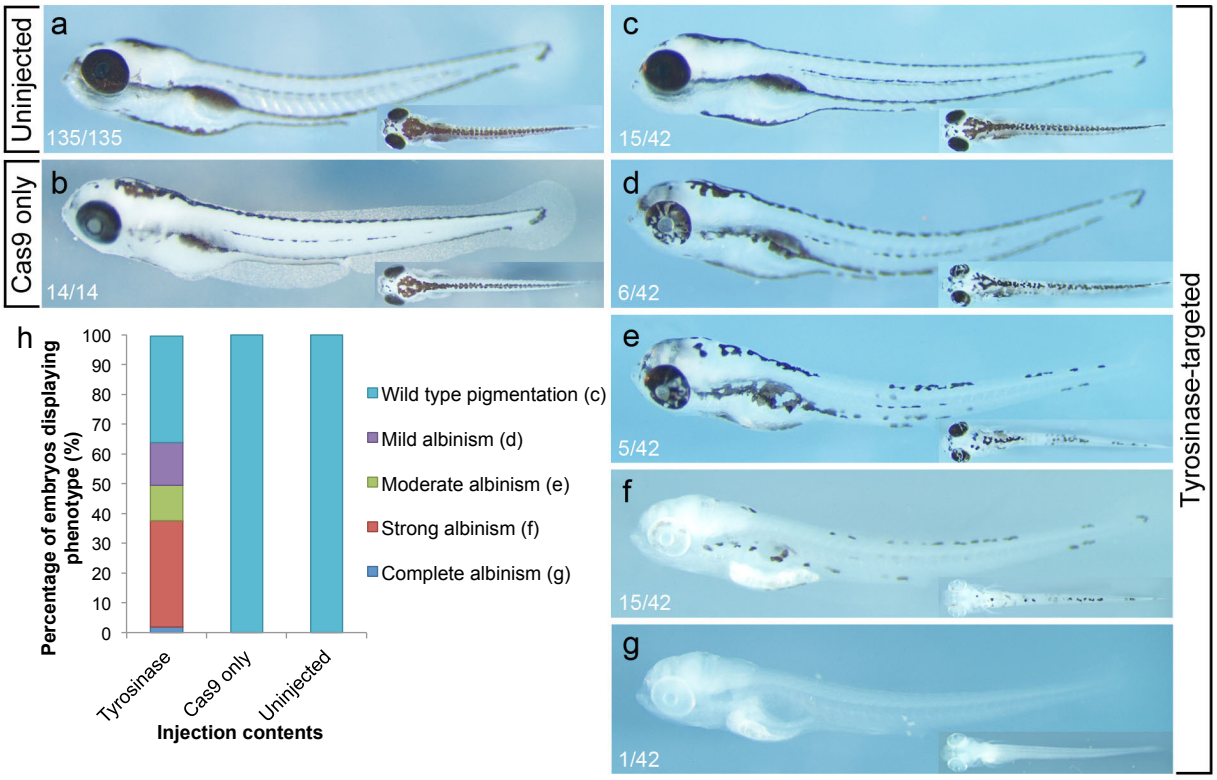

Figure 35: Testing the Cas9 protein and recruiting sgRNA sequence by targeting *tyrosinase*. (a) uninjected WT phenotype, (b) Cas9 only injected WT phenotype, (c) Cas9 and sgRNA injected WT phenotype, (d) mild albinism phenotype, (e) moderate albinism phenotype, (f) strong albinism phenotype, (g) complete albinism phenotype, (h) quantification of a-g. WT=wild type. Lateral and dorsal views of embryos at 5 days post fertilisation. This experiment was performed once.

To test the efficacy of the Cas9 protein and the ability of the *in vitro* transcribed sgRNA molecules to guide gene targeting, the *tyrosinase* gene was targeted (designed and synthesised by Elliot Jokl). Tyrosinase is necessary to generate the pigmentation seen in embryos from approximately two days post fertilisation (Burgoyne et al. 2015), and in its absence, albinism results. Using sgRNA targeting this gene, co-injected with Cas9 protein, albinism was observed to varying severity in the F0 generation, with most of the successfully targeted embryos showing strong albinism (35%, n=42, Figure 35).

In *N1-Src* targeted embryos, no obvious phenotype was observed (data not shown). Embryos were screened for the desired mutation by analysing the size of the genomic locus using PCR. The wild type (WT) sequence contains the 18 base pairs encoding the N1-Src microexon and using the PCR primers used here, produces a fragment of 184 base pairs (indicated by the black arrow on Figure 36). Following homologous recombination, the locus should contain 18 fewer base pairs, once the microexon has been excised. In embryos injected with the necessary components to guide homologous recombination-mediated *N1-Src* excision, a PCR product can be detected that is smaller than the wild type product seen in untargeted embryos (indicated by the grey arrow on Figure 36), which may represent the product of this recombination event. To confirm that homologous recombination has taken place, it is necessary to sequence the products. Due to time restrictions, it was not possible to do so during this project.

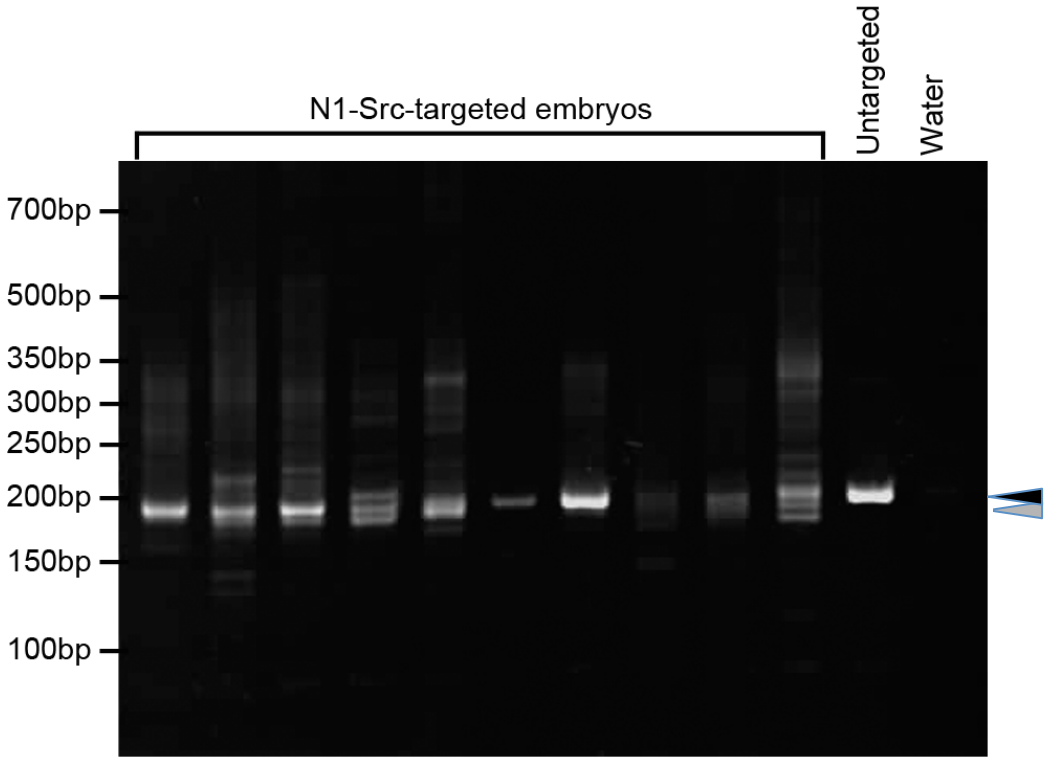

Figure 36: Screen for excision of the *N1-Src* microexon. PCR amplification of a region of the *Src* gene that contains the *N1-Src* microexon yields a product of the size expected for the wild type gene (indicated by the black arrow) and smaller fragments, which may represent *N1-Src* microexon excision, creating a product that is 18 base pairs shorter (indicated by the grey arrow). This experiment was performed with different embryos but in a single experiment.

Discussion

3.3.12 Antisense-morpholino oligo knockdown of neural *Src* splice variants

Figure 22 shows that in *Xenopus tropicalis* the AMOs designed by Philip Lewis can be used singularly or in combination to knockdown the expression of both neural *Src* splice variants, whereas they have previously been used only in combination (Lewis, 2014). It was not possible to specifically target the *xN1-Src* variant using AMO A, as was predicted in Table 7 however by reducing the number of AMOs injected, we may hypothesise that the probability of off-target effects by sequence homology to other transcripts decreases.

It was not possible to demonstrate the specificity of the LNA probe using AMO-injected embryos. Whilst this may indicate non-specific binding of the probe to other transcripts in the embryo, it may also indicate that upon AMO injection, the cells that would ordinarily express these variants retain unspliced pre-mRNA (Eisen & Smith 2008). This unspliced mRNA may be the target of probe binding. Though the RT-PCR on AMO-injected embryos did not detect any such products, the intervening intron retained due to the AMO binding may be too large for detection using the PCR settings used, though the possibility of off-target binding cannot be overlooked. This highlights the necessity for generating an *N1-Src* knockout zebrafish line, in which the spatial expression pattern shown in wild type (WT) embryos can be verified by *in situ* hybridisation in mutant embryos. It is possible that CRISPR could be used to demonstrate the specificity of the *Xenopus* neural *Src* probes. Due to the likelihood of mosaicism, whole-organism functional analyses would be difficult in embryos subjected to CRISPR-mediated homologous recombination, however mosaic organisms could be used for LNA probe validation, as the *in situ* hybridisation signal should be reduced in clonal patches.

To study the isoforms in isolation, splice-blocking AMOs used here (that should not affect synthetic mRNA synthesised from a spliced cDNA

template), could be co-injected with ‘rescue’ levels of each variant, though the amounts of mRNA injected would have to be demonstrated to be physiologically relevant, otherwise the effects of knockdown of one variant and the overexpression of the other may be observed. Equally, rescue experiments of this nature cause the expression in the entire embryo, including tissues in which endogenous expression does not occur, potentially causing additional artefacts. Therefore, we remain unable to cleanly knockdown the expression of each neural *Src* variant in isolation in order to study its function, whilst leaving the expression of the other unaffected, highlighting the need for a knockout organism.

3.3.13 The effects of *xN1-Src* and *xN3-Src* knockdown on the locomotive responses of *Xenopus tropicalis* to touch stimuli

In embryos injected with AMO A, shorter distances travelled and a higher number of ‘twitch’ rather than ‘dart’ swimming phenotypes were observed in response to a touch stimulus to the tail, in agreement with previous data (Lewis 2014). The distance travelled by embryos in response to the touch stimulus was measured as a straight line, which does not necessarily reflect the absolute movement of the embryo, but is indicative of whether the embryo was able to respond normally, by the swimming away from the stimulus.

An additional caveat of this experimental approach was that some embryos exhibited different swimming behaviour when stimulated to the behaviour observed outside of the experimental procedure; showing little response to the touch stimulus when normal swimming behaviour had previously been observed, and therefore were discounted. This may be due to inconsistencies in the touch stimulus intensity as very light stimuli may provoke a different response. Perhaps this reflects a need for repeated stimulations per embryo and acclimatisation of the embryos to the surroundings before the experimental stimulation takes place.

3.3.14 *xN1-Src* and *xN3-Src* knockdown causes expanded expression of the proliferative neural plate marker *sox3* and decreased expression of the differentiation markers *n. tubulin* and *phox2a*

In accordance with the findings of Philip Lewis (Thesis, 2015), expansion of s*ox3* expression and reduced *n. tubulin* expression were observed in the injected hemispheres of embryos injected unilaterally with AMO A. To define an arbitrary cut-off of expansion, the ratios of left to right *sox3* positive domain widths were compared and analysed for an increase of 1% relative to the other domain. Increasing the cut off to a 10% change reduced the percentage of embryos showing expansion in the AMO A-injected hemisphere by 5% but also reduced the percentage of embryos showing expansion in the uninjected hemisphere by 6%, with the percentage of embryos showing no asymmetry increasing. The physiologically relevant threshold for the expansion in open neural plate proliferation is unknown and therefore any threshold used remains arbitrary, however we can conclude that an expansion has indeed occurred in AMO A-injected hemispheres. In these experiments the width of the longitudinal domain of *sox3* expression was measured at a point in the anterior neural plate where stained and unstained cells could be distinguished. If the expansion is irregular along the neural plate, measuring the area of the *sox3* positive domain rather than the width at one point may disregard this irregularity and reflect more reproducibly the size of the proliferative neural plate.

In tailbud stage embryos, once the neural plate had rolled up and fused to form the neural tube, no difference was detected between the widths of the *sox3*-positive domain on either side of the midline. It is possible that at this stage, measuring the dorsal width of the neural tube on either side of the midline is of insufficient sensitivity for measuring this three dimensional structure.

In accordance with the increased size of the proliferative domain (measured as the domain of *sox3* expression), reduced *n. tubulin*

expression was observed in the AMO A-injected hemispheres at neurula stages and a subtle reduction was observed in the longitudinal length of the *phox2a* positive domain in early tailbud stage embryos. We may hypothesise that the decrease in expression of markers of neural and neural crest differentiation *n. tubulin* and *phox2a*, accompanied by the increase in the expression of the proliferative marker *sox3* reflects a role of neural Src isoforms in neural differentiation.

3.3.15 The effect of *xN1-Src* and *xN3-Src* overexpression on embryo morphology and the spatial expression pattern of *sox3, n. tubulin* and *phox2a*

Existing data has shown that *xN1-Src* transfection is able to induce neurite-like projections in cell culture (Lewis 2014) and its high levels correlate with improved prognosis of neuroblastoma cancer (Bjelfman et al. 1990), however there was no effect of microinjecting mRNA encoding xN1-Src on embryo morphology or on the expression of neural or neural crest markers (or possibly a subtle effect in the case of *sox3*), despite mammalian *N1-Src* mRNA microinjection being able to induce craniofacial defects and embryo posteriorisation in *Xenopus laevis* (Lewis 2014).

xN3-Src was cloned into the pCS2+ plasmid, from which synthetic mRNA was transcribed *in vitro* for overexpression analyses in *Xenopus* embryos. Sequencing revealed a D111N missense mutation present in the cloned product, which may represent a PCR error as the mutation occurs at a highly conserved residue, however Phusion polymerase was used throughout the cloning process due to its proofreading capability, and therefore this mutation may represent a naturally occurring polymorphism at this locus. It may be hypothesised that if this sequence discrepancy does represent a PCR error, due to the position of the mutated amino acid at the extreme C-terminus, where there is no recognised conserved domain, it would not alter the function of the product in the overexpression analyses. However, this cannot be ignored and a

construct of the wild type sequence which can be aligned to the published genomic sequenced and identified by Philip Lewis (thesis, 2014) should be cloned for the transcription and injection of synthetic mRNA to confirm that the effects on eye pigmentation and *phox2a* expression are also observed.

Further experiments are required to support the effects observed on locomotive responses, phenotypes and neural and neural crest marker expression profiles. Repeated experiments are essential to calculate the statistical significance of the effects observed here. Additionally, control morpholinos designed to target a transcript not expressed in *Xenopus tropicalis* and control mRNA, such as mRNA encoding *TdTomato* must be injected. This would control for the effect of microinjection and injection of morpholinos/mRNA. Comparing the AMO-injected embryos with control embryos should also be performed to control for natural differences/asymmetry that may occur between the two hemispheres. A time course RT-PCR analysis of AMO A-injected embryos should be performed to investigate the stages of development at which neural *Src* isoforms are knocked down and when expression is no longer inhibited, to predict which stages of neurogenesis are affected. Moreover, rescue experiments should be performed where mRNA encoding each of the splice variants is co-injected alongside the morpholino, however a caveat of this approach is that the mRNA would then be ubiquitously expressed throughout the embryo, rather than its restricted neural expression and thus may have different effects.

Whilst *sox3* and *phox2a* expression domains were measured using ImageJ (except for *xN3-Src* mRNA-injected embryos), *n. tubulin* expression changes were judged ‘by eye’ and therefore represent more subjective analyses. If clearer staining with less background was present, particularly in the case of *n. tubulin*, the individual cells or domains of expression could be counted or measured and compared. Due to time constraints, it was not possible to optimise these *in situ* hybridisations to a sufficient standard for these sorts of analyses.

3.3.17 Generating the necessary reagents to perform CRISPR-mediated homologous recombination and excision of the *N1-Src* microexon in zebrafish

In addition to analysing the effects of reduced protein levels in morphant embryos, such analyses could be performed in embryos of a null *N1-Src* knockout line, the generation of which may be possible in zebrafish using CRISPR/Cas9 -mediated homologous recombination at the *N1-Src* locus. It is advantageous to use this technology in zebrafish rather than *Xenopus* due to their faster generation time. This is required because a specific homologous-recombination-mediated mutation is required; a process of low efficiency (Chu et al. 2015), which is expected to generate the mutation at low frequency, thus forming mosaic organisms. Because of this, germ-line transmission is required to generate non-mosaic organisms with this specific mutation and therefore fast generation times are advantageous. Due to time constraints, such lines have not yet been created, however it been demonstrated that the reagents may be in place to do so.

In conclusion, these data support a role for the expression of neural *Src* variants in balancing proliferation and differentiation of neural precursors. In addition, the reagents required to study their functions are being developed, including morpholino oligos and the components required to generate an *N1-Src* knockout zebrafish line.

Chapter 4: Discussion

Expression analyses of the neural *Src* splice variants

Evolutionary expression analyses

Thus far, the most primitive species in which the *N1-Src* splice variant has been detected is the Catshark. The sharks and rays are the most ancient of the jawed fish, preceded in the evolution of the vertebrates only by the jawless fish – the Lampreys and Hagfish (Holland et al. 1994). In the absence of extensive transcriptome data, and once sufficiently annotated, the Lamprey and Hagfish genomes may offer further insight into the evolutionary emergence of *N1-Src.* By analysing the genomic sequence between exons 3 and 4 of *C-Src*, it may be possible to predict whether this region has the capacity to encode an N1-Src isoform, analogous to those that we see in more modern vertebrates.

The amino acid sequences encoded by *N1-Src* microexons vary in length at either five or six amino acids long, putatively caused by the loss or gain of a positively charged lysine residue at position two of the insert. Within this insert, we may predict that the highly conserved amino and carboxy-terminal arginine residues and the third position hydrophobic amino acids are more important for N1-Src function than other amino acids, for example by directing substrate specificity and binding. To study the importance of these conserved amino acids, overexpression analyses in *Xenopus* and zebrafish embryos could be performed in which the sequence encoding particular amino acids has been mutated.

The expression of N2-Src in mammals such as humans coincides with higher cognition that we see in such species. Whilst the expression of the *N3-Src* variant has only been detected in *Xenopus tropicalis,* the expression of *Src* splice variants of this nature may in fact be more widespread. If the function of this isoform relies upon the encoding of the N-terminal region, the unique domain, an intermediate sequence and then a stop codon, it may not be possible to detect the expression of

orthologous Src isoforms in other organisms using BLAST searches, particularly if the sequence between the end of exon 3 and the stop codon does not infer function and thus is less likely to be conserved. The *N3-Src* variant itself cannot be detected in *Xenopus tropicalis* using BLAST searches of ESTs, but only transcript-specific RT-PCR, therefore the available transcriptome data may be of insufficient sensitivity for detecting variants of this expression level.

The *N4-Src* variant was identified in the Catshark, and detected in the Stinkbird and the Tonguefish; representing species from the sharks, the ray finned fish and the teleosts. Thus far, a function of this isoform has not been elucidated, however its tissue-specific expression points to a neural function. Functional analyses are required to further the research into this variant. Using *Xenopus,* where a variant of this nature has not been detected, injecting synthetic mRNA encoding a hypothetical construct encoding N4-Src may provide some insight. Additionally, RT-PCR using primers that amplify the entire *Src* sequence may reveal isoforms that have not yet been identified.

Temporal and spatial analyses of *xN1-Src* and *xN3-Src*

Using RT-PCR, it was shown in this project that neural *Src* splice variants are upregulated during neural induction and that overexpression mRNA encoding the neural inducer Noggin leads to a putative and subtle upregulation of these variants in *noggin* mRNA-injected animal cap explants, compared to uninjected control explants. This is in-keeping with the observations made by Collett & Steele 1993 who showed *xN1-Src* upregulation in *Xenopus laevis* animal cap explants cultured with the adjacent mesoderm (the germ layer in which the secreted Noggin protein is synthesised). They observed that expression was activated from an undetectable baseline, whereas Figure 17c shows a basal level of expression in animal caps from uninjected embryos, however this may be due to a higher detection sensitivity of the RT-PCR used here. The basal levels of expression detected in the control animal caps may represent

maternally deposited *xN1-Src* and *xN3-Src* transcripts, which were detected in the RT-PCR time course analyses and the *in situ* hybridisation experiments; where it was shown that *xN3-Src* is localised to the animal hemisphere pre-MBT at stage 5; the future ectoderm, which in part gives rise to the neuroectoderm from which neural tissue derives.

As neurulation and neurogenesis proceed, the neural *Src* variants increase and peak in their expression levels and become localised to the neural plate as neurons become specified and the neural tube rolls up, fuses and lowers ventrally into the embryo to form the neural tube. This spatial restriction of *xN1-Src* expression during neurulation supports the results of Collett & Steele (1992), who showed that *xN1-Src* expression could be detected at much higher levels in the dissected *Xenopus leavis* neural plate, than the rest of the embryo.

Towards the end of gastrulation and during neurulation, primary neurogenesis is at its highest levels, with the majority of neural precursors being specified to differentiate into functional neurons and becoming post-mitotic (Wullimann et al. 2005). Previous data has shown that specific neural populations including Rohon Beard sensory neurons and primary motor neurons are specified during neurogenesis at gastrula stages (Lamborghini 1980), which then continues during neurula stages (Wullimann et al. 2005). At this point the neural differentiation marker *n. tubulin* can be detected as longitudinal domains marking the three neural subpopulations (motor neurons, interneurons and Rohon Beard sensory neurons (Nieber et al. 2009)). It is at these stages that the expression levels of neural *Src* splice variants are at their highest. These analyses of the temporal and spatial expression patterns therefore place the expression of these variants at the correct time and place for roles in primary neurogenesis.

Once primary neurogenesis is complete and the tail-flick response has become established at tailbud stage, stage 35 (Thuret et al. 2015; Roberts et al. 2000), the expression of *N-Src* variants decrease and

becomes restricted to the neural tube, the eye and neural crest. The expression of these variants then increases again at the beginning of secondary neurogenesis. This is a previously unstudied time point in which neurogenesis occurs in the neural tube via pathways that are highly conserved between primary and secondary neurogenesis and the neurogenesis that occurs in other vertebrate organisms (Wullimann et al. 2005). The spatial expression patterns of neural *Src* variants at these later stages have not yet been studied. To explore the expression of neural *Src* variants during secondary neurogenesis in more detail, later stages should be analysed, as the stages studied here represent early stages of secondary neurogenesis, beginning at stage 46 in *Xenopus* (Wullimann et al. 2005) and at 28hpf in zebrafish (Zhao et al. 2011). In the temporal analyses of primary neurogenesis, neural *Src* variants are expressed early in the neurogenic process however particularly in the case of the zebrafish, expression levels are at their highest relatively late in the primary neurogenic pathway; towards the end of neurulation at stage 19 in *Xenopus tropicalis* and at 24hpf in zebrafish. This may also be the case during secondary neurogenesis and therefore later stages of secondary neurogenesis should be analysed in detail. Such stages of secondary neurogenesis in which neurogenesis occurs in the hollow neural tube have been more closely likened to the neurogenesis of amniotes such as humans, than the neurogenesis that occurs in the open neural plate, thus highlighting the importance of their detailed analyses. However, the pathways that regulate primary and secondary neurogenesis show high conservation (Wullimann et al. 2005), therefore the relevance of studying nonamniotic primary neurogenesis, as a model of human neurogenesis should not be undervalued.

The spatial expression analyses of neural *Src* variants focused on early stages of *Xenopus tropicalis* development. In addition to the temporal expression analyses of secondary neurogenesis, spatial expression analyses should also be performed at these later stages to investigate the tissues in which these variants are expressed. To provide an additional example of vertebrate development, zebrafish embryos should also be

analysed for the spatial expression pattern of *N1-Src* during primary and secondary neurogenesis.

xN1-Src and *xN3-Src* expression was detected in the adult *Xenopus tropicalis* brain. It can therefore be concluded that in addition to *xN1-Src, xN3-Src* expression is maintained into adulthood. Expression of neither variant was detected in the other ectodermal tissue studied; the skin, nor was either detected in the endodermal derivatives the lung or liver; in line with the findings of Pyper & Bolen (1990), who showed *N1-Src* was expressed in the human adult brain but not in the lung, liver or pancreas. Surprisingly, in this experiment *xN1-Src* and *xN3-Src* expression were also detected in the heart. It could be hypothesised that this is due to the high level of autonomic neuron innervation necessary for the heart's contractile function (Vaseghi & Shivkumar 2008), however expression of neither variant was detected in the muscle; an additional mesodermal derivative with high levels of motor neuron innervation (Purves et al. 2001). *C-Src* expression was detectable in all adult tissues studied, fitting with evidence that shows its ubiquitous expression (Pyper & Bolen 1990). The expression analyses of *Src* variants in *Xenopus tropicalis* adult tissues showed the expression of *xN1-Src* and a product of approximately the same size as *xN3-Src* in the brain, supporting previous findings by Pyper & Bolen (1990). The expression of these variants was also detected in the heart; a previously unstudied tissue. *In situ* hybridisation using neural *Src* LNA probes did not reveal embryonic staining of the myocardium, which can be visualised as a domain of *nkx2.5* expression; a transcriptional regulator of heart development visible at the cardiac crescent of tailbud stage embryos (Brade et al. 2007). This suggests that if the expression detected in the heart does exist, expression must be restricted to later embryonic development and to the adult heart, though these experiments must be repeated to conform that these products do not represent sample contamination and the products cloned to confirm their identities.

Comparing the expression of neural *Src* splice variants during *Xenopus tropicalis* and zebrafish early embryogenesis

Whilst both *C-Src* and *xN1-Src* levels begin at relatively low levels in the maternal mRNA pool of *Xenopus tropicalis* embryos and then increase during neural induction and the beginning of neurogenesis at gastrula stages, the expression of *C-Src* and *N1-Src* can be detected at much higher starting levels at the equivalent zebrafish cleavage stages, relative to the expression levels at other time points. Their expression levels then decrease at the beginning of neurogenesis during gastrula stages, before increasing as primary neurogenesis continues during somitogenesis stages, which occurs alongside the formation of the neural tube (Schmidt et al. 2013). Whilst *N1-Src* expression increases later in zebrafish than *Xenopus tropicalis*, occurring after gastrulation, both species exhibit increases in *N-Src* expression levels during neurogenesis that occurs alongside the formation of the neural tube. There was then an additional increase in *N1-Src* expression during secondary neurogenesis at 28hpf (Zhao et al. 2011), as was observed in *Xenopus tropicalis*, though in the zebrafish developmental stages studied, the *N1-Src* expression level did not decrease between primary and secondary neurogenesis. A more detailed time course is required between these time points to investigate the detailed dynamics of *N1-Src* expression levels.

Functional analyses of neural Src isoforms using knockdown technology

The data presented in this project show that bilateral microinjection of AMO A, which inhibits the expression of neural *Src* variants, result in locomotive defects and recapitulate the findings of Lewis (2014). After the initial sensory perception of the stimulus, de-regulated locomotion responses may reflect dysfunction at many levels. Coordinated free swimming can be observed from stage 33, at which point the uninucleate myotomes, innervated by motor neurons are able to coordinate swimming upon sensory stimulation (Muntz 1975). At the stage of development analysed here (approximately stage 40-41), defects in coordinated

swimming may reflect faults in the development of axial musculature, neural circuitry or neuromuscular junctions. If the defects were in the neural circuitry, they are unlikely to result from deficiencies in hindbrain development, as the free swimming responses analysed here can be evoked in stage 37/38 *Xenopus laevis* embryos in which the hindbrain had been removed (Khan & Roberts 1982), and therefore if neuronal circuitry defects are the cause, they are likely to reside in the spinal cord neural circuitry and may be to some extent explained by the unilateral injection results, which showed an increase in the size of the proliferative neural plate (marked by *sox3* expression) and a reduction in the number of differentiated neurons (marked by *n. tubulin* staining)..

A reduction in the number of mature neurons forming reflex arcs during primary neurogenesis would account for the inability of embryos to respond to a touch stimulus with the reflex swimming response displayed at tailbud stages (Roberts et al. 2000). The morphant embryos appeared able to sense the stimulus but were unable to respond with coordinated movements. This effect could be ascribed to defects in motor neuron differentiation however *n. tubulin* staining in unilaterally injected embryos did not reveal a specific subset of neurons was affected by the AMO-mediated knockdown more than the others. To investigate this more precisely, the effects on specific neural populations should be investigated using *in situ* hybridisation probes that mark sensory neurons, interneurons and motor neurons, such as the Rohon Beard sensory neuron marker *runx1* (Hulstrand & Houston 2013), the interneuron markers *vsx1* (D'Autilia et al. 2006) and *gsh2* (Illes et al. 2009) and the motor neuron markers *xHB9* (Saha et al. 1997) and *nkx6.1* (Illes et al. 2009). In addition, to confirm that the effect observed is due to an effect on neural circuitry and not an effect on the axial musculature that is necessary for coordinated swimming, future experiments should consider the possible effects on myogenesis that may also cause the locomotive phenotype seen here. To do so, the expression of myogenic markers such as *myoD* and *myf-5* (Hopwood et al. 1991) in morphant embryos should be analysed.

In unilaterally injected morphant embryos, in which the neural plate expresses *C-Src* but not *xN1-src,* the proliferation increased (shown as an increase in *sox3* staining) and the differentiation decreased (shown as a decrease in *n. tubulin* staining). This concept of increased proliferation and decreased differentiation in the presence of C-Src and absence of N1-Src mirrors the observations made by Bjelfman et al. (1990) who showed that neuroblastoma cancer tumour samples that expressed higher levels of N1-Src than C-Src had better prognosis, resulting from tumour differentiation and spontaneous regression. Additionally, a subtle reduction was observed in the expression domain of the noradrenergic neuron marker *phox2a* in tailbud stage embryos, which marks the cells whose human equivalents develop into neuroblastoma cancer (Wylie et al. 2015). When studied in greater detail, *Xenopus* neurogenesis therefore provides a strong model by which neural Src function can be studied in the context of neuroblastoma cancer.

RT-PCR analyses did not reveal a gross upregulation of *C-Src* levels upon neural *Src* knockdown (Figure 22) however AMO-mediated knockdown of neural *Src* variants may cause an increase in *C-Src* expression specifically in the cells that ordinarily express neural *Src* variants, due to the lack of availability of other splice sites. Whilst a gross upregulation of *C-Src* was not detected using RT-PCR, it is possible that the upregulation is restricted to the cells that normally express the neural *Src* variants and therefore was undetectable using this method. Increased C-Src levels may increase the proliferative capacity of these cells, as promoting proliferation is a known function of the C-Src isoform (Kilkenny et al. 2003), and may explain the increased size of the *sox3* expression domain. Dissecting the neural plate and performing RT-PCR on this specific structure may show subtle upregulation of *C-Src* mRNA in this structure if this is the case. Alternatively, a *C-Src*-specific LNA *in situ* hybridisation probe could be designed to span exons 3 and 4, excluding neural *Src* binding. Increased signal detected from this probe in morphant embryos would indicate whether the levels of this transcript increase.

These analyses investigate the effects of the knockdown of both *xN1-Src* and *xN3-Src* as it was not possible to target *xN1-Src* alone using AMO A, as predicted (Table 7, Figure 22). It may be possible to knockdown *xN3-Src* specifically by targeting the splice acceptor site of this transcript however it has not been possible to target *xN1-Src* specifically, therefore demonstrating a limitation of this approach. In addition, using the zebrafish model organism, discrepancies have been shown between the phenotypes identified in morphant and mutant embryos, which have in part been attributed to the off-target activation of p53-dependent apoptosis (Robu et al. 2007). Equally, abolishing the levels of a protein of interest may yield different effects to merely reducing protein levels using knockdown approaches. Knockout model organisms provide the cleanest manner by which protein function can be studied *in vivo* and we hypothesise that a zebrafish *N1-Src* knockout line could be generated using CRISPR-mediated homologous recombination. Homozygous null embryos could be bred from heterozygous parents; a process beyond the time limits of this project. Whilst it was not shown here that such lines have been created, it was shown that the reagents might now be in place to do so.

The transparency of zebrafish embryos provide additional benefits as the CRISPR could be performed in transgenic lines with fluorescent proteins expressed in neural and neural crest populations. The effects of knockdown could then be analysed in time course experiments on live embryos using light sheet microscopy, without the need for in situ hybridisation.

Functional analyses of neural Src isoforms using mRNA overexpression

In situ hybridisation showed that the *xN1-Src* and *xN3-Src* microexons are expressed in neural structures including the neural plate and tube and neural crest structures such as branchial arches. Whilst *xN1-Src* overexpression resulted in no observable phenotype, *xN3-Src* mRNA

overexpression resulted in the reduction of eye size and/or pigmentation and a reduction in *phox2a* staining of the noradrenergic neurons at tailbud stages. Analysing earlier stages of development may reveal a specific time point at which the development of these structures becomes deregulated, perhaps offering insight into effector functions of xN3-Src in the development of the eye and this neural crest subpopulation. The co-localisation of *xN3-Src* expression and the structures whose development was inhibited by *xN3-Src* overexpression suggests that the observed effects reflect an endogenous function of xN3-Src, rather than a non-specific artefact of overexpression in the whole organism.

xN3-Src overexpression caused an inhibition of eye and noradrenergic neuron development in the absence of SH3 domain-mediated substrate binding, owing to a stop codon in this domain. This may reflect a regulatory function of this isoform, for example by binding to C-Src, xN1-Src or other SFK proteins via its unique domain (Pérez et al. 2013). To explore this possibility, tagging the xN3-Src N-terminus, for example with a HA tag, would allow this interaction to be assessed via co-immunoprecipitation experiments. Analysing COS7 fibroblast cells transfected with the *xN3-Src*-pCS2+ plasmid generated in this project and the *xN1-Src*-pCS2+ plasmid cloned by Philip Lewis for the outgrowth of neurites (Lewis 2014) may also indicate whether xN3-Src is able to inhibit xN1-Src function.

In knockout, morphant and mRNA-injected embryos, large-scale analyses, such as RNA-seq may reveal additional genes in the pathway of neurogenesis whose expression levels are regulated by neural Src isoforms, to be validated using techniques such as *in situ* hybridisation and immunostaining.

Concluding remarks

This project builds on the work by Philip Lewis (2014) and shows in detail the temporal and spatial expression patterns of the neural *Src* variants

whose expression in neural tissues during periods of neurogenesis indicate that they may have roles in the development of the nervous system. In addition, experiments in this project have shown that molecular tools, including morpholino oligos and putatively the reagents necessary to generate a *N1-Src* knockout zebrafish line are being gathered to help study the roles of these isoforms in *Xenopus tropicalis* and zebrafish neurogeneses. By studying the function of these isoforms during such processes, we aim to elucidate their functions during vertebrate neurogenesis, which may offer insight into how N1-Src levels determine neuroblastoma cancer prognosis.

References

Amanchy, R. et al., 2007. A curated compendium of phosphorylation motifs. *Nature biotechnology*, 25(3), pp.285–6.

Amata, I., Maffei, M. & Pons, M., 2014. Phosphorylation of unique domains of Src family kinases. *Frontiers in genetics*, 5, p.181.

Baluda, M.A., 1972. Widespread presence, in chickens, of DNA complementary to the RNA genome of avian leukosis viruses. *Proceedings of the National Academy of Sciences of the United States of America*, 69(3), pp.576–80.

Baumgartner, M. et al., 2008. c-Src-mediated epithelial cell migration and invasion regulated by PDZ binding site. *Molecular and cellular biology*, 28(2), pp.642–55.

Benson, D.A. et al., 2009. GenBank. *Nucleic acids research*, 37(Database issue), pp.D26–31.

Bhatt, A.S. et al., 2005. Adhesion signaling by a novel mitotic substrate of src kinases. *Oncogene*, 24(34), pp.5333–43.

biobyte solutions GmbH, 2014. phyloT: a tree generator. Available at: http://phylot.biobyte.de/index.html [Accessed November 1, 2015].

Bjelfman, C. et al., 1990. Expression of the neuronal form of pp60c-src in neuroblastoma in relation to clinical stage and prognosis. *Cancer research*, 50(21), pp.6908–14.

Braasch, D.A. & Corey, D.R., 2001. Locked nucleic acid (LNA): fine-tuning the recognition of DNA and RNA. *Chemistry & Biology*, 8(1), pp.1–7.

Brade, T. et al., 2007. The amphibian second heart field: Xenopus islet-1 is required for cardiovascular development. *Developmental biology*, 311(2), pp.297–310.

Brewster, R., Lee, J. & Ruiz i Altaba, A., 1998. Gli/Zic factors pattern the neural plate by defining domains of cell differentiation. *Nature*, 393(6685), pp.579–83.

Brodeur, G.M. & Bagatell, R., 2014. Mechanisms of neuroblastoma regression. *Nature Reviews Clinical Oncology*, 11(12), pp.704–713.

Brugge, J.S. et al., 1985. Neurones express high levels of a structurally

modified, activated form of pp60c-src. *Nature*, 316(6028), pp.554–7.

Burgoyne, T. et al., 2015. Regulation of melanosome number, shape and movement in the zebrafish retinal pigment epithelium by OA1 and PMEL. *Journal of Cell Science*, 128(7), pp.1400–1407.

Cao, Y., Zhao, H. & Grunz, H., 2002. XETOR regulates the size of the proneural domain during primary neurogenesis in Xenopus laevis. *Mechanisms of Development*, 119(1), pp.35–44.

Chu, V.T. et al., 2015. Increasing the efficiency of homology-directed repair for CRISPR-Cas9-induced precise gene editing in mammalian cells. *Nature Biotechnology*, 33(5), pp.543–548.

Ciccarone, V. et al., 1989. Phenotypic diversification in human neuroblastoma cells: expression of distinct neural crest lineages. *Cancer research*, 49(1), pp.219–25.

Collett, J.W. & Steele, R.E., 1993. Alternative splicing of a neural-specific Src mRNA (Src+) is a rapid and protein synthesis-independent response to neural induction in Xenopus laevis. *Developmental biology*, 158(2), pp.487–95.

Collett, J.W. & Steele, R.E., 1992. Identification and developmental expression of Src+ mRNAs in Xenopus laevis. *Developmental biology*, 152(1), pp.194–8.

Courtneidge, S.A. et al., 1993. Activation of Src family kinases by colony stimulating factor-1, and their association with its receptor. *The EMBO journal*, 12(3), pp.943–50.

D'Autilia, S. et al., 2006. Cloning and developmental expression of the Xenopus homeobox gene Xvsx1. *Development genes and evolution*, 216(12), pp.829–34.

Darnell, D.K. et al., 2010. Whole mount in situ hybridization detection of mRNAs using short LNA containing DNA oligonucleotide probes. *RNA (New York, N.Y.)*, 16(3), pp.632–7.

David-Pfeuty, T., 1990. Immunolocalization of the cellular src protein in interphase and mitotic NIH c-src overexpresser cells. *The Journal of Cell Biology*, 111(6), pp.3097–3116.

Dou, Y., Andersson-Lendahl, M. & Arner, A., 2008. Structure and function of skeletal muscle in zebrafish early larvae. *The Journal of general*

physiology, 131(5), pp.445–53.

Eisen, J.S. & Smith, J.C., 2008. Controlling morpholino experiments: don't stop making antisense. *Development (Cambridge, England)*, 135(10), pp.1735–43.

Exiqon, LNA™ Oligo Tm Prediction. Available at: https://www.exiqon.com/ls/pages/exiqontmpredictiontool.aspx [Accessed February 28, 2015].

Fahrbach, S.E., 2013. *Developmental Neuroscience: A Concise Introduction*, Princeton: Princeton University Press.

Fehr, J. et al., 2007. Expression of the G-protein alpha-subunit gustducin in mammalian spermatozoa. *Journal of comparative physiology. A, Neuroethology, sensory, neural, and behavioral physiology*, 193(1), pp.21–34.

Filippakopoulos, P., Müller, S. & Knapp, S., 2009. SH2 domains: modulators of nonreceptor tyrosine kinase activity. *Current opinion in structural biology*, 19(6), pp.643–9.

Forehand, C.J. & Farel, P.B., 1982. Spinal cord development in anuran larvae: I. Primary and secondary neurons. *The Journal of comparative neurology*, 209(4), pp.386–94.

Gagnon, J.A. et al., 2014. Efficient mutagenesis by Cas9 protein-mediated oligonucleotide insertion and large-scale assessment of single-guide RNAs. *PloS one*, 9(5), p.e98186.

Gingrich, J.R. et al., 2004. Unique domain anchoring of Src to synaptic NMDA receptors via the mitochondrial protein NADH dehydrogenase subunit 2. *Proceedings of the National Academy of Sciences of the United States of America*, 101(16), pp.6237–42.

Gonfloni, S. et al., 1997. The role of the linker between the SH2 domain and catalytic domain in the regulation and function of Src. *The EMBO journal*, 16(24), pp.7261–71.

Groveman, B.R. et al., 2011. Roles of the SH2 and SH3 domains in the regulation of neuronal Src kinase functions. *The FEBS journal*, 278(4), pp.643–53.

Guan, J.L., 1997. Role of focal adhesion kinase in integrin signaling. *The international journal of biochemistry & cell biology*, 29(8-9), pp.1085–

96.

Guille, M., 1999. *Molecular Methods in Developmental Biology: Xenopus and Zebrafish*, Springer Science & Business Media.

Guiral, E.C., Faas, L. & Pownall, M.E., 2010. Neural crest migration requires the activity of the extracellular sulphatases XtSulf1 and XtSulf2. *Developmental biology*, 341(2), pp.375–88.

Harland, R.M., 1991. In situ hybridization: an improved whole-mount method for Xenopus embryos. *Methods in cell biology*, 36, pp.685–95.

Hirsch, N., Zimmerman, L.B. & Grainger, R.M., 2002. Xenopus, the next generation: X. tropicalis genetics and genomics. *Developmental dynamics : an official publication of the American Association of Anatomists*, 225(4), pp.422–33.

Hoey, J.G., Summy, J. & Flynn, D.C., 2000. Chimeric constructs containing the SH4/Unique domains of cYes can restrict the ability of Src(527F) to upregulate heme oxygenase-1 expression efficiently. *Cellular signalling*, 12(9-10), pp.691–701.

Holland, P.W. et al., 1994. Gene duplications and the origins of vertebrate development. *Development (Cambridge, England). Supplement*, pp.125–33.

Holley, S.A. et al., 1996. The Xenopus Dorsalizing Factor noggin Ventralizes Drosophila Embryos by Preventing DPP from Activating Its Receptor. *Cell*, 86(4), pp.607–617.

Hopwood, N.D., Pluck, A. & Gurdon, J.B., 1991. Xenopus Myf-5 marks early muscle cells and can activate muscle genes ectopically in early embryos. *Development (Cambridge, England)*, 111(2), pp.551–60.

Huang, H. et al., 2008. Defining the specificity space of the human SRC homology 2 domain. *Molecular & cellular proteomics : MCP*, 7(4), pp.768–84.

Hulstrand, A.M. & Houston, D.W., 2013. Regulation of neurogenesis by Fgf8a requires Cdc42 signaling and a novel Cdc42 effector protein. *Developmental biology*, 382(2), pp.385–99.

Huxley, J.S. & Beer, G.R. de, 2015. *The Elements of Experimental Embryology*, Cambridge: Cambridge University Press.

Illes, J.C., Winterbottom, E. & Isaacs, H. V, 2009. Cloning and expression analysis of the anterior parahox genes, Gsh1 and Gsh2 from Xenopus tropicalis. *Developmental dynamics : an official publication of the American Association of Anatomists*, 238(1), pp.194–203.

Irby, R.B. & Yeatman, T.J., 2000. Role of Src expression and activation in human cancer. *Oncogene*, 19(49), pp.5636–42.

Irtegun, S. et al., 2013. Tyrosine 416 is phosphorylated in the closed, repressed conformation of c-Src. *PloS one*, 8(7), p.e71035.

iTOL, iTOL INTERACTIVE TREE OF LIFE. Available at: http://itol.embl.de/index.shtml [Accessed November 1, 2015].

Jevtić, P. & Levy, D.L., 2015. Nuclear size scaling during Xenopus early development contributes to midblastula transition timing. *Current biology : CB*, 25(1), pp.45–52.

Johnson, L.N., 2009. The regulation of protein phosphorylation. *Biochemical Society transactions*, 37(Pt 4), pp.627–41.

Kane, D.A. & Kimmel, C.B., 1993. The zebrafish midblastula transition. *Development (Cambridge, England)*, 119(2), pp.447–56.

Kato, G. & Maeda, S., 1999. Neuron-specific Cdk5 Kinase Is Responsible for Mitosis-Independent Phosphorylation of c-Src at Ser75 in Human Y79 Retinoblastoma Cells. *Journal of Biochemistry*, 126(5), pp.957–961.

Kawabuchi, M. et al., 2000. Transmembrane phosphoprotein Cbp regulates the activities of Src-family tyrosine kinases. *Nature*, 404(6781), pp.999–1003.

Khan, J.A. & Roberts, A., 1982. Experiments on the Central Pattern Generator for Swimming in Amphibian Embryos. *Philosophical Transactions of the Royal Society B: Biological Sciences*, 296(1081), pp.229–243.

Kilkenny, D.M. et al., 2003. c-Src regulation of fibroblast growth factor-induced proliferation in murine embryonic fibroblasts. *The Journal of biological chemistry*, 278(19), pp.17448–54.

Kimmel, C.B. et al., 1995. Stages of embryonic development of the zebrafish. *Developmental dynamics : an official publication of the American Association of Anatomists*, 203(3), pp.253–310.

Koegl, M. et al., 1994. Palmitoylation of multiple Src-family kinases at a homologous N-terminal motif. *The Biochemical journal*, 303 (Pt 3, pp.749–53.

Koestner, U. et al., 2008. Semaphorin and neuropilin expression during early morphogenesis of Xenopus laevis. *Developmental dynamics : an official publication of the American Association of Anatomists*, 237(12), pp.3853–63.

Kuroda, H., Wessely, O. & De Robertis, E.M., 2004. Neural induction in Xenopus: requirement for ectodermal and endomesodermal signals via Chordin, Noggin, beta-Catenin, and Cerberus. *PLoS biology*, 2(5), p.E92.

Lamborghini, J.E., 1980. Rohon-beard cells and other large neurons in Xenopus embryos originate during gastrulation. *The Journal of comparative neurology*, 189(2), pp.323–33.

Lambrechts, A. et al., 2000. cAMP-dependent protein kinase phosphorylation of EVL, a Mena/VASP relative, regulates its interaction with actin and SH3 domains. *The Journal of biological chemistry*, 275(46), pp.36143–51.

Lee, J.E. et al., 1995. Conversion of Xenopus ectoderm into neurons by NeuroD, a basic helix-loop-helix protein. *Science (New York, N.Y.)*, 268(5212), pp.836–44.

Letunic, I. & Bork, P., 2007. Interactive Tree Of Life (iTOL): an online tool for phylogenetic tree display and annotation. *Bioinformatics (Oxford, England)*, 23(1), pp.127–8.

Letunic, I. & Bork, P., 2011. Interactive Tree Of Life v2: online annotation and display of phylogenetic trees made easy. *Nucleic acids research*, 39(Web Server issue), pp.W475–8.

Lewis, P.A., 2014. The role of N-Src kinases in neuronal differentiation.

Lim, J. & Thiery, J.P., 2012. Epithelial-mesenchymal transitions: insights from development. *Development (Cambridge, England)*, 139(19), pp.3471–86.

Lindfors, H.E., Drijfhout, J.W. & Ubbink, M., 2012. The Src SH2 domain interacts dynamically with the focal adhesion kinase binding site as demonstrated by paramagnetic NMR spectroscopy. *IUBMB life*,

64(6), pp.538–44.

Lo, L. et al., 1999. Specification of neurotransmitter identity by Phox2 proteins in neural crest stem cells. *Neuron*, 22(4), pp.693–705.

Ma, Q., Kintner, C. & Anderson, D.J., 1996. Identification of neurogenin, a vertebrate neuronal determination gene. *Cell*, 87(1), pp.43–52.

Maffei, M. et al., 2015. The SH3 Domain Acts as a Scaffold for the N-Terminal Intrinsically Disordered Regions of c-Src. *Structure (London, England : 1993)*, 23(5), pp.893–902.

Marchler-Bauer, A. et al., 2014. CDD: NCBI's conserved domain database. *Nucleic acids research*, 43(Database issue), pp.D222–6.

Martinez, R. et al., 1987. Neuronal pp60c-src contains a six-amino acid insertion relative to its non-neuronal counterpart. *Science (New York, N.Y.)*, 237(4813), pp.411–5.

Maruyama, T. et al., 2015. Increasing the efficiency of precise genome editing with CRISPR-Cas9 by inhibition of nonhomologous end joining. *Nature Biotechnology*, 33(5), pp.538–542.

McCurley, A.T. & Callard, G. V, 2008. Characterization of housekeeping genes in zebrafish: male-female differences and effects of tissue type, developmental stage and chemical treatment. *BMC molecular biology*, 9(1), p.102.

Meadus, W.J., 2003. A semi-quantitative RT-PCR method to measure the in vivo effect of dietary conjugated linoleic acid on porcine muscle PPAR gene expression. *Biological procedures online*, 5, pp.20–28.

Mitra, S.K. & Schlaepfer, D.D., 2006. Integrin-regulated FAK-Src signaling in normal and cancer cells. *Current opinion in cell biology*, 18(5), pp.516–23.

Miyagi, Y. et al., 2002. Delphilin: a novel PDZ and formin homology domain-containing protein that synaptically colocalizes and interacts with glutamate receptor delta 2 subunit. *The Journal of neuroscience : the official journal of the Society for Neuroscience*, 22(3), pp.803–14.

Mizuseki, K., Kishi, M., Shiota, K., et al., 1998. SoxD: an essential mediator of induction of anterior neural tissues in Xenopus embryos. *Neuron*, 21(1), pp.77–85.

Mizuseki, K., Kishi, M., Matsui, M., et al., 1998. Xenopus Zic-related-1 and Sox-2, two factors induced by chordin, have distinct activities in the initiation of neural induction. *Development (Cambridge, England)*, 125(4), pp.579–87.

Muntz, L., 1975. Myogenesis in the trunk and leg during development of the tadpole of Xenopus laevis (Daudin 1802). *Journal of embryology and experimental morphology*, 33(3), pp.757–74.

Nakayama, T. et al., 2014. Cas9-based genome editing in Xenopus tropicalis. *Methods in enzymology*, 546, pp.355–75.

NCBI, NCBI Conserved Domain Search. Available at: http://www.ncbi.nlm.nih.gov/Structure/cdd/wrpsb.cgi [Accessed December 27, 2015a].

NCBI, NCBI Taxonomy Browser. Available at: http://www.ncbi.nlm.nih.gov/Taxonomy/Browser/wwwtax.cgi [Accessed November 1, 2015b].

Newport, J. & Kirschner, M., 1982. A major developmental transition in early xenopus embryos: I. characterization and timing of cellular changes at the midblastula stage. *Cell*, 30(3), pp.675–686.

Nieber, F., Pieler, T. & Henningfeld, K.A., 2009. Comparative expression analysis of the neurogenins in Xenopus tropicalis and Xenopus laevis. *Developmental dynamics : an official publication of the American Association of Anatomists*, 238(2), pp.451–8.

Nieuwkoop, P.D. & Faber, J., 1994. *Normal Table of Xenopus laevis (Daudin)*, New York: Garland Publishing Inc.

Okada, M., 2012. Regulation of the SRC family kinases by Csk. *International journal of biological sciences*, 8(10), pp.1385–97.

Oneyama, C. et al., 2008. The lipid raft-anchored adaptor protein Cbp controls the oncogenic potential of c-Src. *Molecular cell*, 30(4), pp.426–36.

Pan, Q. et al., 2011. Cdk5 targets active Src for ubiquitin-dependent degradation by phosphorylating Src(S75). *Cellular and molecular life sciences : CMLS*, 68(20), pp.3425–36.

Pera, E.M. et al., 2003. Integration of IGF, FGF, and anti-BMP signals via Smad1 phosphorylation in neural induction. *Genes & development*,

17(24), pp.3023–8.

Pérez, Y. et al., 2013. Lipid binding by the Unique and SH3 domains of c-Src suggests a new regulatory mechanism. *Scientific reports*, 3, p.1295.

te Poele, R.H. & Joel, S.P., 1999. Schedule-dependent cytotoxicity of SN-38 in p53 wild-type and mutant colon adenocarcinoma cell lines. *British journal of cancer*, 81(8), pp.1285–93.

Pownall, M.E. & Isaacs, H. V., 2010. *FGF Signalling in Vertebrate Development*, San Rafael: Morgan & Claypool Life Sciences.

Purves, D. et al., 2001. *The Motor Unit*, Sunderland: Sinauer Associates.

Pyper, J.M. & Bolen, J.B., 1990. Identification of a novel neuronal C-SRC exon expressed in human brain. *Molecular and cellular biology*, 10(5), pp.2035–40.

Ran, F.A. et al., 2013. Genome engineering using the CRISPR-Cas9 system. *Nature protocols*, 8(11), pp.2281–308.

Raulf, F., Robertson, S.M. & Schartl, M., 1989. Evolution of the neuron-specific alternative splicing product of the c-src proto-oncogene. *Journal of neuroscience research*, 24(1), pp.81–8.

Resh, M., 1993. Interaction of tyrosine kinase oncoproteins with cellular membranes. *Biochimica et Biophysica Acta (BBA) - Reviews on Cancer*, 1155(3), pp.307–322.

Resh, M.D., 1994. Myristylation and palmitylation of Src family members: The fats of the matter. *Cell*, 76(3), pp.411–413.

Reynolds, C.P., 2002. Ras and Seppuku in neuroblastoma. *Journal of the National Cancer Institute*, 94(5), pp.319–21.

Roberts, A., Hill, N.A. & Hicks, R., 2000. Simple mechanisms organise orientation of escape swimming in embryos and hatchling tadpoles of Xenopus laevis. *The Journal of experimental biology*, 203(Pt 12), pp.1869–85.

Robu, M.E. et al., 2007. p53 activation by knockdown technologies. *PLoS genetics*, 3(5), p.e78.

Rogers, C.D. et al., 2009. Xenopus Sox3 activates sox2 and geminin and indirectly represses Xvent2 expression to induce neural progenitor formation at the expense of non-neural ectodermal derivatives.

Mechanisms of development, 126(1-2), pp.42–55.

Rogers, C.D., Ferzli, G.S. & Casey, E.S., 2011. The response of early neural genes to FGF signaling or inhibition of BMP indicate the absence of a conserved neural induction module. *BMC developmental biology*, 11, p.74.

Saha, M.S., Miles, R.R. & Grainger, R.M., 1997. Dorsal-ventral patterning during neural induction in Xenopus: assessment of spinal cord regionalization with xHB9, a marker for the motor neuron region. *Developmental biology*, 187(2), pp.209–23.

Saksela, K. & Permi, P., 2012. SH3 domain ligand binding: What's the consensus and where's the specificity? *FEBS letters*, 586(17), pp.2609–14.

Sanes, D.H., Reh, T.A. & Harris, W.A., 2011. *Development of the Nervous System*, San Diego: Academic Press.

Sasai, Y. et al., 1994. Xenopus chordin: a novel dorsalizing factor activated by organizer-specific homeobox genes. *Cell*, 79(5), pp.779–90.

Sayers, E.W. et al., 2009. Database resources of the National Center for Biotechnology Information. *Nucleic acids research*, 37(Database issue), pp.D5–15.

Schartl, M. & Barnekow, A., 1982. The expression in eukaryotes of a tyrosine kinase which is reactive with pp60v-src antibodies. *Differentiation; research in biological diversity*, 23(2), pp.109–14.

Schlosser, G., Koyano-Nakagawa, N. & Kintner, C., 2002. Thyroid hormone promotes neurogenesis in the Xenopus spinal cord. *Developmental dynamics : an official publication of the American Association of Anatomists*, 225(4), pp.485–98.

Schmidt, R., Strähle, U. & Scholpp, S., 2013. Neurogenesis in zebrafish – from embryo to adult. *Neural Development*, 8(1), p.3.

Schroeder, T.E., 1970. Neurulation in Xenopus laevis. An analysis and model based upon light and electron microscopy. *J Embryol Exp Morphol*, 23(2), pp.427–462.

Shi, Y. & Massagué, J., 2003. Mechanisms of TGF-beta signaling from cell membrane to the nucleus. *Cell*, 113(6), pp.685–700.

Shuldiner, A.R. et al., 1991. Two nonallelic insulin genes in Xenopus laevis are expressed differentially during neurulation in prepancreatic embryos. *Proceedings of the National Academy of Sciences of the United States of America*, 88(17), pp.7679–83.

Silva, A.-C. et al., 2006. Developmental expression of Shisa-2 in Xenopus laevis. *The International journal of developmental biology*, 50(6), pp.575–9.

Silverman, L., Sudol, M. & Resh, M.D., 1993. Members of the src family of nonreceptor tyrosine kinases share a common mechanism for membrane binding. *Cell growth & differentiation : the molecular biology journal of the American Association for Cancer Research*, 4(6), pp.475–82.

Sindelka, R., Ferjentsik, Z. & Jonák, J., 2006. Developmental expression profiles of Xenopus laevis reference genes. *Developmental dynamics : an official publication of the American Association of Anatomists*, 235(3), pp.754–8.

Slack, J.M. & Forman, D., 1980. An interaction between dorsal and ventral regions of the marginal zone in early amphibian embryos. *Journal of embryology and experimental morphology*, 56, pp.283–99.

Smida, J. & Smidová, V., 1969. Enhanced virus content of chicken tumours induced by the Schmidt-Ruppin strain of Rous sarcoma virus. *Neoplasma*, 16(4), pp.463–6.

Smith, W.C. & Harland, R.M., 1992. Expression cloning of noggin, a new dorsalizing factor localized to the Spemann organizer in Xenopus embryos. *Cell*, 70(5), pp.829–40.

Spemann, H. & Mangold, H., 1924. über Induktion von Embryonalanlagen durch Implantation artfremder Organisatoren. *Archiv für Mikroskopische Anatomie und Entwicklungsmechanik*, 101(1-3), pp.458–458.

Spemann, H. & Mangold, H., 1924. über Induktion von Embryonalanlagen durch Implantation artfremder Organisatoren. *Archiv für Mikroskopische Anatomie und Entwicklungsmechanik*, 100(3-4), pp.599–638.

Stehelin, D. et al., 1976. DNA related to the transforming gene(s) of avian

sarcoma viruses is present in normal avian DNA. *Nature*, 260(5547), pp.170–3.

Summy, J.M. et al., 2003. The SH4-Unique-SH3-SH2 domains dictate specificity in signaling that differentiate c-Yes from c-Src. *Journal of cell science*, 116(Pt 12), pp.2585–98.

Sweetman, D., 2011. In situ detection of microRNAs in animals. *Methods in molecular biology (Clifton, N.J.)*, 732, pp.1–8.

Thomas, S.M. & Brugge, J.S., 1997. Cellular functions regulated by Src family kinases. *Annual review of cell and developmental biology*, 13, pp.513–609.

Thuret, R., Auger, H. & Papalopulu, N., 2015. Analysis of neural progenitors from embryogenesis to juvenile adult in Xenopus laevis reveals biphasic neurogenesis and continuous lengthening of the cell cycle. *Biology open*, p.bio.013391–.

Tindall, A.J. et al., 2007. Expression of enzymes involved in thyroid hormone metabolism during the early development of Xenopus tropicalis. *Biology of the cell / under the auspices of the European Cell Biology Organization*, 99(3), pp.151–63.

Trainor, P.A., 2005. Specification and patterning of neural crest cells during craniofacial development. *Brain, behavior and evolution*, 66(4), pp.266–80.

Ulmer, T.S., Werner, J.M. & Campbell, I.D., 2002. SH3-SH2 Domain Orientation in Src Kinases. *Structure*, 10(7), pp.901–911.

Válóczi, A. et al., 2004. Sensitive and specific detection of microRNAs by northern blot analysis using LNA-modified oligonucleotide probes. *Nucleic acids research*, 32(22), p.e175.

Vaseghi, M. & Shivkumar, K., 2008. The role of the autonomic nervous system in sudden cardiac death. *Progress in cardiovascular diseases*, 50(6), pp.404–19.

Ward, J.D., 2015. Rapid and precise engineering of the Caenorhabditis elegans genome with lethal mutation co-conversion and inactivation of NHEJ repair. *Genetics*, 199(2), pp.363–77.

Warrander, F. et al., 2015. Lin28 proteins promote expression of 17∼92 family miRNAs during amphibian development. *Developmental*

dynamics : an official publication of the American Association of Anatomists, [Epub ahea.

Westhoff, M.A. et al., 2004. SRC-mediated phosphorylation of focal adhesion kinase couples actin and adhesion dynamics to survival signaling. *Molecular and cellular biology*, 24(18), pp.8113–33.

Willars, G.B. & Challiss, R.A.J., 2004. *Receptor Signal Transduction Protocols: 259* 2nd ed., Totowa: Springer Science & Business Media.

Willingham, M.C., Jay, G. & Pastan, I., 1979. Localization of the ASV src gene product to the plasma membrane of transformed cells by electron microscopic immunocytochemistry. *Cell*, 18(1), pp.125–34.

Winterbottom, E.F., Ramsbottom, S.A. & Isaacs, H. V, 2011. Gsx transcription factors repress Iroquois gene expression. *Developmental dynamics : an official publication of the American Association of Anatomists*, 240(6), pp.1422–9.

Wullimann, M.F. et al., 2005. Secondary neurogenesis in the brain of the African clawed frog, Xenopus laevis, as revealed by PCNA, Delta-1, Neurogenin-related-1, and NeuroD expression. *The Journal of comparative neurology*, 489(3), pp.387–402.

Wylie, L.A. et al., 2015. Ascl1 phospho-status regulates neuronal differentiation in a Xenopus developmental model of neuroblastoma. *Disease models & mechanisms*, 8(5), pp.429–41.

Yan, B., Neilson, K.M. & Moody, S.A., 2009. Notch signaling downstream of foxD5 promotes neural ectodermal transcription factors that inhibit neural differentiation. *Developmental dynamics : an official publication of the American Association of Anatomists*, 238(6), pp.1358–65.

Yanagi, T. et al., 2015. The Spemann organizer meets the anterior-most neuroectoderm at the equator of early gastrulae in amphibian species. *Development, growth & differentiation*, 57(3), pp.218–31.

Yasuo, H. & Lemaire, P., 2001. Generation of the germ layers along the animal-vegetal axis in Xenopus laevis. *The International journal of developmental biology*, 45(1), pp.229–35.

You, Y. et al., 2006. Design of LNA probes that improve mismatch discrimination. *Nucleic acids research*, 34(8), p.e60.

Yu, H. et al., 1992. Solution structure of the SH3 domain of Src and identification of its ligand-binding site. *Science (New York, N.Y.)*, 258(5088), pp.1665–8.

Zarrinpar, A., Bhattacharyya, R.P. & Lim, W.A., 2003. The structure and function of proline recognition domains. *Science's STKE : signal transduction knowledge environment*, 2003(179), p.RE8.

Zhao, X. et al., 2011. High mobility group box-1 (HMGB1; amphoterin) is required for zebrafish brain development. *The Journal of biological chemistry*, 286(26), pp.23200–13.